https://www.mdc-berlin.de/de/veroeffentlichungstypen/clinical-journal-club

Als gemeinsame Einrichtung von MDC und Charité fördert das Experimental and Clinical Research Center die Zusammenarbeit zwischen Grundlagenwissenschaftlern und klinischen Forschern. Hier werden neue Ansätze für Diagnose, Prävention und Therapie von Herz-Kreislauf- und Stoffwechselerkrankungen, Krebs sowie neurologischen Erkrankungen entwickelt und zeitnah am Patienten eingesetzt. Sie sind eingeladen, uns beizutreten. Bewerben Sie sich!

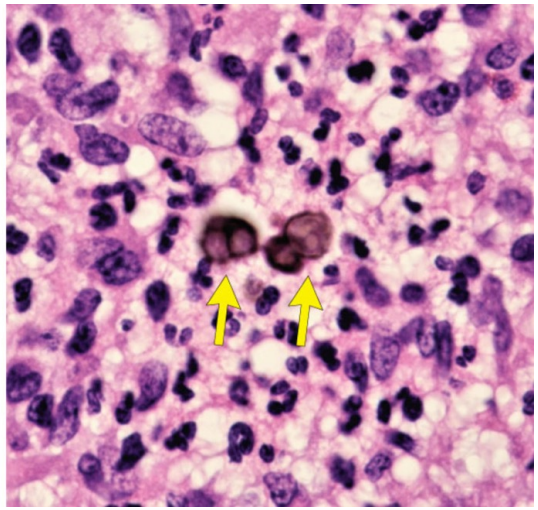

38-year-old pregnant woman at 30 weeks' gestation was referred to the dermatology clinic for evaluation of an itchy lesion on her abdomen that had first appeared 9 years earlier and subsequently slowly expanded. The lesion first appeared after the patient had emigrated from Honduras, where she had worked in agriculture. Physical examination of the 15-cm lesion and the histopathological analysis of a skin-biopsy sample are shown. Which of the following is the most likely diagnosis?

Blastomycosis

Chromoblastomycosis

Cutaneous leishmaniasis

Lobomycosis

Tinea corporis

The histopathological analysis showed pseudoepitheliomatous hyperplasia with dermal granulomatous infiltrates — consistent with cicatricial morphologic features — and thick-walled, brown, septate spores called muriform cells (also known as Medlar bodies, sclerotic bodies, or copper pennies), which are pathognomonic for chromoblastomycosis. A fungal culture grew a pigmented mold, which showed septate hyphae with loosely branched clavate conidia and prominent denticles on microscopy.

Die **Chromoblastomykose** (oft auch als *Chromoblastosis* oder *Chromomykose* bezeichnet) ist eine **chronische, langsam fortschreitende Pilzinfektion der Haut** und des Unterhautgewebes. Sie wird durch bestimmte geschwärzte, pigmentierte Pilze (sogenannte Schwärzepilze oder Dematiaceen) verursacht.

Die Erreger (häufig Pilzarten wie *Fonsecaea pedrosoi* oder *Cladophialophora carrionii*) leben im Erdboden, auf Holz und an Pflanzen.

•**Infektionsweg:** Die Sporen gelangen meist durch **kleine Hautverletzungen** – beispielsweise durch Dornen, Holzsplitter oder bei der Gartenarbeit – in den Körper.

•**Verbreitung:** Die Erkrankung tritt vorwiegend in ländlichen Regionen der **Tropen und Subtropen** bei immunkompetenten Menschen auf.

Der Begriff **IVUS** steht für Intravaskulärer Ultraschall (intravascular ultrasound). Bei der „left main“ handelt es sich um den **linken Hauptstamm** des Herzens, das wichtigste Blutgefäß, das den Herzmuskel versorgt. Die Kombination von IVUS am linken Hauptstamm ist in der Kardiologie ein entscheidender Standard zur genauen Diagnostik und Behandlungsplanung.

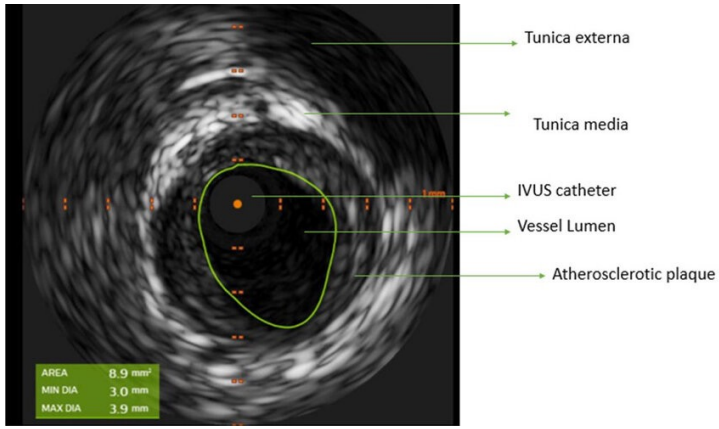

Warum ist IVUS am linken Hauptstamm so wichtig?

•**Präzise Beurteilung:** Die normale Herzkatheteruntersuchung (Angiografie) zeigt das Gefäß nur als zweidimensionalen Schatten. Ein IVUS liefert jedoch detaillierte Querschnittsbilder und macht die Gefäßwände sowie Plaque-Ablagerungen direkt sichtbar.

•**Entscheidungshilfe:** Oft ist im Röntgenbild unklar, ob eine Verengung (Stenose) am Hauptstamm den Blutfluss tatsächlich behindert. IVUS hilft dabei, den Schweregrad exakt zu quantifizieren und die Notwendigkeit von Stents oder einer Bypass-Operation festzulegen.

•**Leitfaden für Stents:** Die Ultraschalluntersuchung zeigt dem Arzt genau, welche Stentgröße gewählt werden muss und ob der Stent nach dem Einsetzen optimal an der Gefäßwand anliegt.

IVUS-Guided versus Angiography-Guided PCI in Unprotected Left Main Coronary Disease

Percutaneous coronary intervention (PCI) is increasingly used for revascularization of unprotected left main coronary artery disease. Whether intravascular ultrasonographic (IVUS) guidance during PCI results in better clinical outcomes than conventional angiographic guidance alone is uncertain.

In an international, multicenter, open-label trial, we randomly assigned patients with unprotected left main coronary artery disease in a 1:1 ratio to undergo either IVUS-guided PCI or angiography-guided PCI. The primary end point was a patient-oriented composite of any stroke, any myocardial infarction, any revascularization, or death from any cause at the longest follow-up.

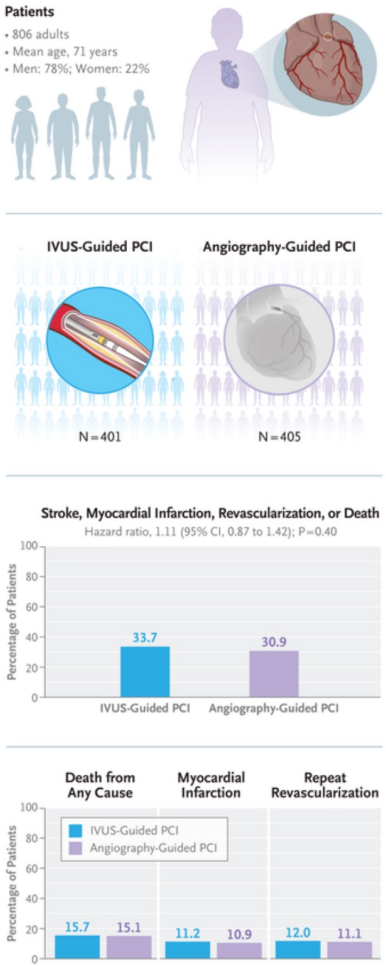

Unprotected left main coronary artery disease is detected in 4 to 6% of patients undergoing diagnostic coronary angiography and is associated with a substantial risk of ischemia in the myocardium and an adverse prognosis. Coronary-artery bypass grafting has long been the preferred method of coronary revascularization when unprotected left main coronary artery disease is present, but randomized trials have established percutaneous coronary intervention (PCI) as an acceptable alternative in patients with low-to-intermediate anatomical complexity and have shown a similar incidence of major adverse cardiac events with the two procedures. However, PCI for left main coronary artery disease poses technical challenges, such as ensuring adequate stent expansion, apposition, and lesion coverage, which may influence long-term outcomes.

Intravascular ultrasonography (IVUS) provides high-resolution tomographic imaging to assess lesion characteristics, guide stent selection and placement, and evaluate postprocedural results. Observational studies and meta-analyses have shown that IVUS guidance during PCI for left main coronary artery disease is associated with a reduced incidence of death, myocardial infarction, and stent thrombosis and is used in more than 50% of PCI procedures for this disease in contemporary practice.

The funders (Philips Image Guided Therapy Devices and Boston Scientific) provided unrestricted grants but had no role in the design, conduct, or oversight of the trial; collection, management, or analysis of the data; interpretation of results; or preparation, review, or approval of the manuscript. There were no restrictions on reporting on the basis of agreements among the sponsor, the funders, and the authors. The first two authors wrote the manuscript and, together with the last author, made the decision to submit the manuscript for publication. All the authors vouch for the accuracy and completeness of the data and for the fidelity of the trial to the protocol.

Patients

Patients 18 years of age or older were eligible if they had unprotected left main coronary artery disease with a stenosis diameter of at least 50% (as visually estimated on angiography) deemed by the local heart team or the treating interventional cardiologist to be suitable for PCI and if they had evidence of moderate or severe ischemia on noninvasive testing or had symptoms despite receiving guideline-directed medical therapy. Qualifying lesions included ostial lesions in the left anterior descending artery, the ostial left circumflex artery, or both.

End Points

The primary end point was a patient-oriented composite of any stroke, any myocardial infarction, any revascularization, or death from any cause at the longest follow-up.

Characteristic	IVUS-Guided PCI (N=401)	Angiography-Guided PCI (N=405)
Age — yr	71.1±11.0	71.7±10.4
Male sex — no. (%)	315 (78.6)	317 (78.3)
Initial presentation — no./total no. (%)		
Non–ST-segment elevation myocardial infarction†	158/400 (39.5)	157/405 (38.8)
Unstable angina	44/400 (11.0)	37/405 (9.1)
Chronic coronary syndrome	198/400 (49.5)	211/405 (52.1)
Medical history — no./total no. (%)		
Hypertension	318/400 (79.5)	321/405 (79.3)
Insulin-dependent diabetes mellitus	3/401 (0.7)	3/405 (0.7)
Non–insulin-dependent diabetes mellitus	144/401 (35.9)	130/405 (32.1)
Dyslipidemia	296/400 (74.0)	315/405 (77.8)
Current smoking	52/400 (13.0)	61/405 (15.1)
Previous PCI	105/400 (26.2)	100/405 (24.7)
Previous CABG	14/400 (3.5)	3/405 (0.7)
Previous myocardial infarction	100/400 (25.0)	90/405 (22.2)
Peripheral vascular disease	59/400 (14.8)	50/405 (12.3)
Chronic obstructive pulmonary disease	39/400 (9.8)	40/405 (9.9)
Previous heart failure	103/400 (25.8)	80/405 (19.8)
Left ventricular ejection fraction — %‡	53.2±11.1	53.4±10.4
Body-mass index§	28.0±5.3	27.4±4.7
Creatinine clearance <60 ml/min — no./total no. (%)	123/384 (32.0)	139/388 (35.8)
Anatomical SYNTAX score — units¶	30.1±13.0	29.3±12.1

Lesion and Procedural Characteristics.

Characteristic	IVUS-Guided PCI (N=401)	Angiography-Guided PCI (N=405)
No. of target lesions per patient	1.59±0.85	1.61±0.84
Anatomical three-vessel disease — no./total no. (%)†	215/371 (58.0)	216/374 (57.8)
AHA classification per lesion — no./total no. (%)‡		
A	32/394 (8.1)	47/403 (11.7)
B1	104/394 (26.4)	120/403 (29.8)
B2	238/394 (60.4)	204/403 (50.6)
C	121/394 (30.7)	140/403 (34.7)
Lesion preparation performed — no./total no. (%)	371/394 (94.2)	372/403 (92.3)
Lesion preparation devices — no./total no. (%)		
Compliant balloon	143/394 (36.3)	135/403 (33.5)
Noncompliant balloon	259/394 (65.7)	247/403 (61.3)
Cutting balloon	56/394 (14.2)	40/403 (9.9)
Rotablator	37/394 (9.4)	29/403 (7.2)
Intravascular lithotripsy	46/394 (11.7)	22/403 (5.5)
Dilation after stent placement — no./total no. (%)	382/394 (97.0)	387/403 (96.0)
Use of IVUS per patient — no./total no. (%)§		
Before stenting	261/401 (65.1)	10/403 (2.5)
After stenting	385/401 (96.0)	9/403 (2.2)
At any time	391/401 (97.5)	12/403 (3.0)
Balloon inflation in the proximal part of the stent after stent placement — no./total no. (%)¶	352/393 (89.6)	342/402 (85.1)
No. of stents used per patient	2.48±1.57	2.40±1.42
Total stent length per patient — mm	58.68±40.53	57.64±37.37
Maximum stent diameter per patient — mm	3.71±0.43	3.66±0.40
Total procedure duration — min	88.6±50.2	63.9±37.6
Periprocedural complications — no./total no. (%)	29/394 (7.4)	29/403 (7.2)

Primary and Secondary End Points.

Outcome	IVUS-Guided PCI (N=401)		Angiography-Guided PCI (N=405)		Hazard Ratio (95% CI)*
	no. (%)	*events/100 patient-yr*	*no. (%)*	*events/100 patient-yr*	
Primary end point					
Patient-oriented composite end point†	135 (33.7)	14.1	125 (30.9)	12.7	1.11 (0.87–1.42)‡
Secondary end points§					
Device-oriented composite end point¶	90 (22.4)	9.0	83 (20.5)	8.1	1.10 (0.82–1.49)
Vessel-oriented composite end point‖	97 (24.2)	9.8	87 (21.5)	8.6	1.14 (0.85–1.52)
Death from any cause	63 (15.7)	5.5	61 (15.1)	5.2	1.06 (0.74–1.50)
Death from cardiovascular causes	38 (9.5)	3.3	29 (7.2)	2.5	1.34 (0.83–2.17)
Stroke	12 (3.0)	1.1	4 (1.0)	0.3	3.11 (1.00–9.65)
Myocardial infarction	45 (11.2)	4.3	44 (10.9)	4.2	1.04 (0.68–1.57)
Target-vessel–related myocardial infarction	42 (10.5)	4.0	41 (10.1)	3.9	1.04 (0.67–1.59)
Non–procedure-related myocardial infarction**	22 (5.5)	2.0	16 (4.0)	1.4	1.41 (0.74–2.68)
Procedure-related myocardial infarction**	24 (6.0)	2.2	30 (7.4)	2.8	0.81 (0.47–1.38)
Non–target-vessel–related myocardial infarction	5 (1.2)	0.4	4 (1.0)	0.3	1.29 (0.35–4.80)
Repeat revascularization††	48 (12.0)	4.6	45 (11.1)	4.2	1.10 (0.73–1.65)
Target-vessel revascularization	40 (10.0)	3.8	38 (9.4)	3.5	1.08 (0.69–1.69)
Target-lesion revascularization	32 (8.0)	3.0	36 (8.9)	3.3	0.91 (0.56–1.46)
Clinically indicated target-lesion revascularization	28 (7.0)	2.6	30 (7.4)	2.7	0.96 (0.57–1.60)
Stent thrombosis‡‡					
Definite	3 (0.7)	0.3	1 (0.2)	0.1	3.07 (0.32–29.53)
Probable or definite	8 (2.0)	0.7	3 (0.7)	0.3	2.73 (0.72–10.27)

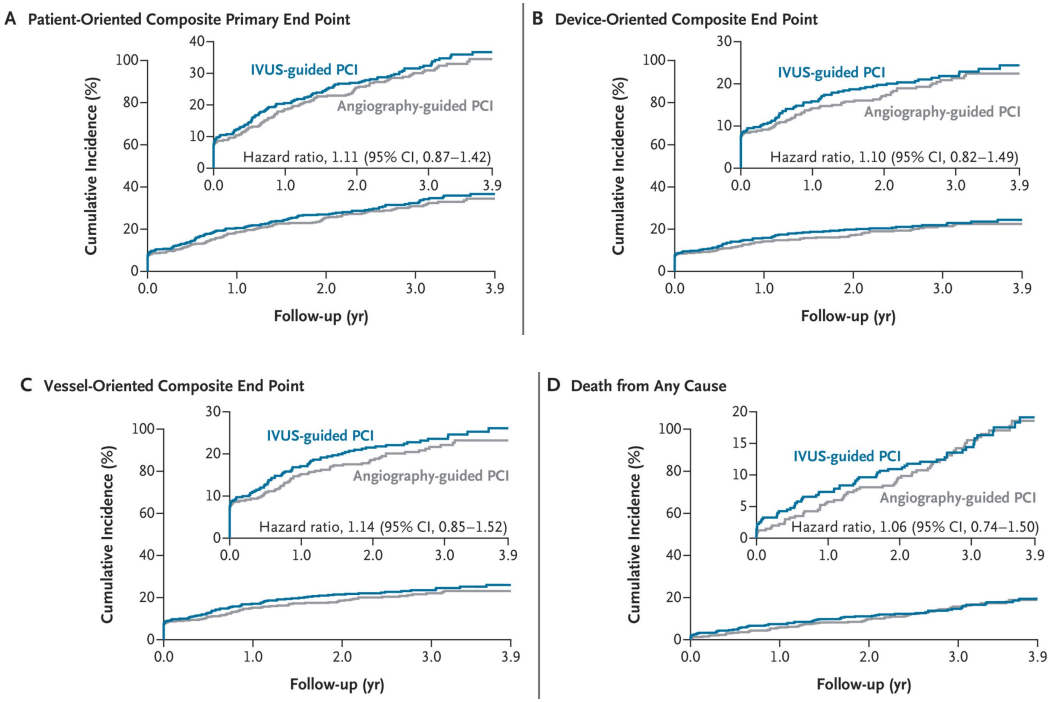

Time-to-Event Curves for the Primary and Secondary End Points.

Panel A shows the cumulative incidence of a patient-oriented composite of any stroke, any myocardial infarction, any revascularization, or death from any cause (the primary end point). Panels B, C, and D show the cumulative incidence of a device-oriented composite of death from cardiovascular causes, target-vessel myocardial infarction, or clinically indicated target-lesion revascularization (Panel B); a vessel-oriented composite of death from cardiovascular causes, target-vessel myocardial infarction, or target-vessel revascularization (Panel C); and death from any cause (Panel D), all secondary end points. Hazard ratios are from Cox models. The insets show the same data on an expanded y axis.

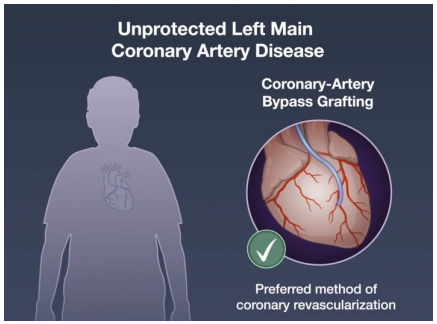
Unprotected Left Main Coronary Artery Disease
Coronary-Artery Bypass Grafting
Preferred method of coronary revascularization

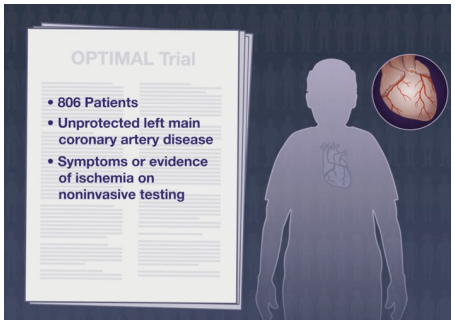
OPTIMAL Trial
• 806 Patients
• Unprotected left main coronary artery disease
• Symptoms or evidence of ischemia on noninvasive testing

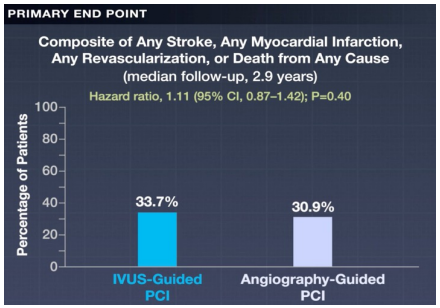
PRIMARY END POINT
Composite of Any Stroke, Any Myocardial Infarction, Any Revascularization, or Death from Any Cause
(median follow-up, 2.9 years)
Hazard ratio, 1.11 (95% CI, 0.87–1.42); P=0.40
Percentage of Patients
100
80
60
40
20
0
33.7%
30.9%
IVUS-Guided PCI
Angiography-Guided PCI

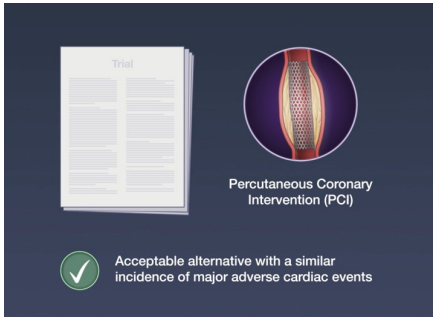
Trial
Percutaneous Coronary Intervention (PCI)
Acceptable alternative with a similar incidence of major adverse cardiac events

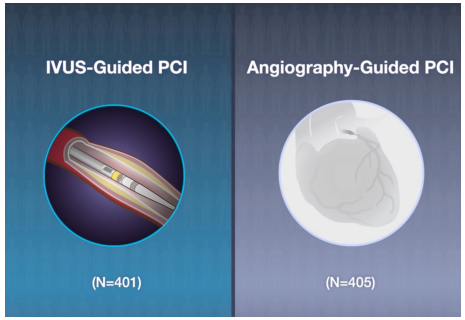
IVUS-Guided PCI
Angiography-Guided PCI
(N=401)
(N=405)

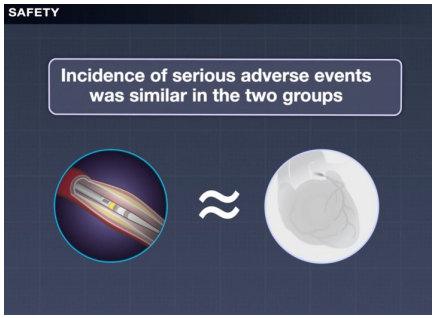
SAFETY
Incidence of serious adverse events was similar in the two groups

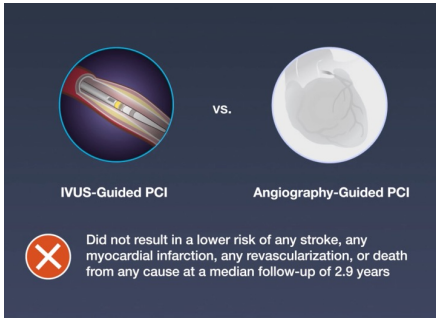
vs.
IVUS-Guided PCI
Angiography-Guided PCI
Did not result in a lower risk of any stroke, any myocardial infarction, any revascularization, or death from any cause at a median follow-up of 2.9 years

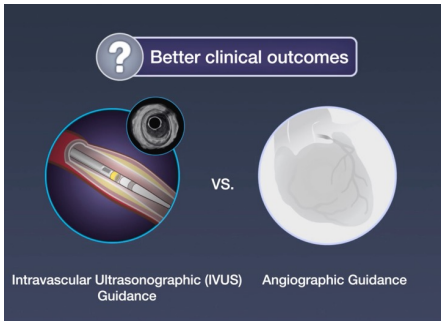
Better clinical outcomes
vs.
Intravascular Ultrasonographic (IVUS) Guidance
Angiographic Guidance

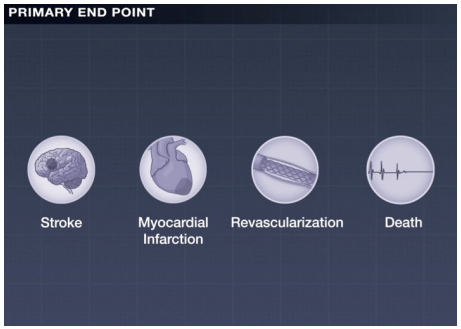
PRIMARY END POINT
Stroke
Myocardial Infarction
Revascularization
Death

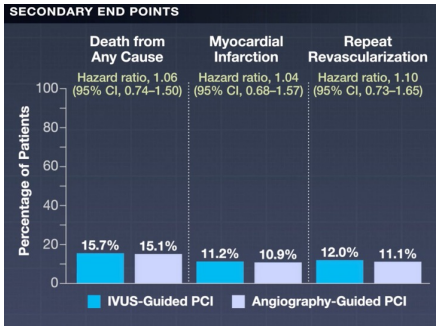
SECONDARY END POINTS
Death from Any Cause
Myocardial Infarction
Repeat Revascularization
Hazard ratio, 1.06 (95% CI, 0.74–1.50)
Hazard ratio, 1.04 (95% CI, 0.68–1.57)
Hazard ratio, 1.10 (95% CI, 0.73–1.65)
Percentage of Patients
100
80
60
40
20
0
15.7%
15.1%
11.2%
10.9%
12.0%
11.1%
IVUS-Guided PCI
Angiography-Guided PCI

Der **intravaskuläre Ultraschall (IVUS)** ist eine moderne Ultraschalluntersuchung direkt im Inneren der Herzkranzgefäße, die bei einer **perkutanen Koronarintervention (PCI)** – also einer minimalinvasiven Herzkatheter-Erweiterung mittels Stent – als entscheidendes Steuerungswerkzeug dient. Bei sogenannten **High-Risk PCIs** (Hochrisiko-Eingriffen bei anatomisch komplexen Gefäßverengungen) verbessert der Einsatz von IVUS die Langzeitergebnisse und die Patientensicherheit drastisch.

In der modernen Kardiologie gilt die IVUS-gesteuerte PCI laut den aktuellen Leitlinien der European Society of Cardiology (ESC) als **Klasse-I-Empfehlung (Evidenzniveau A)** für komplexe Läsionen.

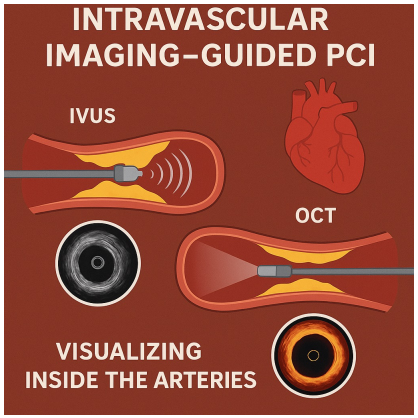

Der Ultraschallkatheter liefert während des Eingriffs drei kritische Informationen:

•**Gefäßbeschaffenheit**: Exakte Beurteilung von Kalkablagerungen und der Plaque-Last vor der Dehnung.

•**Stent-Dimensionierung**: Präzise Messung des echten Gefäßdurchmessers, um die perfekte Stentgröße zu wählen.

•**Ergebnis-Verifizierung**: Kontrolle, ob der Stent vollständig an der Gefäßwand anliegt (Vermeidung von Malappositionen) und maximal entfaltet ist.

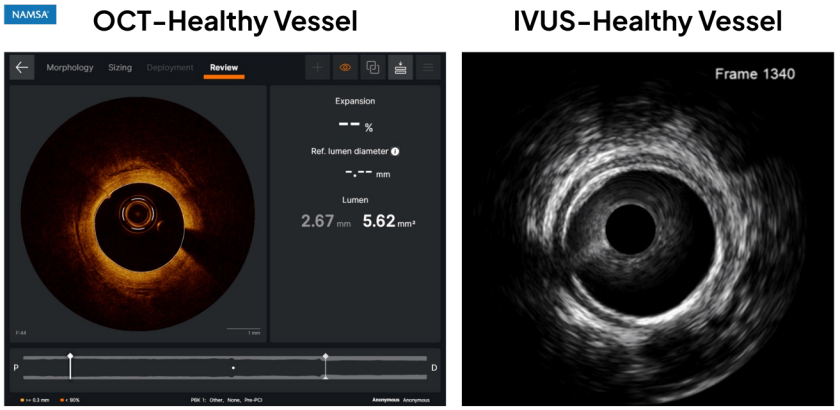

Intravascular Ultrasound–Guided or Angiography-Guided Complex High-Risk PCI

Intravascular ultrasound (IVUS) guidance during percutaneous coronary intervention (PCI) has been associated with increased stent optimization and reduced adverse events among patients with complex coronary-artery lesions, but adoption of this strategy in Western countries remains low. Although practice guidelines recommend intracoronary imaging for anatomically complex lesions, evidence from current European practice is limited. In this investigator-initiated, international, open-label, randomized, controlled trial, we assigned patients undergoing complex PCI to either IVUS-guided PCI, performed with the use of prespecified stent-optimization criteria, or angiography-guided PCI. The primary end point was target-vessel failure, defined as a composite of death from cardiac causes, target-vessel myocardial infarction, or clinically indicated target-vessel revascularization.

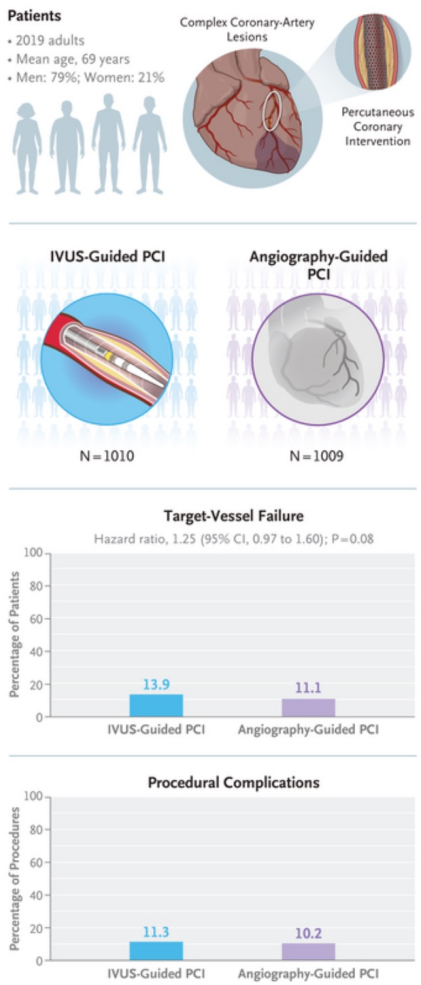

Intravascular ultrasound (IVUS) guidance during percutaneous coronary intervention (PCI) has been associated with increased stent optimization, including adequate stent expansion and apposition, and with reductions in geographic miss (failure of the coronary stent to cover the entire lesion) and adverse clinical events as compared with angiography-guided PCI alone. Meta-analyses and randomized trials that were conducted predominantly in Asian countries have shown a consistent benefit of this strategy, particularly in patients with complex coronary-artery anatomy. In Western countries, however, routine adoption of intracoronary imaging remains low.
Patients undergoing PCI of complex coronary-artery lesions — such as severe calcifications, lesions due to left main coronary artery disease or ostial disease, true bifurcation lesions, chronic total occlusions, in-stent restenosis, or long segments with an indication for extensive stenting — are at heightened risk for stent failure and subsequent ischemic events.

Patients

Patients 18 years of age or older were eligible for enrollment in the trial if they presented with a non–ST-segment elevation acute coronary syndrome (non–ST-segment elevation myocardial infarction or unstable angina) or stable ischemic heart disease (stable angina or silent ischemia) and were scheduled to undergo PCI of at least one angiographically complex coronary-artery lesion or had an indication for PCI with planned mechanical circulatory support. Complex lesions were defined as angiographic severe calcifications, ostial lesions, true bifurcation lesions with a side branch at least 2.5 mm in diameter, left main coronary-artery lesions, chronic total occlusions, in-stent restenosis, or lesions more than 28 mm in length. Key exclusion criteria were ST-segment elevation myocardial infarction, cardiogenic shock, planned PCI of a diseased aortocoronary bypass graft, and an absolute contraindication to the use of iodinated contrast material or prolonged dual antiplatelet therapy or an allergy to such agents that could not be premedicated.

Procedures

The trial protocol specified that all target lesions were to be treated with everolimus-eluting platinum–chromium stents (Synergy or Synergy Megatron, Boston Scientific). In the IVUS-guided PCI group, patients underwent IVUS for assessment of stent optimization after the intervention.

Characteristic	IVUS-Guided PCI (N=1010)	Angiography-Guided PCI (N=1009)
Age — yr	69.5±10.3	69.1±10.3
Male sex — no. (%)	804 (79.6)	800 (79.3)
Initial presentation — no. (%)		
Acute coronary syndrome	294 (29.1)	259 (25.7)
Non–ST-segment elevation myocardial infarction	212 (21.0)†	187 (18.5)
Unstable angina	82 (8.1)	72 (7.1)
Stable ischemic heart disease	716 (70.9)	750 (74.3)
Stable angina	549 (54.4)	561 (55.6)
Silent ischemia	167 (16.5)	189 (18.7)
Medical history — no. (%)		
Hypertension	762 (75.4)	784 (77.7)
Insulin-dependent diabetes mellitus	92 (9.1)	98 (9.7)
Non–insulin-dependent diabetes mellitus	218 (21.6)	224 (22.2)
Dyslipidemia	719 (71.2)	708 (70.2)
Current smoking	181 (17.9)	170 (16.8)
Previous PCI	472 (46.7)	481 (47.7)
Previous coronary-artery bypass grafting	78 (7.7)	69 (6.8)
Previous myocardial infarction	297 (29.4)	318 (31.5)
Peripheral vascular disease	136 (13.5)	168 (16.7)
Chronic obstructive pulmonary disease	92 (9.1)	83 (8.2)
Previous heart failure	222 (22.0)	221 (21.9)
Left ventricular ejection fraction — %‡	52.6±11.0	53.3±11.5
Body-mass index§	27.5±4.3	27.3±4.4
Creatinine clearance <60 ml/min — no./total no. (%)	237/933 (25.4)	226/945 (23.9)

Lesion and Procedural Characteristics.

Characteristic	IVUS-Guided PCI (N=999)	Angiography-Guided PCI (N=1002)
No. of target lesions†	1.42±0.71	1.42±0.69
Anatomical SYNTAX score‡		
No. of patients with data	787	809
Score	25.4±14.4	24.9±14.0
Target lesion type — no. (%)		
Angiographic severe calcification	458 (45.8)	423 (42.2)
Ostial lesion	275 (27.5)	267 (26.6)
Bifurcation	331 (33.1)	323 (32.2)
Left main coronary-artery lesion	198 (19.8)	177 (17.7)
Chronic total occlusion	220 (22.0)	222 (22.2)
In-stent restenosis	167 (16.7)	186 (18.6)
Long lesion	616 (61.7)	603 (60.2)
Concurrent treatment of noncomplex lesions — no. (%)	100 (10.0)	109 (10.9)
Use of mechanical circulatory support — no. (%)	5 (0.5)	9 (0.9)
Lesion preparation performed — no. (%)	917 (91.8)	904 (90.2)
Lesion-preparation method used — no. (%)		
Semicompliant balloon angioplasty	464 (46.4)	465 (46.4)
Noncompliant balloon angioplasty	585 (58.6)	502 (50.1)
Scoring balloon angioplasty	51 (5.1)	58 (5.8)
Cutting balloon angioplasty	77 (7.7)	59 (5.9)
Rotablation	65 (6.5)	73 (7.3)
Intravascular lithotripsy	106 (10.6)	75 (7.5)
Orbital atherectomy	25 (2.5)	27 (2.7)
Dilation with balloon angioplasty performed after stent implantation — no. (%)	912 (91.3)	847 (84.5)
Maximum balloon diameter after stent implantation		
No. of patients with data	908	842
Diameter — mm	3.90±0.70	3.72±0.67
Use of IVUS at any time during the procedure — no. (%)	986 (98.7)	9 (0.9)
No. of stents placed	2.35±1.38	2.19±1.35
Total stent length		
No. of patients with data	983	978
Length — mm	64.0±38.7	59.6±37.3
Maximum stent diameter		
No. of patients with data	983	978
Diameter — mm	3.50±0.54	3.38±0.52
Total procedure duration — min	88.8±47.3	66.2±41.3
Total volume of contrast material		
No. of patients with data	984	998
Volume — ml	185.0±94.5	175.7±87.2
Procedural complications — no. (%)	113 (11.3)	102 (10.2)

Primary and Secondary End Points.

End Point	IVUS-Guided PCI (N=1010)			Angiography-Guided PCI (N=1009)			Hazard Ratio (95% CI)
	no. of events	*% of patients with event*	*no. of events/ 100 patient-yr*	*no. of events*	*% of patients with event*	*no. of events/ 100 patient-yr*	
Primary end point							
Target-vessel failure: composite of death from cardiac causes, target-vessel myocardial infarction, or clinically indicated target-vessel revascularization	140	13.9	9.6	112	11.1	7.7	1.25 (0.97–1.60)†
Key secondary end points							
Composite of target-vessel myocardial infarction or clinically indicated target-vessel revascularization	112	11.1	7.7	92	9.1	6.3	1.22 (0.92–1.60)
Clinically indicated target-vessel revascularization	75	7.4	5.0	61	6.0	4.0	1.22 (0.87–1.71)
Composite of death from cardiac causes or target-vessel myocardial infarction	94	9.3	6.3	78	7.7	5.2	1.20 (0.89–1.62)
Target-lesion failure: composite of death from cardiac causes, target-vessel myocardial infarction, or clinically indicated target-lesion revascularization	133	13.2	9.1	109	10.8	7.4	1.22 (0.94–1.57)
Target-lesion revascularization	75	7.4	5.0	67	6.6	4.5	1.11 (0.80–1.54)
Death from cardiac causes	34	3.4	2.2	27	2.7	1.7	1.24 (0.75–2.05)
Other prespecified secondary end points‡							
Death from any cause	50	5.0	3.2	58	5.7	3.7	0.85 (0.58–1.24)
Myocardial infarction	69	6.8	4.6	65	6.4	4.4	1.05 (0.75–1.48)
Target-vessel myocardial infarction§	66	6.5	4.4	58	5.7	3.9	1.13 (0.80–1.61)
Nonprocedural myocardial infarction	23	2.3	1.5	25	2.5	1.6	0.90 (0.51–1.59)
Periprocedural myocardial infarction	44	4.4	2.9	35	3.5	2.3	1.26 (0.81–1.96)
Non–target-vessel myocardial infarction	4	0.4	0.3	8	0.8	0.5	0.49 (0.15–1.62)
Repeat revascularization	107	10.6	7.3	99	9.8	6.7	1.07 (0.82–1.41)
Target-vessel revascularization	83	8.2	5.5	74	7.3	5.0	1.11 (0.81–1.52)
Definite stent thrombosis	2	0.2	0.1	10	1.0	0.6	0.20 (0.04–0.90)
Definite or probable stent thrombosis	5	0.5	0.3	15	1.5	1.0	0.33 (0.12–0.90)

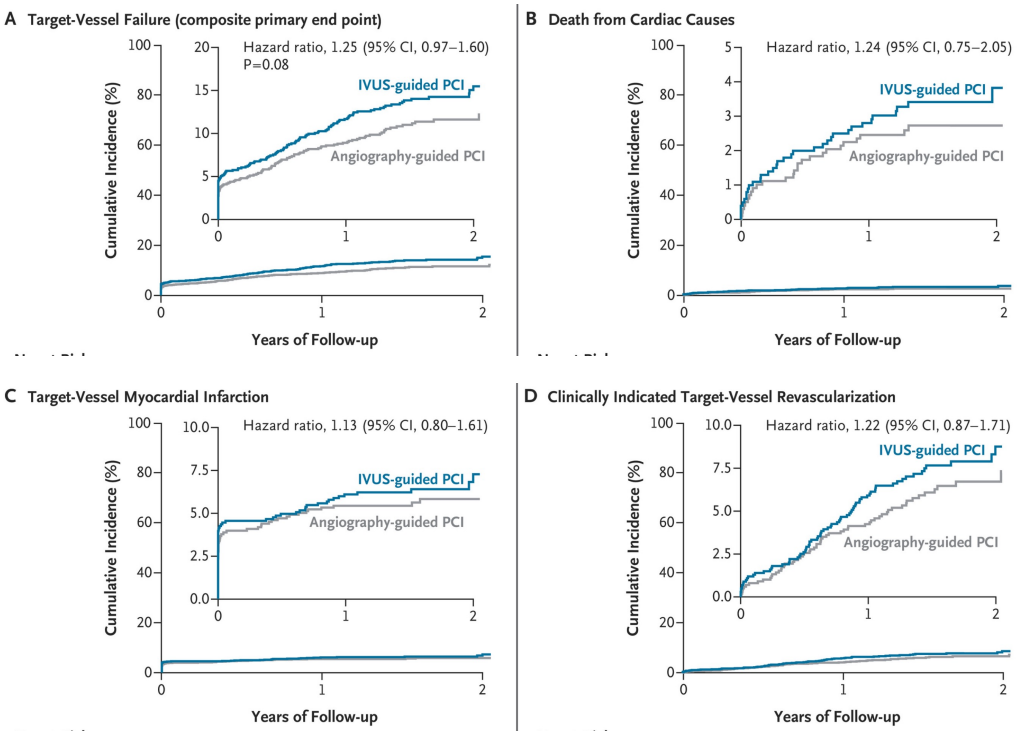

Time-to-First-Event Curves for the Primary and Secondary End Points.

Shown is the cumulative incidence of the primary end point, target-vessel failure (Panel A), defined as a composite of death from cardiac causes (Panel B), target-vessel myocardial infarction (Panel C), or clinically indicated target-vessel revascularization (Panel D). Hazard ratios are derived from Cox proportional-hazards models; the P value is derived from a log-rank test. The curves are truncated at the latest time point at which 15% or more of the patients remained at risk. For the individual components of the primary end point, which were assessed as secondary end points, the widths of the confidence intervals have not been adjusted for multiplicity and should not be used to infer definitive treatment effects. The insets show the same data on an enlarged y axis.

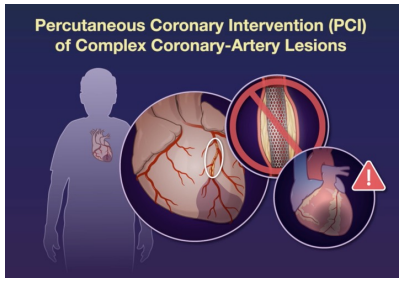
Percutaneous Coronary Intervention (PCI)
of Complex Coronary-Artery Lesions

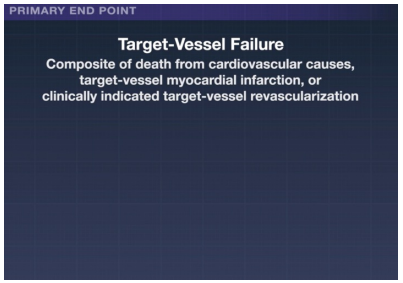
PRIMARY END POINT
Target-Vessel Failure
Composite of death from cardiovascular causes,
target-vessel myocardial infarction, or
clinically indicated target-vessel revascularization

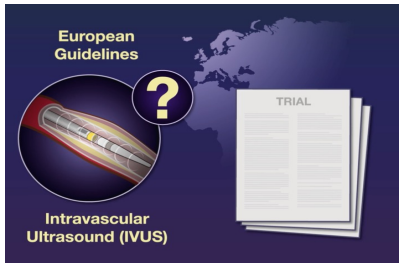
European
Guidelines
?
TRIAL
Intravascular
Ultrasound (IVUS)

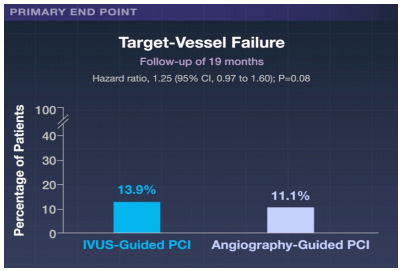
PRIMARY END POINT
Target-Vessel Failure
Follow-up of 19 months
Hazard ratio, 1.25 (95% CI, 0.97 to 1.60); P=0.08
Percentage of Patients
100
40
30
20
10
0
13.9%
11.1%
IVUS-Guided PCI
Angiography-Guided PCI

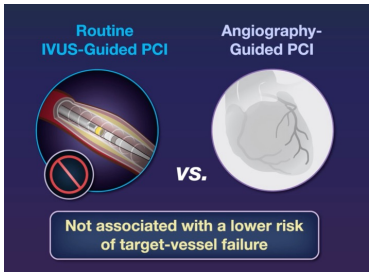
Routine
IVUS-Guided PCI
Angiography-
Guided PCI
vs.
Not associated with a lower risk
of target-vessel failure

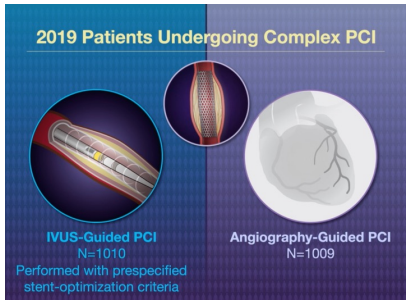
2019 Patients Undergoing Complex PCI
IVUS-Guided PCI
N=1010
Performed with prespecified
stent-optimization criteria
Angiography-Guided PCI
N=1009

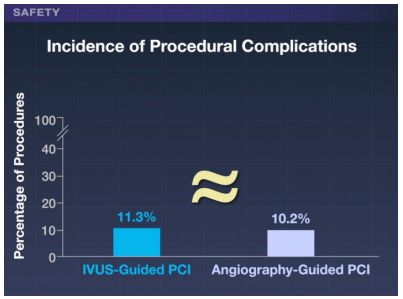
SAFETY
Incidence of Procedural Complications
Percentage of Procedures
100
40
30
20
10
0
≈
11.3%
10.2%
IVUS-Guided PCI
Angiography-Guided PCI

Interleukin 10 (IL-10) ist eines der wichtigsten entzündungshemmenden Zytokine (Botenstoffe) des menschlichen Immunsystems. Es wirkt immunregulierend, schützt den Körper vor überschießenden Entzündungen und spielt eine zentrale Rolle bei der Entwicklung der Immuntoleranz.

Funktionen im Überblick

•**Entzündungshemmung:** IL-10 unterdrückt die Produktion pro-inflammatorischer Zytokine (wie TNF-α, IL-1 und Interferon-gamma).

•**Immunmodulation:** Es verhindert, dass das Immunsystem körpereigenes Gewebe angreift und beugt so Autoimmunerkrankungen vor.

•**Infektionsschutz:** Bei akuten Infektionen hilft IL-10, Kollateralschäden im Gewebe zu begrenzen, die durch eine zu starke Immunreaktion entstehen könnten

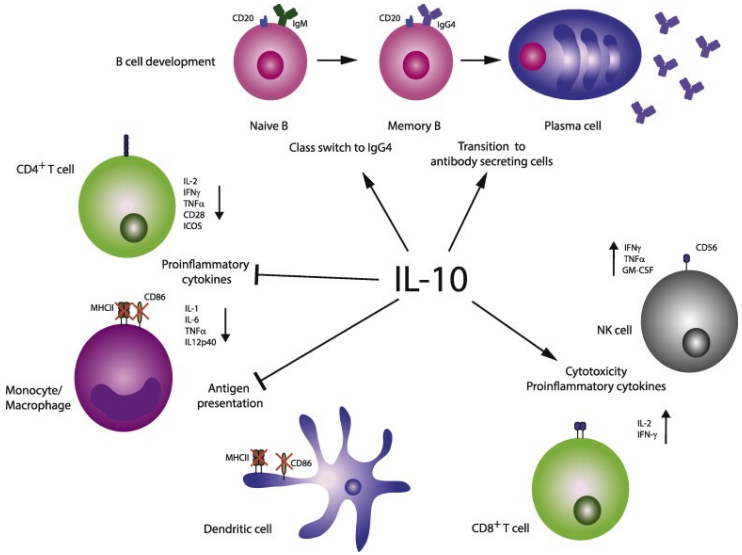

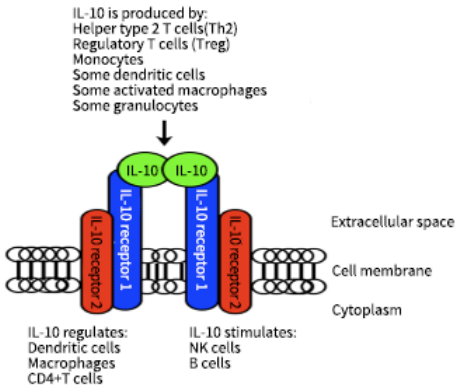

Autoantibodies against Cytokines — From Infection to Inflammation

Interleukin-10

An antiinflammatory cytokine produced by several types of leukocytes, including regulatory T cells. Interleukin-10 acts on various cell types, including myeloid cells such as macrophages. It reduces inflammation by antagonizing proinflammatory cytokines, in particular interferon-γ.

Autoantibodies against Cytokines

Autoantibodies neutralizing type I interferons were first reported in 1984 in a patient with disseminated zoster. The field lay dormant until 2004, when cases involving patients with atypical mycobacterial disease and autoantibodies neutralizing type II interferon were reported. Remarkably, patients with autoantibodies neutralizing type II interferon had the same mycobacterial infections as patients with monogenic inborn errors of type II interferon or its receptor.

Rare Interleukin-10 Autoantibodies

The authors reported two children with autoantibodies neutralizing interleukin-10. The clinical manifestations of these patients were inflammatory rather than infectious.

Common Interleukin-10 Autoantibodies

Gharahdaghi et al. have built, in spectacular fashion, on their initial observation. They report that approximately 3.5% of adult patients with IBD have autoantibodies neutralizing interleukin-10.

In humans, the **IL10 gene** is located on the **long (q) arm of chromosome 1**.

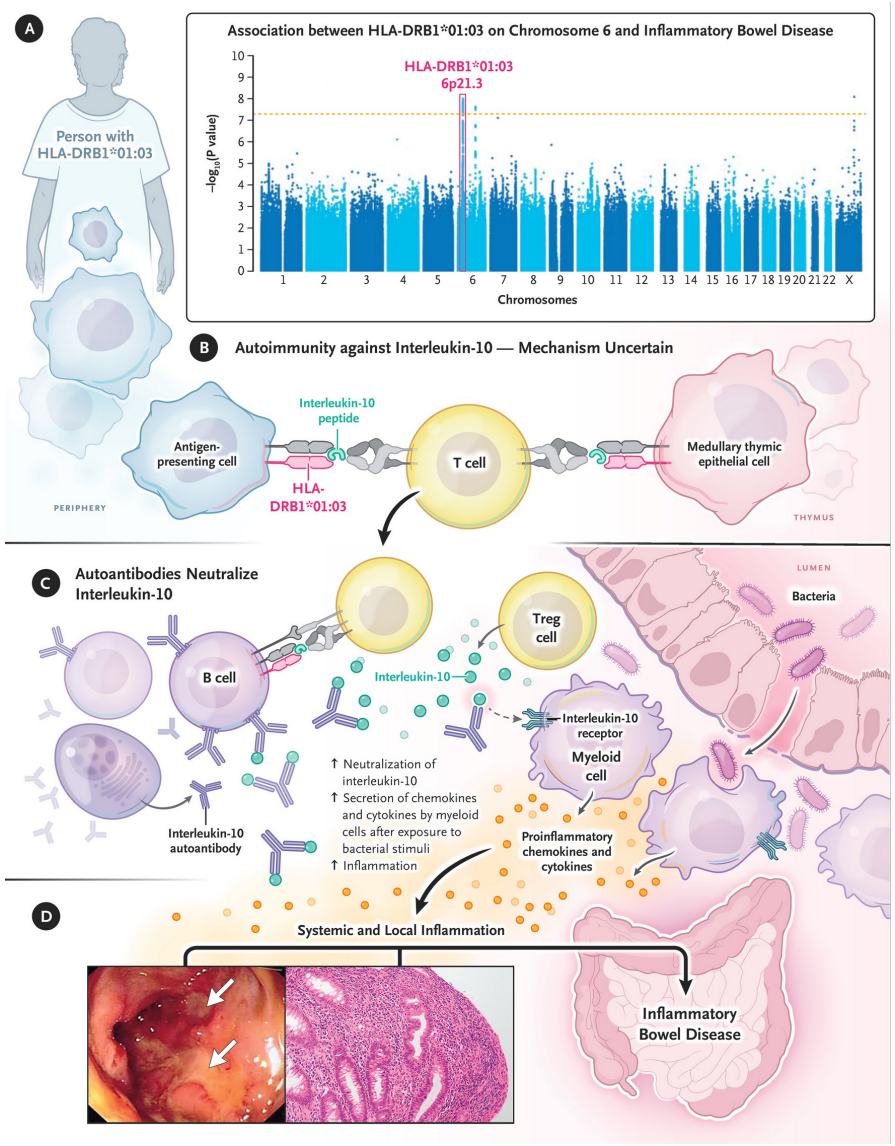

HLA Risk Allele and Autoantibodies against Interleukin-10 in Inflammatory Bowel Disease (IBD).

HLA association studies have identified a common HLA allele, HLA-DRB1*01:03, that is associated with Crohn's disease and ulcerative colitis (Panel A).[10] The study by Gharahdaghi et al.[1] uncovers the pathophysiological underpinnings of this association. As a hypothetical mechanism, interleukin-10 peptide is embedded into the DRB1 HLA and recognized by interleukin-10–HLA-specific CD4 T cells, interacting with B cells (Panel B). Gharahdaghi et al. describe autoantibodies neutralizing interleukin-10, a key antiinflammatory cytokine (Panel C). Such autoantibodies are found in 3.5% of patients with IBD and cause higher levels of inflammation when blood leukocytes are tested in vitro, because interleukin-10, produced by regulatory T (Treg) cells and other cell types, is neutralized, unleashing phagocytic responses to bacterial stimuli. This reaction may occur in the intestinal mucosa in vivo. Patients harboring these autoantibodies could be treated with B-cell–depleting agents. A study of interleukin-10 autoantibodies in a previous issue of the *Journal*[8] described the presence of intestinal inflammation (Panel D), both macroscopic (arrows indicate ulcerations) and microscopic (histologic analysis of samples of colon tissue with hematoxylin and eosin staining, showing mild distortion of glandular architecture associated with an increase in the cellularity of the lamina propria and admixed acute and chronic inflammation). These lesions underlie IBD.

Interleukin-10 Autoantibodies and HLA-DRB1*01:03 in Inflammatory Bowel Disease

Neutralizing autoantibodies against interleukin-10 can result in a phenocopy of monogenic defects of interleukin-10 signaling in children and may be associated with inflammatory bowel disease (IBD). The allele HLA-DRB1*01:03 is the strongest genetic risk factor for ulcerative colitis.

Methods

We used a cellular interleukin-10 reporter assay and a confirmatory competitive enzyme-linked immunosorbent assay to assess neutralizing interleukin-10 autoantibodies in serum samples obtained from patients with IBD in the Oxford and U.K. IBD BioResource cohorts and from persons without IBD (controls). An in vitro cytokine-release bioassay was performed in a subgroup of patients to assess interleukin-10, interleukin-23, interleukin-1β, tumor necrosis factor, and interleukin-6. We performed HLA association analysis using imputation and high-resolution sequencing.

Conclusions

Neutralizing interleukin-10 autoantibodies were present in a subgroup of patients with IBD and were strongly associated with HLA-DRB1*01:03.

Inflammatory bowel disease (IBD) is linked to more than 300 genetic susceptibility loci that have been identified in genomewide association studies. One of the strongest and most consistent genetic associations is located within the HLA region. The allele HLA-DRB1*01:03 is the strongest genetic risk factor not only for susceptibility to ulcerative colitis but also for complicated phenotypes, including acute severe ulcerative colitis and an increased likelihood of surgical resection. However, the underlying pathogenic mechanism linking this HLA allele to disease remains unclear.

Interleukin-10 is an antiinflammatory cytokine essential for maintaining immune homeostasis in the gastrointestinal tract. Interleukin-10 is produced by monocytes, macrophages, regulatory T cells, and subsets of B cells, and its signaling in monocytes and macrophages is necessary to control inflammation. Autosomal recessive, loss-of-function variants in genes encoding interleukin-10 or its receptor (encoded by *IL10RA* and *IL10RB*) cause infantile-onset IBD. The *IL10RA* variant p.Pro295Leu (c.884C→T; reported odds ratios, 1.7 and 2.1) can contribute to adult-onset IBD.

We previously described two children with IBD who had neutralizing autoantibodies against interleukin-10 (anti–interleukin-10). In one child, anti–interleukin-10 titers and disease activity responded to B-cell–depleting anti-CD20 therapy. This finding exemplifies a phenomenon whereby acquired immune dysfunction caused by anticytokine autoantibodies can lead to phenocopies of inborn errors of immunity. The contribution of anti–interleukin-10 to the spectrum of Crohn's disease and ulcerative colitis in adolescents and adults is unclear. In this study, we measured the seroprevalence of anti–interleukin-10 in cohorts of patients with IBD and persons without IBD (controls) to investigate a genetic association between anti–interleukin-10 positivity and HLA.

HLA-DRB1 ist ein Gen, das für die Beta-Kette des **HLA-DR-Proteinkomplexes** kodiert, einem essenziellen Bestandteil des menschlichen Immunsystems. Dieses Protein gehört zum **Haupthistokompatibilitätskomplex der Klasse II** (MHC-II). Seine Hauptaufgabe besteht darin, dem Immunsystem körpereigene sowie fremde Eiweißfragmente (Antigene) zu präsentieren. Bestimmte Varianten dieses Gens (Allele) stehen in starkem Verdacht, das Risiko für verschiedene **Autoimmunerkrankungen** drastisch zu erhöhen.

Beta chain of the HLA-DR protein complex

Methods

Study Design

We investigated the seroprevalence of anti–interleukin-10 among patients with IBD and controls. Neutralization capacity was assessed by means of a cellular interleukin-10 reporter assay and a confirmatory competitive enzyme-linked immunosorbent assay (ELISA). A cytokine release assay was performed in a subgroup of patients, and HLA association studies were conducted.

Patient Cohorts and Ethics

We analyzed data from patients with IBD from two main cohorts: the Oxford cohort (which comprised the Oxford IBD Discovery cohort and the Oxford IBD Validation cohort) and the U.K. IBD BioResource cohort. These cohorts were compared with persons without IBD (controls); pediatric controls were from the Oxford subset of the Antibody Diagnostics in Paediatric Coeliac Disease study, and adult controls were health care workers recruited as part of the Protective Immunity through T Cells in Healthcare Workers (PITCH) program.

Interleukin-10 Autoantibody Neutralization Assays

In the Oxford IBD Discovery cohort, we used a set of five assays to detect IgG class anti–interleukin-10 neutralizing autoantibodies.

Genetic Analysis

HLA haplotyping was performed in a subgroup of the Oxford cohorts and the U.K. IBD BioResource cohort on the basis of HLA imputation of high-resolution genotyping data with the use of a multiancestry HLA imputation reference panel.

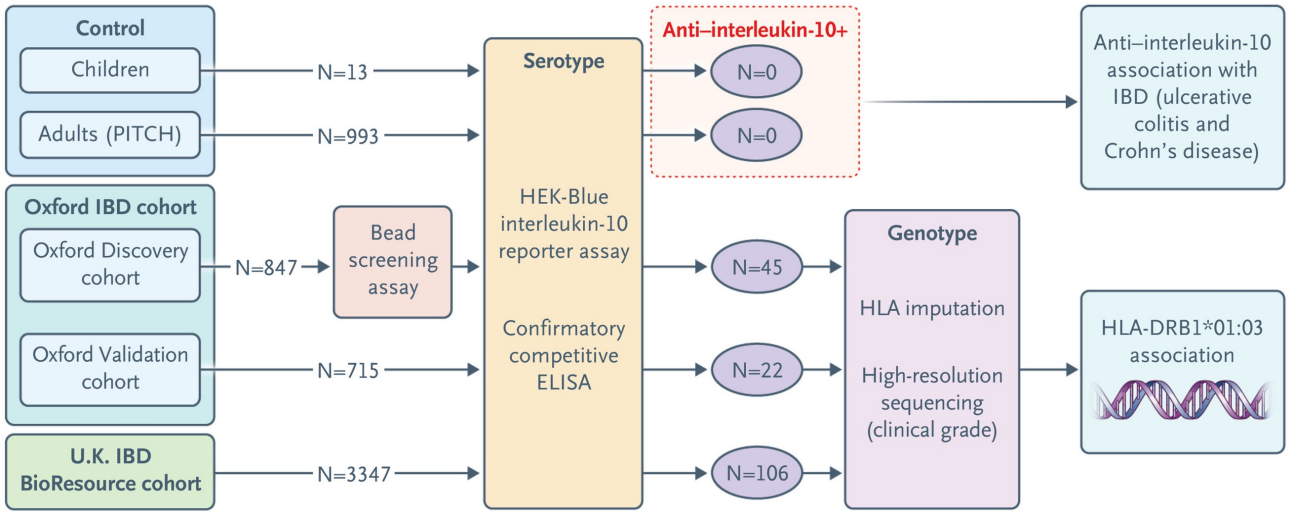

Study Flow Diagram.

Shown is the design of the study, including the cohorts of patients with inflammatory bowel disease (IBD) and persons without IBD (controls), serum testing, and genotyping. Data from two main cohorts of patients were used: the Oxford cohort (which comprised the Oxford IBD Discovery cohort and the Oxford IBD Validation cohort) and the U.K. IBD BioResource cohort. Pediatric controls were from the Oxford subset of the Antibody Diagnostics in Paediatric Coeliac Disease study, and adult controls were health care workers recruited as part of the Protective Immunity through T Cells in Healthcare Workers (PITCH) program. ELISA denotes enzyme-linked immunosorbent assay, and HEK human embryonic kidney.

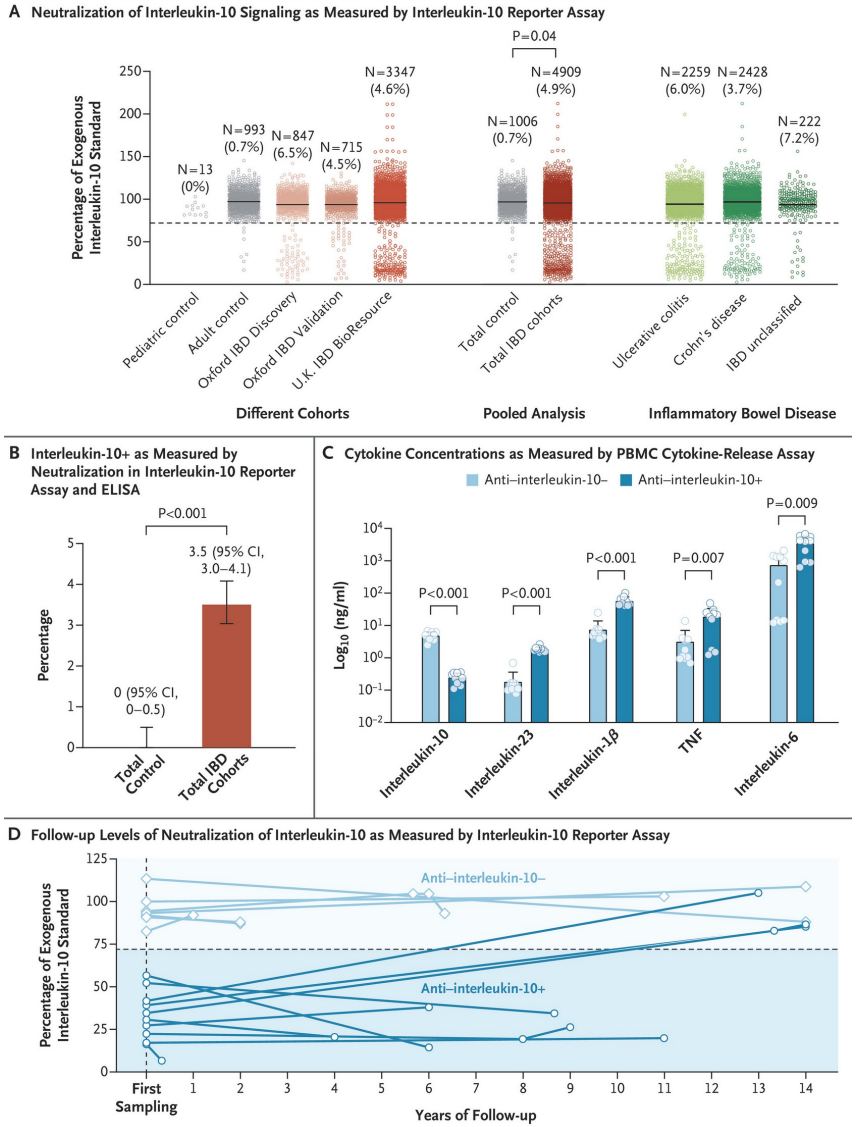

Association of Neutralizing Anti–Interleukin-10 Autoantibody with IBD.

Neutralization of interleukin-10 signaling was measured by an interleukin-10 reporter assay (HEK-Blue IL-10) (Panel A). Serum was incubated with exogenous recombinant interleukin-10 (50 ng per milliliter), and reporter activity (secreted alkaline phosphatase) is shown as a percentage of the interleukin-10 standard. Analyses were performed according to cohort (separately and pooled) and IBD subtype (ulcerative colitis, Crohn's disease, or IBD unclassified). The dashed line indicates the neutralization threshold, and solid lines indicate means. In the pooled analysis, higher levels of interleukin-10–neutralization activity were seen among the 4909 patients than among the 1006 controls (P=0.04 by the Mann–Whitney U test). The percentages of patients and controls (pooled cohorts) with anti–interleukin-10 positivity, as defined by neutralization in the interleukin-10 reporter assay and neutralization in the competitive ELISA, are shown in Panel B (P<0.001 by the chi-square test). I bars indicate the 95% confidence interval. The results of a cytokine-release assay of peripheral-blood mononuclear cells (PBMCs) from a healthy donor are shown in Panel C. Cells were stimulated with lipopolysaccharide in the presence of patient serum, and the concentrations of various cytokines (interleukins 10, 23, 1β, and 6 and tumor necrosis factor [TNF]) are shown according to anti–interleukin-10 status. In the bar graphs, dots indicate individual samples, bars indicate means, and T bars indicate standard deviations. P values were obtained by means of multiple Mann–Whitney U tests with the use of adjustment for the Benjamini–Hochberg false discovery rate. Panel D shows follow-up levels of neutralization of interleukin-10 signaling indicated by the interleukin-10 reporter assay (HEK-Blue IL-10) over time among 7 patients who were negative for anti–interleukin-10 at baseline (diamonds) and among 10 patients who were positive for anti–interleukin-10 (dots). Diamonds and dots indicate individual patient samples over time, and the dashed line indicates the neutralization threshold.

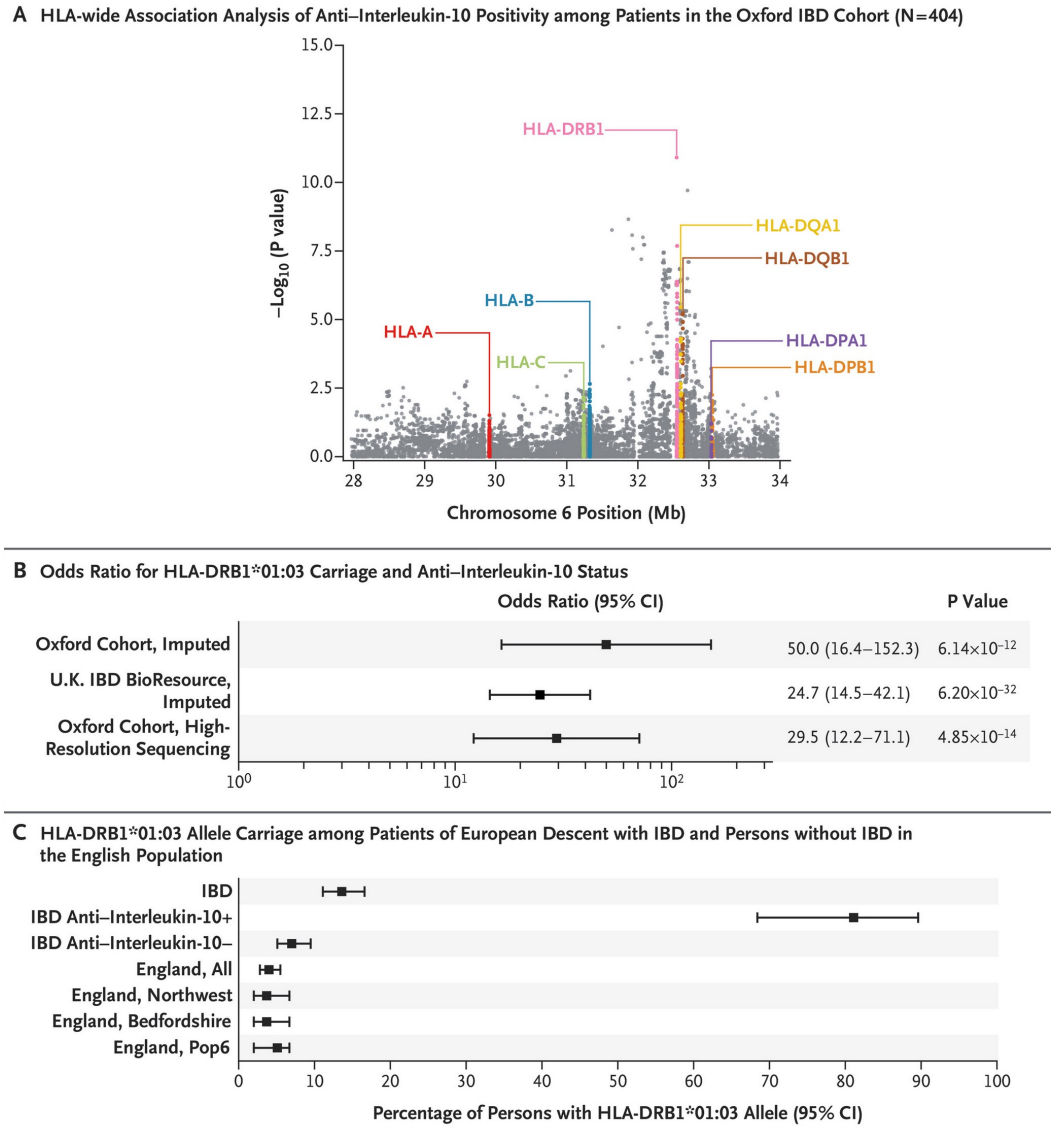

Association of Anti–Interleukin-10 and HLA-DRB1*01:03.

Panel A shows the HLA-wide association analysis of anti–interleukin-10 positivity among 404 patients from the Oxford IBD cohort who underwent genotyping. Shown are genomic positions of chromosome 6 (genome build 37) and $-\log_{10}$ P values obtained from two-sided regression analyses for single-nucleotide polymorphisms (gray dots) and classical HLA alleles. Logistic-regression model testing of association with biallelic variant alleles (counts of presence vs. absence), with sex and age included as fixed-effect covariates, was conducted. Panel B shows the odds ratios for HLA-DRB1*01:03 presence and anti–interleukin-10 positivity. Analyses were performed in a subgroup of the Oxford IBD cohort and the U.K. IBD BioResource cohort, with the incorporation of imputed data and high-resolution sequencing data (the Oxford IBD cohort). Panel C shows the percentage of persons with HLA-DRB1*01:03 carrier status among both patients with IBD (Oxford IBD cohort) and persons without IBD who were of European descent in the English population (with general population frequencies derived from https://allelefrequencies.net).[17] Details regarding the four English cohorts (all, Northwest, Bedfordshire, and Pop6) are provided in the Supplementary Appendix.

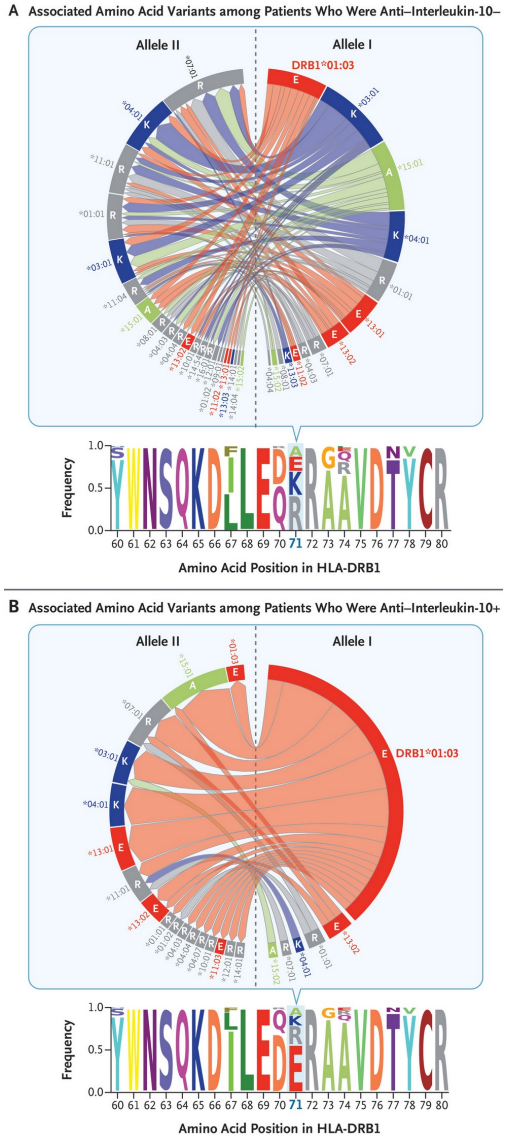

HLA-DRB1 Allele Pairing and Amino Acid Composition.

Shown are Circos diagrams and sequence logos, which illustrate HLA-DRB1 allele pairing and amino acid composition among 234 patients in the Oxford cohort, with stratification according to anti–interleukin-10 autoantibody status (negative [Panel A] and positive [Panel B]). In the Circos plots, the circumferential length of the arc corresponds to the frequency of each HLA-DRB1 allele, and the width of the ribbon corresponds to the frequency of each specific genotype pairing. The central dashed line bisects the plot into allele I (right hemisphere) and allele II (left hemisphere). The sequence logos depict the frequency of amino acids at positions 60 to 80 of the HLA-DRB1 molecule within each group, with the size of the letter for each amino acid indicating the frequency of each amino acid residue at that position. The color scheme for the Circos plots corresponds to the amino acid at position 71.

Discussion

The results of our study challenge the current paradigm of IBD in several areas. Neutralizing anti–interleukin-10 autoantibodies were identified in 3.5% of the patients with IBD in our study, thus defining an immunologically distinct subgroup. The genetic association between HLA-DRB1*01:03 and anti–interleukin-10 autoreactivity provides mechanistic insight into one of the strongest known genetic susceptibility factors for IBD, with possible diagnostic, prognostic, and therapeutic implications.

Our discovery of anti–interleukin-10 in both children and adults with IBD adds to the emerging understanding of humoral autoimmunity as a pathogenic mechanism. Anti–interleukin-10 is associated with an acquired phenocopy of inborn errors of the interleukin-10 pathway and has been modeled in mice receiving interleukin-10–neutralizing antibodies. Our in vitro data show that blocking of interleukin-10 amplifies proinflammatory responses by means of IBD-relevant cytokines, as occurs in inborn errors of the interleukin-10 pathway. Although epithelial, phagocytic, T-cell, and cytokine defects have been widely studied in the pathogenesis of IBD, the contribution of B-cell responses and humoral immunity has been less clear. Single-cell sequencing has highlighted the involvement of B-cell and plasma-cell responses in persons with ulcerative colitis. Autoantibodies have previously been described against a spectrum of autoantigens and microbial antigens in patients with IBD as disease-associated biomarkers, but anti–interleukin-10 appears to be likely to play a pathogenic and disease-modifying role in IBD.

Die **X-chromosomale Retinoschisis (XLRS)** ist eine seltene, genetisch bedingte Netzhauterkrankung, die fast ausschließlich Männer betrifft und eine der häufigsten Ursachen für makuläre Degeneration im Kindes- und Jugendalter darstellt. Sie ist durch eine fortschreitende **Spaltung (Schisis) der Netzhautschichten** charakterisiert, was zu einer zunehmenden Beeinträchtigung der Sehkraft führt.

Ursachen und Genetik

Die Erkrankung basiert auf **Mutationen im *RS1*-Gen**, welches auf dem X-Chromosom liegt.

•**Funktion des Gens**: Das Gen kodiert das Protein *Retinoschisin*. Dieses fungiert wie ein zellulärer Klebstoff, der die einzelnen Schichten der Netzhaut zusammenhält.

•**Erbgang**: Da die Vererbung **X-chromosomal-rezessiv** erfolgt, bricht die Krankheit bei Männern (XY) aus, wenn ihr einziges X-Chromosom mutiert ist. Frauen (XX) besitzen meist ein zweites, gesundes X-Chromosom, welches den Defekt kompensiert; sie sind in der Regel beschwerdefreie Überträgerinnen (Konduktorinnen).

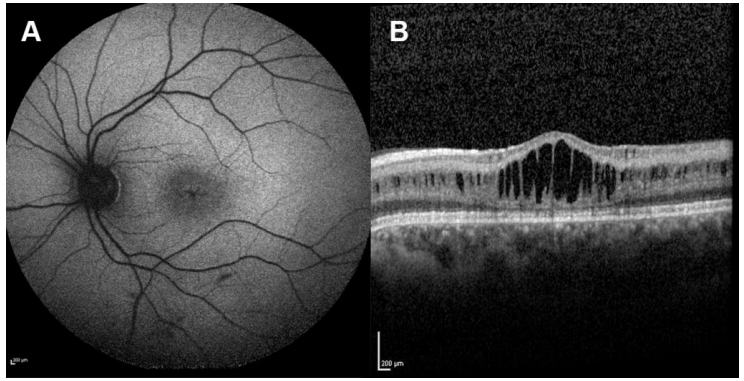

Subretinal Gene Therapy for X-Linked Retinoschisis

X-linked retinoschisis is a recessive disease characterized by progressive macular degeneration and vision loss due to pathogenic variation in *RS1*. We administered a single subretinal injection of an AAV8 vector containing human *RS1* complementary DNA (scAAV8-hRS1) into one eye of patients 5 to 18 years of age who had X-linked retinoschisis. The primary end point was safety during the 52-week period after injection. Secondary end points included the change from baseline to week 52 in the best corrected visual acuity (BCVA), retinal structure (assessed with swept-source optical coherence tomography; SS-OCT), the function of photoreceptor and bipolar cells (assessed with full-field electroretinography), and macular sensitivity to light (assessed with microperimetry).

Conclusions

In this study of subretinal gene therapy with scAAV8-hRS1 in 12 patients with X-linked retinoschisis, there were no reports of adverse events of grade 3 or higher or ocular inflammation. Further clinical testing of scAAV8-hRS1 is warranted. (Funded by the National Natural Science Foundation of China and others; Chinese Clinical Trial Registry number, ChiCTR2300076682.)

X-linked retinoschisis (Online Mendelian Inheritance in Man [OMIM] number, 312700) is a recessive retinal disorder that is characterized by loss of vision, macular schisis, and a marked reduction in the b-wave amplitude on full-field electroretinography. (The b-wave amplitude is a measure primarily of the function of ON bipolar cells, which are second-order retinal neurons that depolarize in response to light increments and transmit visual signals from photoreceptors to downstream retinal neurons.) The disease predominantly affects males and has a prevalence ranging from 1 in 25,000 males to 1 in 5000 males worldwide. X-linked retinoschisis results from mutations at Xp22.13 in the *RS1* gene (OMIM number, 300839), which encodes an extracellular adhesion protein critical to retinal structure and photoreceptor–bipolar cell signaling. Loss of vision typically starts in the first decade of life, with a best corrected visual acuity (BCVA) ranging from 20/20 to 20/600 (0.00 to 1.48 logarithm of the minimum angle of resolution [logMAR]). The BCVA deteriorates to 20/200 (1.00 logMAR) by the sixth or seventh decade of life owing to outer retinal atrophy.

To overcome the limited retinal transduction seen in previous trials of intravitreal X-linked retinoschisis gene therapy, we adopted a subretinal delivery approach, which should provide greater exposure of photoreceptor cells to AAV than intravitreal delivery. The investigational product, scAAV8-hRS1, is a self-complementary AAV8 vector that encodes a codon-optimized human *RS1* transgene driven by the rhodopsin kinase promoter for selective expression in photoreceptors. We report 1-year safety and efficacy outcomes of a single-group study of subretinally delivered scAAV8-hRS1 in pediatric patients with X-linked retinoschisis.

The last author (an experienced retinal surgeon) removed the central core of the vitreous humor by means of pars plana vitrectomy using a 25-gauge, three-port vitrectomy system. The scAAV8-hRS1 vector was to be administered according to a 3+3 design in escalating doses of 7.5×10^{10}, 1×10^{11}, and 1.5×10^{11} vg. Patients were to receive their designated dose in a total injection volume of 100 µL administered subretinally under intraoperative optical coherence tomographic (OCT) guidance. The target injection site was temporal to the macula, between the superior and inferior retinal vascular arcades, with the injection bleb covering the macular region

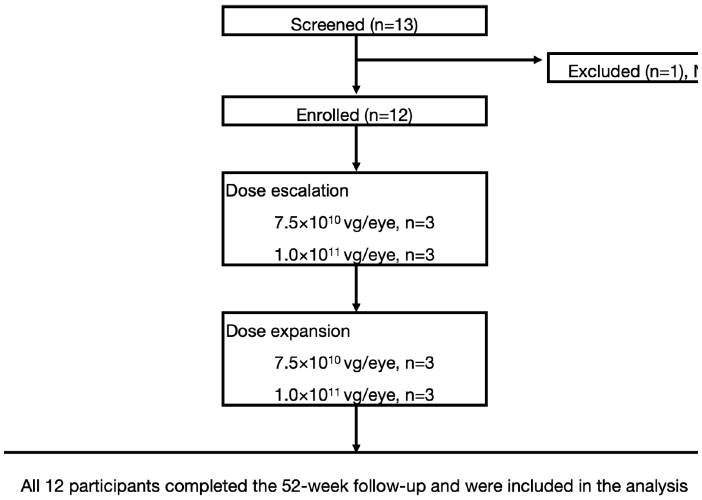

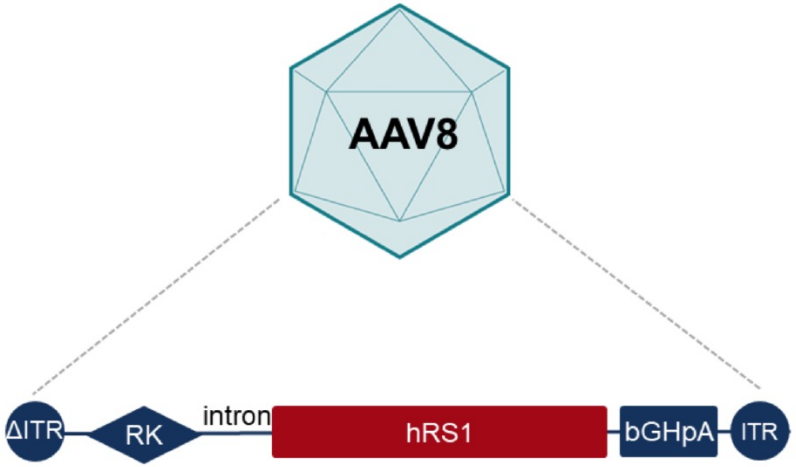

Schematic representation of scAAV8-hRS1 construct design.

Demographic and Clinical Characteristics at Baseline.

Characteristic	scAAV8-hRS1, 7.5×10^{10} vg						scAAV8-hRS1, 1×10^{11} vg					
	Patient 1	Patient 2	Patient 3	Patient 7	Patient 8	Patient 9	Patient 4	Patient 5	Patient 6	Patient 10†	Patient 11	Patient 12†
Age — yr	7	6	7	10	7	6	8	11	7	5	5	8
Ethnic group‡	Han	Han	Han	Han	Han	Gelao	Han	Han	Han	Han	Han	Han
Anti-AAV8 NAb titer	<1:5	1:5	<1:5	1:200	<1:5	1:200	1:35	<1:5	<1:5	1:5	<1:5	<1:5
RSI genotype	Exon 6, c.577C→T (p.Pro 193Ser)	Exon 4, c.304C→T (p.Arg 102Trp)	Exon 4, c.216G→T (p.Glu 72Asp)	Exon 5, c.421C→T (p.Arg 141Cys)	Exon 5, c.436G→A (p.Glu 146Lys)	chrX: g.18,671,528 to 18,675,852del	Exon 4, c.305G→A (p.Arg 102Gln)	Exon 4, c.214G→A (p.Glu 72Lys)	Exon 4, c.214G→A (p.Glu 72Lys)	Exon 4, c.214G→A (p.Glu 72Lys)	Exon 4, c.304C→T (Arg 102Trp)	Exon 5, c.421C→T (Arg 141Cys)
Treated eye	Left	Left	Left	Left	Right	Right	Left	Left	Left	Right	Right	Left
BCVA — no. of letters												
Treated eye	19	48	59	17	58	53	37	37	56	56	50	58
Untreated eye	52	59	59	63	62	61	72	72	62	52	54	38

Adverse Events during Follow-up.

Adverse Event	Grade	scAAV8-hRS1, 7.5×10^{10} vg (N=6)		scAAV8-hRS1, 1×10^{11} vg (N=6)	
		Patients	Events	Patients	Events
		no. (%)	*no.*	*no. (%)*	*no.*
Ocular adverse events					
Ocular hypertension†	2	4 (67)	5	5 (83)	8
Ocular hypotension†	2	4 (67)	4	4 (67)	4
Corneal trauma	2	1 (17)	1	0	0
Allergic conjunctivitis	2	1 (17)	1	0	0
Macular hole	2	0	0	1 (17)	1
Conjunctival hyperemia	1	4 (67)	4	1 (17)	1
Conjunctival hemorrhage	1	3 (50)	3	2 (33)	2
Eye pain	1	1 (17)	1	1 (17)	1
Retinal atrophy	2	1 (17)	1	0	0
Strabismus	2	0	0	1 (17)	1
Retinal nerve fiber layer thinning	2	0	0	2 (33)	2
Systemic adverse events					
Upper respiratory tract infection	2	2 (33)	3	3 (50)	4
Acute bronchitis	2	0	0	1 (17)	1
Hematuria	1	1 (17)	1	0	0
Asymptomatic sinoatrial-to-atrial wandering pacemaker rhythm	1	1 (17)	1	0	0
Asymptomatic accelerated junctional rhythm	1	0	0	1 (17)	1
Asymptomatic incomplete interference atrioventricular dissociation	1	0	0	1 (17)	1
Asymptomatic intraventricular aberrant conduction	1	0	0	1 (17)	1
Headache	2	0	0	1 (17)	1
Nasal congestion	2	0	0	1 (17)	1
Hyperuricemia	1	0	0	1 (17)	1

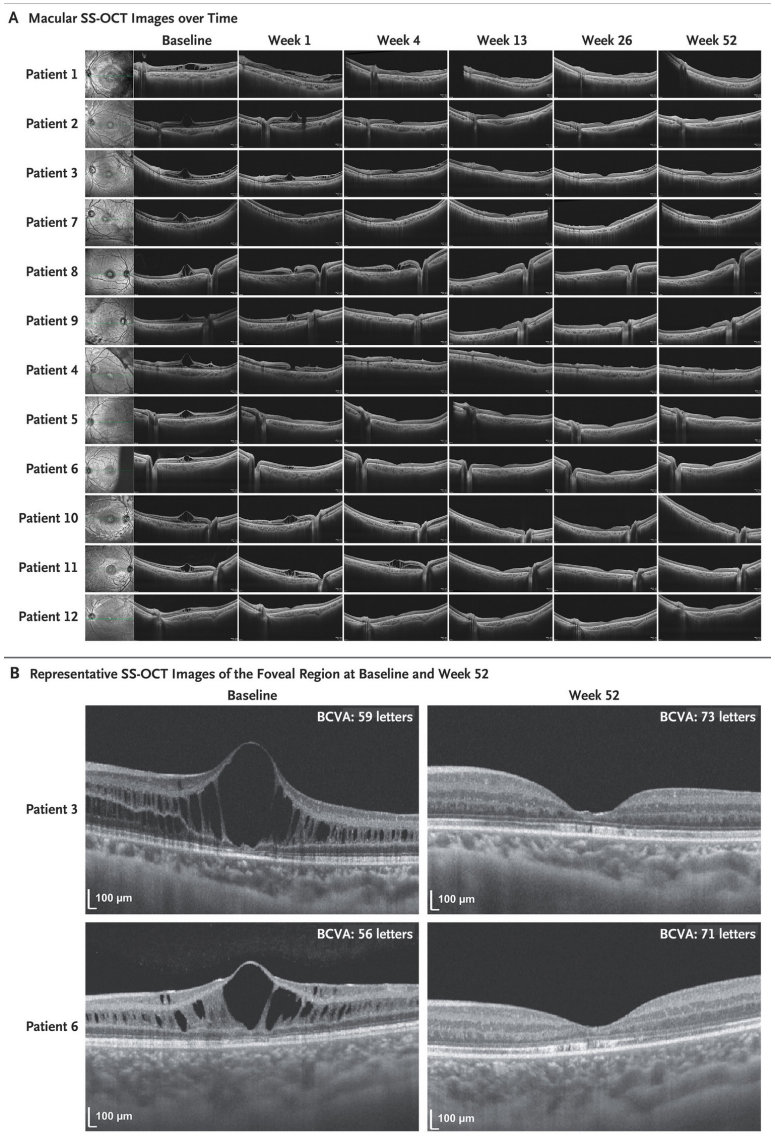

Macular Imaging of Treated Eyes over Time.

Panel A shows macular swept-source optical coherence tomographic (SS-OCT) images at baseline and after subretinal injection of an AAV8 vector containing human *RS1* complementary DNA (scAAV8-hRS1) into one eye of patients with X-linked retinoschisis. Patients 1 to 3 and 7 to 9 received a dose of 7.5×10^{10} vector genomes (vg), and Patients 4 to 6 and 10 to 12 received a dose of 1×10^{11} vg. The scanning procedure involved acquisition of 33 line scans through the macula to ensure consistent scanning at the same location across visits. Each image represents a single line scan across the fovea. Gradual closure of the schisis cavity occurred over time; the foveal contour started to emerge by week 4, and the schisis cavity was completely closed by week 13. A macular hole was evident in Patient 4 at week 4 and was successfully repaired with surgery. Panel B shows representative SS-OCT images of the schisis cavity in the macular foveal region of the treated eye at baseline and resolution of the cavity at week 52. Best corrected visual acuity (BCVA) was assessed as letters on the Early Treatment Diabetic Retinopathy Study chart (scores range from 0 to 100 letters, with higher scores indicating better visual acuity).

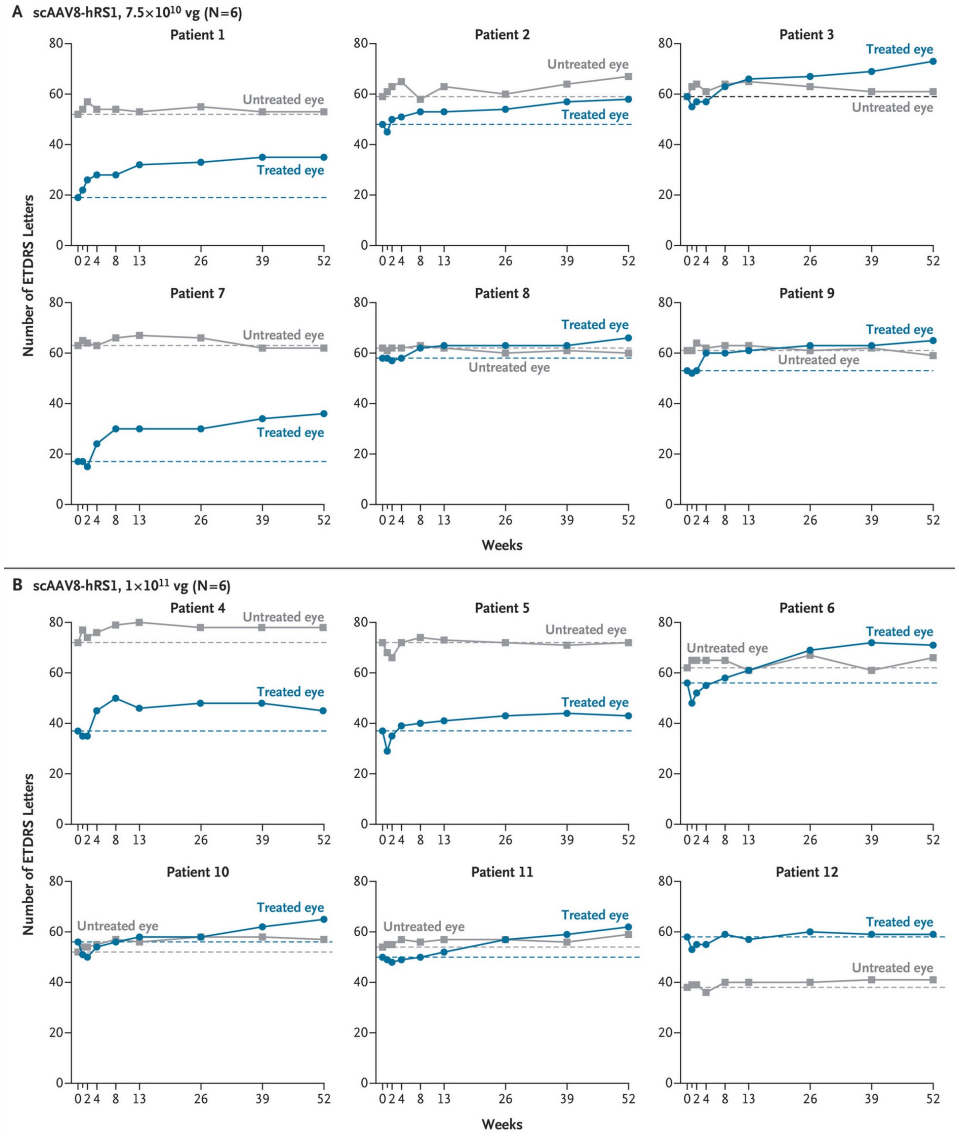

Best Corrected Visual Acuity over Time.

Shown is the BCVA of the treated and untreated eyes in patients in the 7.5×10^{10} vg cohort (Panel A) and those in the 1×10^{11} vg cohort (Panel B). All treated eyes had a BCVA at baseline of up to 63 letters. Increases from baseline in the BCVA indicate improvement, and decreases from baseline indicate worsening. A change of 10 letters is considered to be the minimal clinically meaningful difference.[14] Blue dashed lines indicate baseline values for treated eyes, and gray dashed lines baseline values for untreated eyes. The black dashed line in the graph for Patient 3 indicates the baseline value for both eyes.

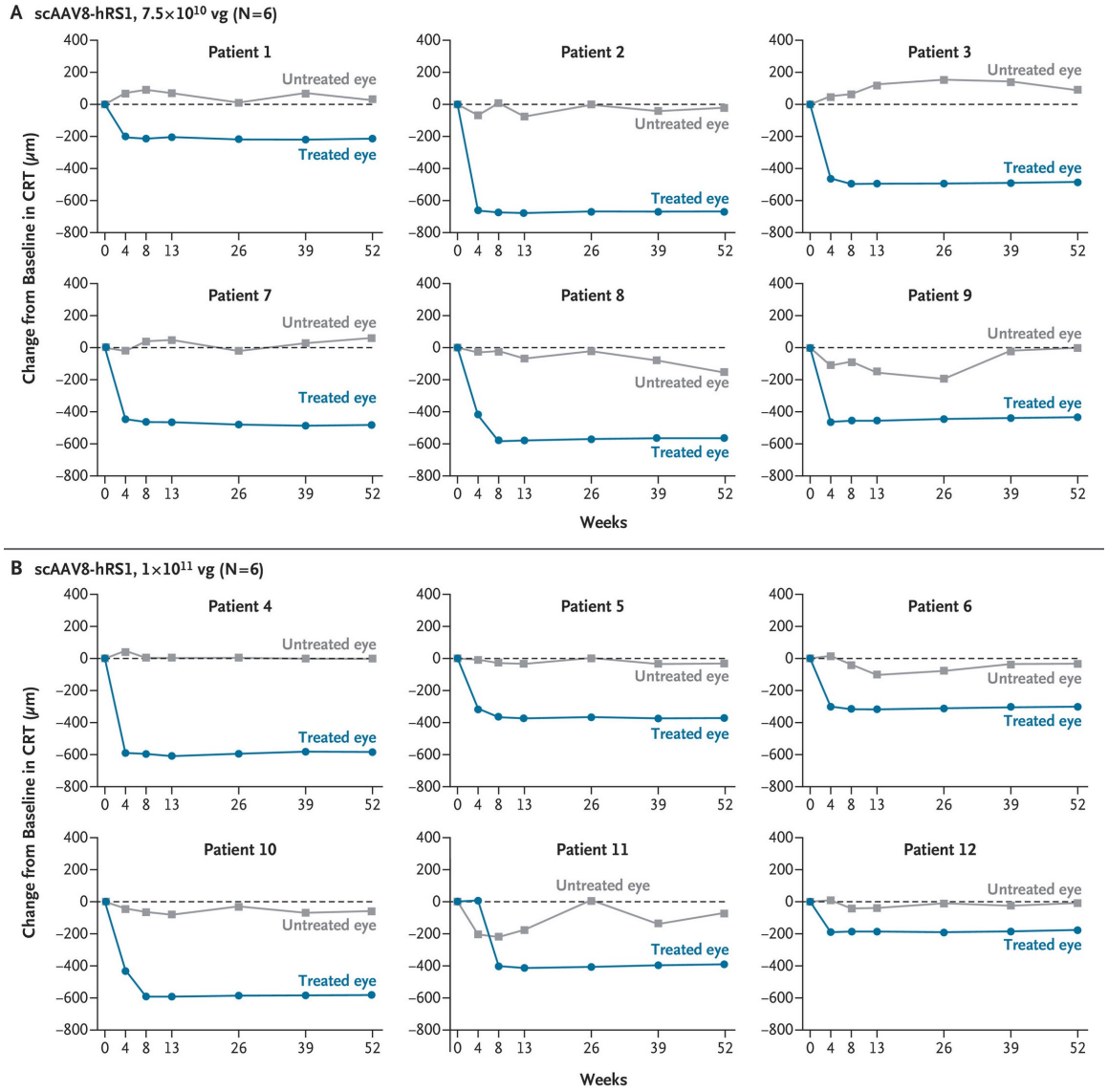

Change from Baseline in Central Retinal Thickness.

Shown are changes from baseline (dashed lines) in central retinal thickness (CRT) in the treated and untreated eyes, as assessed with SS-OCT imaging, in the 7.5×10^{10} and 1×10^{11} vg cohorts.

Discussion

In the current study involving 12 patients with X-linked retinoschisis who received a subretinal injection of scAAV8-hRS1, we observed 56 adverse events of grade 1 or 2 but no adverse events of grade 3 or higher during the 52-week follow-up period. These findings are consistent with those from previous trials of subretinal gene therapy. We did not detect inflammatory responses in any of the patients. A macular hole, which was related to surgery, occurred in 1 patient. Given the thin maculae in patients with X-linked retinoschisis, minimal macular manipulation is advised, especially in children, who have strong vitreomacular adhesion. No patients had retinal detachment.

Ocular hypertension was observed in 9 patients; this finding is consistent with pediatric sensitivity to glucocorticoids. All cases of abnormal intraocular pressure resolved without sequelae. As in other gene-therapy studies, we observed relatively high neutralizing antibody titers after treatment. However, vector shedding was undetectable by week 4, and none of the patients had a T-cell response to the AAV8 capsid or RS1 protein.

Within the confines of these limitations, subretinal administration of a scAAV8-hRS1 vector was safe and accompanied by improvement in retinal structure in patients with X-linked retinoschisis. These results support further clinical testing of the scAAV8-hRS1 vector in the treatment of X-linked retinoschisis.

Antidotes for Anticoagulation Reversal

Summary

The global rise in anticoagulant use has increased the number of major bleeding events that warrant timely and effective pharmacologic reversal. Reversal strategies should be informed by the pharmacodynamic and pharmacokinetic features of the anticoagulant and antidote, regulatory indications, quality of evidence, patient-specific factors, and availability of treatment options. Protamine sulfate neutralizes unfractionated heparin, whereas no specific antidotes exist for low-molecular-weight heparins or fondaparinux. Four-factor prothrombin complex concentrates effectively reverse vitamin K antagonists. Idarucizumab specifically reverses dabigatran, although delayed dabigatran rebound can occur. Andexanet alfa targets direct oral factor Xa inhibitors, but uncertainties regarding the efficacy–safety balance, monitoring, rebound, perioperative use, and cost have prompted off-label use of four-factor prothrombin complex concentrates, for which stronger evidence is needed. Key challenges remain, including determination of appropriate dosing, standardization and validation of laboratory monitoring, mitigation of thrombotic risk, and development of guidelines for perioperative treatment. Emerging agents aim to broaden targets and improve safety. Building high-quality evidence remains essential to advancing global, patient-centered anticoagulant and hemostatic care.

Antidotes for Anticoagulation Reversal

- Protamine remains the unfractionated heparin–specific antidote; however, a determination of appropriate dosing and monitoring requires further studies. No antidotes are approved for neutralizing low-molecular-weight heparins, fondaparinux, or danaparoid.
- In bleeding associated with vitamin K antagonists, four-factor prothrombin complex concentrates with vitamin K achieve faster correction of the international normalized ratio than three-factor formulations and fresh-frozen plasma, with better hemostasis and safety than fresh-frozen plasma. The efficacy and safety of fixed doses as compared with standard doses of four-factor prothrombin complex concentrates remain uncertain.
- Idarucizumab and andexanet alfa provide specific, rapid, nearly complete pharmacodynamic reversal of uncontrolled or life-threatening bleeding with dabigatran and factor Xa inhibitors, respectively. Andexanet elicits regulatory concerns owing to early thrombosis risk and is not approved for perioperative use, with a warning regarding cardiac surgery. Off-label use of four-factor prothrombin complex concentrates provides safe hemostatic support to the reversal of bleeding associated with factor Xa inhibitors. Head-to-head comparisons of four-factor prothrombin complex concentrates with each specific antidote are lacking.
- The priorities for future study include the development of safer antidotes; standardized, clinically validated laboratory assays; and enhanced understanding of rebound effects. Randomized studies with clinical end points and adequate follow-up are needed.

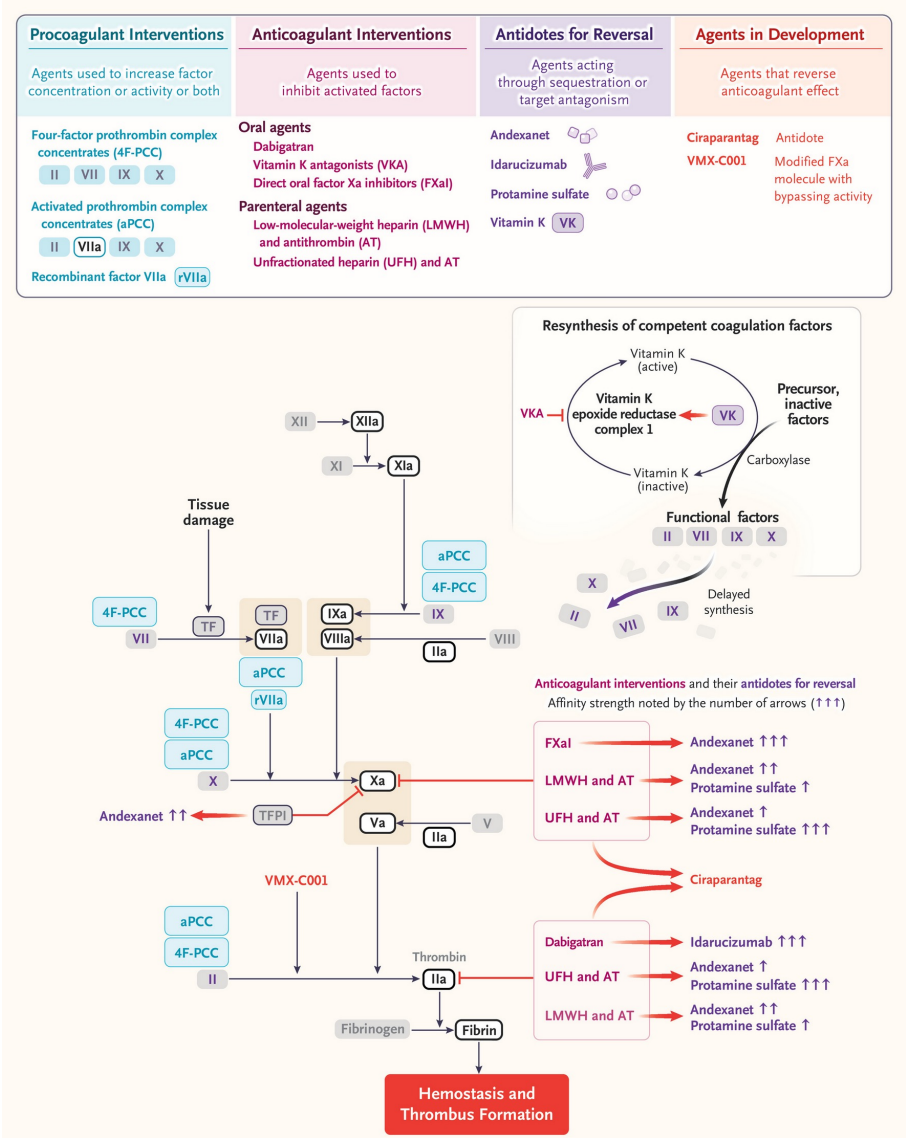

Mechanisms of Action of Specific and Nonspecific Antidotes to Anticoagulant Drugs.

Specific antidotes directly neutralize anticoagulants by means of molecular-specific recognition and selective binding to the agents, whereas nonspecific functional antidotes, including prothrombin complex concentrate, restore hemostasis in a way that is not dependent on the pharmacodynamic features of the anticoagulant. Four-factor prothrombin complex concentrates (4F-PCCs) restore coagulation by supplementing vitamin K–dependent coagulation factors (II, VII, IX, and X), resulting in a variable support of hemostasis, regardless of the anticoagulant's pharmacodynamics; activated 4F-PCCs contain factor VII in the activated form (FVIIa), with bypassing activity through direct, tissue-factor–dependent activation of factor X (FX) and factor IX (FIX), resulting in a rapid burst of thrombin generation; recombinant FVIIa has a similar bypassing activity. As shown on the right side of the figure, anticoagulant drugs have different competing affinities for their coagulation targets and for their specific antidotes. Vitamin K competes with vitamin K antagonists for the vitamin K epoxide reductase complex 1 binding site, enabling gradual resynthesis of competent coagulation factors and correction of the international normalized ratio (INR). Direct factor Xa inhibitors (FXaIs) have higher affinity for andexanet alfa than for factor Xa; the heparin–antithrombin complex also binds andexanet and induces transient heparin resistance. Andexanet binding and inhibition of tissue factor (TF) pathway inhibitor (TFPI) may increase thrombin generation and prothrombotic risk; however, andexanet is no longer marketed in the United States as of December 22, 2025.[38] Unfractionated heparin (UFH) has a very high chemical affinity for protamine sulfate, whereas low-molecular-weight heparin (LMWH) has a low affinity. Dabigatran has a higher affinity for idarucizumab than for thrombin. Ciraparantag, currently in development, can bind multiple oral and parenteral drugs with high affinity. VMX-C001 is a bypassing agent in development.

Characteristics of Available and Emerging Antidotes to Anticoagulant Agents.

Antidote	Composition and Pharmacodynamic Features	Pharmacokinetic Features††	Administration	Approved Indications	Risks and Warnings	Reference Assay
Specific						
Protamine sulfate	Polycationic arginine-rich peptides (approx. 32 AA; MW, approx. 4.5 kDa) Selective binding to UFH forming inert complexes Partial LMWH neutralization (anti-FIIa activity)	Vd: approx. 60 ml/kg Onset: <5 min Half-life: 5–7 min Clearance: hepatic for heparin–protamine complexes, renal for free drug, but no dose adjustment required in kidney disease	Slow IV infusion: ≤1 mg per 100 IU (or 1 mg) UFH considering UFH half-life (30–90 min, nonlinearly dose-dependent)	UFH reversal (FDA, EMA) Not approved for LMWH	Risks: hypotension (1.8–12.4%), pulmonary hypertension (0.6–15.8%), anaphylaxis (0.14–0.7%), fatal ventricular arrhythmias (<0.1%) Prohemostatic effect at high doses Caution with previous exposure and in pregnancy	ACT (high UFH levels) aPTT–anti-FXa (low UFH levels) Viscoelastic assays under study
Vitamin K1	Naphthoquinone (MW, approx. 450.7 Da) Selective competition with VKA at VKORC1 (Kd, ≤10 nM; warfarin Ki, approx. 5 nM) restoring γ-carboxylation of vitamin K–dependent factors	Vd: approx. 290 ml/kg Onset of reversal dependent on coagulation factor, not antidote half-life Half-life: approx. 2 hr Clearance: renal and fecal	IV (5–10 mg) or oral (1–10 mg), depending on INR and bleeding	VKA-associated bleeding or high INR (EMA, FDA)	IV route: risk of anaphylactoid reactions Use the lowest effective dose Avoid intramuscular route Safe in pregnancy	INR Vitamin K–dependent factor levels
Andexanet alfa	Recombinant, modified, FXa decoy (S419A + GLA domain deletion, MW, approx. 40 kDa) Reversible binding of direct FXaI (similar Kd for native and decoy FXa) Binds heparin–AT complex Off-target binding to TFPI	Vd: approx. 75 ml/kg Onset: ≤5 min Half-life: approx. 4–7 hr Clearance: hepatic	IV bolus + 2-hr infusion Dose based on FXaI type, dose, and timing since last intake	Uncontrolled or life-threatening bleeding with apixaban, rivaroxaban (EMA conditional authorization, withdrawn from the U.S. market)‡‡ No approval for edoxaban, LMWH, fondaparinux	Thromboembolic risk Transient UFH resistance Early FXaI rebound Not recommended in pregnancy	Interferes with commercial anti-FXa assays Point-of-care viscoelastic assays under study
Idarucizumab	Humanized mouse Fab fragment (MW, approx. 47.8 kDa) Specific for dabigatran (Kd approx. 2 pM; Kd of dabigatran for thrombin 0.7 nM)	Vd: 60 ml/kg (dabigatran Vd higher than that with idarucizumab by approx. factor of 6) Onset: <5 min Half-life: approx. 10 hr Clearance: renal with prolonged half-life if renal disease	IV: 5 g (2×2.5 g boluses)	Uncontrolled or life-threatening bleeding or emergency surgery with receipt of dabigatran (EMA, FDA)	Late dabigatran rebound (from 24 hr) Contraindicated in pregnancy	ECT dTT aPTT (less sensitive)
Nonspecific						
4-Factor PCC	Plasma-derived concentrate restoring vitamin K–dependent FII, FVII, FIX, FX Protein C, protein S, UFH, AT may be present Final plasma coagulation factor levels up to 1.5 times that of the physiologic concentrations	Vd: variable, from 45±10.7 ml/kg of FVII to 114.3±54.6 ml/kg of FIX Onset: INR correction detectable by 30 min after infusion Half-life: variable (FVII 5±1.9 hr, FIX 42.4±41.6 hr, FX 31.8±8.7 hr, FII 60.4±21.5 hr) Clearance: hepatic	Approved IV dose: 25–50 FIX IU/kg adjusted on INR (max 5000 IU) Fixed dose under investigation	VKA reversal (EMA, FDA) in major bleeding and before surgery or procedures Off-label for DOACs	UFH-containing preparations contraindicated if history of HIT or in DIC Caution if recent (3 mo) major thrombotic event Pregnancy and lactation: only if benefits outweigh risks	INR (VKA) Coagulation factor levels PT (FXaI, depending on reagents) aPTT (dabigatran only) Thrombin generation (all FXaI)
Activated PCC	Plasma-derived concentrate of FVIIa (approx. 1 IU/mg) + FII, IX, X Bypasses intrinsic pathway by FX activation Plasma FVIIa levels increased by a factor of 25 to 100 (based on 50 IU/kg dose in a 70-kg person)§§	Vd: 45–114 ml/kg Onset: 10–30 min Half-life: variable according to the single components Clearance: hepatic	IV Usual dose, 500 IU for INR <5 and 1000 IU for INR ≥5 for VKA reversal; 10–50 IU/kg for DOAC reversal	Off-label for all anticoagulants	High risk of major thrombosis, especially >200 IU/kg/day or in high-risk patients Avoid in pregnancy	INR (for VKA) PT (reagent dependent) aPTT (dabigatran only) Thrombin generation (FXaI)
Recombinant FVIIa	Recombinant FVIIa (MW, approx. 50 kDa) Direct activation of FX FVIIa levels increase by a factor of up to 1500 (dose of 90 μg/kg in a 70-kg person)	Vd: 103 ml/kg Onset: within minutes Half-life: 2.3 hr in patient with bleeding Clearance: hepatic	IV Off-label dose ≤90 μg/kg	Off-label for all anticoagulants	High dose-dependent risk of thrombosis, reduced if <20 IU/kg Avoid in pregnancy	PT (reagent-dependent for FXaI)
Ciraparantag	Synthetic cationе based on the arginine ring (MW, 512 Da) Electrostatic binding to UFH, LMWH, and DOACs	Vd: approx. 300 ml/kg Onset: within minutes Half-life: 12–19 min Clearance: renal	IV, dose under investigation	In development	Off-target binding to proteins and relevant drug interactions possible Safety to be established	Whole-blood clotting time (experimental)
VMX-C001	Modified, recombinant, human FX (MW, approx. 63 kDa) Selective restoration of FX activity independent of FXaI	Vd: approx. 130 ml/kg Onset: within minutes Half-life: 20.5–30.2 hr Clearance: possibly hepatic	IV, dose under investigation	In development	Safety not yet established	Diluted PT Diluted Russell viper venom time

Andexanet Alfa as Compared with PCC.

Study or Trial and Year	Design	Population and Intervention	End Points	Key Results
Diener et al., 2025[25]	Single-group, prospective	137 patients with ICH (47.4% men; mean age, 80 yr; 65.7% apixaban, 34.3% rivaroxaban) Andexanet	Primary: hematoma volume change within 12–72 hr; hematoma growth ≤33% within 12–72 hr Secondary: mortality and in-hospital TEE	Mean hematoma expansion 2.3 ml (95% CI, 0.4–4.2); approx. 90% with hematoma growth ≤33% In-hospital mortality, 21.9% 90-Day mortality, 36.7% In-hospital TEE, 8%
Tsivgoulis et al., 2025[26]	Meta-analysis of 18 studies	Andexanet (1567 patients) or study-defined usual care (1969 patients)	Primary: hematoma expansion ≤35% or ≤6 ml (good hemostasis) Secondary: hematoma expansion ≤20% (excellent hemostasis), functional outcomes (modified Rankin Scale score 0–3), mortality, and TEE	Good hematoma control: higher with andexanet (RR, 1.16; 95% CI, 1.06–1.26) No significant difference in excellent hemostasis, function, mortality, or TEE
Sarhan et. al., 2025[27]	Meta-analysis of 16 studies	2977 patients (58% men; mean age, 77 yr) with ICH PCC (1560 patients) or andexanet (1417 patients)	Primary: anticoagulation reversal, mortality, and TEE Secondary: length of hospital and ICU stay, hematoma expansion	Associated with andexanet: Higher anticoagulant reversal (RR, 1.10; 95% CI, 1.01–1.20; P=0.02) More TEE (RR, 1.47; 95% CI, 1.01–2.15; P=0.046) Longer hospital stay (mean difference in days, 0.64; 95% CI, 0.07–1.22; P=0.03) No meaningful difference in ICU stay, mortality, or hematoma expansion
Ovesen et al., 2025[28]	Systematic review of 2 RCTs	534 patients with FXaI-related critical bleeding PCC, FFP, or andexanet	Mortality TEE Trial-defined hemostatic efficacy Functional outcomes	PCC vs. FFP Faster INR correction (RR, 0.41; 95% CI, 0.32–0.52) Hemostasis nonsignificantly better (RR, 0.68; 95% CI, 0.44–1.06; P=0.09) Similar all-cause mortality and TEE (RR, 3.14; 95% CI, 0.14–72.92) PCC vs. andexanet Lower hemostatic efficacy (RR, 1.46; 95% CI, 1.15–1.85; P=0.002) Similar all-cause mortality and functional outcomes Lower TEE (RR, 0.55; 95% CI, 0.30–1.00; P=0.052)
Connolly et al., 2024[16]	RCT	452 patients with ICH (mean age, 78.9 yr; approx. 55% men; ≤15 hr since the last FXaI dose) Andexanet (263 patients) or usual care (267 patients; 85.5% received PCC preparations)	Primary: hemostatic efficacy on the ANNEXA-A scale Secondary: 30-day mortality, TEE	Hemostatic efficacy: andexanet, 67.0%; usual care, 53.1% (adj. difference, 13.4 percentage points; 95% CI, 4.6–22.2; P=0.003) 30-Day mortality: andexanet, 27.8%; usual care, 25.5% (P=0.51) 30-Day TEE: andexanet, 10.3%; usual care, 5.6% (P=0.048)
White et al., 2024[29]	Meta-analysis of 18 studies†	1725 patients with FXaI-associated major bleeding (mean age, 72 yr; 54% men) Andexanet (645 patients) or PCC products at a dose of 25–50 IU/kg (1080 patients)	Effective hemostasis (study-defined scales, mostly ISTH) TEE 30-Day mortality All studies considered to be at high risk of bias	Associated with andexanet: Higher effective hemostasis (OR, 1.36; 95% CI, 1.01–1.84) Lower 30-day mortality (OR, 0.53; 95% CI, 0.37–0.76) Similar TEE
Dobesh et al., 2023[30]	Retrospective	4395 patients (57% men; mean age, 66 yr) with major bleeding with rivaroxaban or apixaban (1328 ICH, 2567 gastrointestinal bleeding, 500 bleeding in critical compartment or other type) Andexanet (2122 patients) or 4F-PCC (2273)	Effective hemostasis In-hospital stay In-hospital mortality Rate of DOAC restart	Effective hemostasis: andexanet, 73.8%; 4F-PCC, 58.8% (P=0.05) In-hospital mortality: andexanet, 6.0%; 4F-PCC, 10.6% (OR, 0.50; 95% CI, 0.39–0.65) Similar in-hospital stay duration and rate of DOAC restart
Chaudhary et al., 2022[31]	Meta-analysis of 36 studies	1832 patients with ICH (57% men; mean age, 74 yr) while taking DOACs (1123 dabigatran, 180 apixaban, 110 rivaroxaban) 4F-PCC (967 patients), andexanet (525), or idarucizumab (340)	Primary: anticoagulation reversal (mostly ISTH criteria) Secondary: all-cause mortality, TEE	Anticoagulation reversal: PCC, 77%; andexanet, 75%; idarucizumab, 82% All-cause mortality: PCC, 26%; andexanet, 24%; idarucizumab, 11% TEE: PCC, 8%; andexanet, 14%; idarucizumab, 5% 4F-PCC vs. andexanet: no significant difference in anticoagulation reversal, mortality, or TEE
Costa et al., 2022[32]	Observational (propensity-score–weighted analysis)	202 patients with ICH while taking rivaroxaban or apixaban Andexanet (107 patients; 96.6% received low dose) or 4F-PCC (95 patients; 79.3% received 25 U/kg)	Hemostatic effectiveness and 30-day mortality	Hemostatic effectiveness: andexanet, 85.8%; 4F-PCC, 68.1% (OR, 2.73; 95% CI, 1.16–6.42) 30-Day mortality: andexanet, 7.9%; 4F-PCC, 19.6% (OR, 0.36; 95% CI, 0.13–0.98); Similar hematoma growth
Gómez-Outes et al., 2021[33]	Meta-analysis of 60 studies (2 RCTs)	4735 patients (55% men; mean age, 70 yr) with major bleeding (55% ICH) while taking DOACs (dabigatran, 1111 patients; FXaI, 2688 patients) 4F-PCC (25–50 IU/kg) (2688 patients), idarucizumab (1111), or andexanet (936)	Overall mortality Effective hemostasis (ANNEXA-4, ISTH, or Sarode scale) TEE	Differences in death rates and effective hemostasis not significant across reversal agents TEE: andexanet, 10.7%; 4F-PCC, 4.3%; idarucizumab, 3.8% (4F-PCC and idarucizumab, P=0.03 vs. andexanet) Risk of death significantly associated with failure to achieve effective hemostasis (RR, 3.63; 95% CI, 2.56 to 5.16; I^2 = 0%)
Nederpelt et al., 2021[34]	Meta-analysis of 21 studies	1726 patients (53% men; mean age, 70 yr) with FXaI-related bleeding Andexanet (438 patients) or PCC preparations (1278)	Hemostatic effectiveness (Sarode or ISTH scales) at 12 hr and 24 hr TEE In-hospital mortality	Similar hemostatic effectiveness At 12 hr — andexanet, 82%; PCC, 88% At 24 hr — andexanet, 71%; PCC, 76% 30-Day TEE: andexanet 10.7%, PCC 3.1% In-hospital mortality: andexanet 23.3%, PCC 15.8%
Jaspers et al., 2021[35]	Meta-analysis of 21 studies	1428 patients treated with PCC and 396 with andexanet Separate analyses and indirect comparison	Hemostatic effectiveness (ANNEXA-4 criteria) TEE In-hospital mortality	Hemostatic effectiveness: PCC, 85% (95% CI, 80–90); andexanet, 82% (95% CI, 0.78–0.87) TEE: PCC, 3% (95% CI, 0.02–0.04); andexanet, 11% (95% CI. 0.04–0.18)
Connolly et al., 2019[23]	Open-label, single-group (ANNEXA-A)	352 patients (66% men; mean age, 77 yr) with major uncontrolled bleeding (64% with ICH) while taking apixaban (194 patients), rivaroxaban (128), enoxaparin (20), or edoxaban (10) Andexanet	Primary: percent change in anti–FXa activity, hemostatic efficacy at 12 hr Secondary: 30-day TEE and mortality	92% reduction in anti-FXa activity 82% excellent or good hemostasis 14% 30-day mortality 10% TEE

Fixed vs. Standard Doses of 4F-PCC for Reversal of VKA and DOAC.

Study or Trial and Year	Design	Population and PCC Dose	End Points	Key Findings
Alwakeal et al., 2024[70]	Meta-analysis of 19 studies (3 RCTs)	323 patients in RCTs, 1912 in observational studies (approx. 55% men, age approx. 73 yr) 4F-PCC at fixed dose of 750–3000 IU, mean approx. 1500 IU (858 patients) or standard dose (1054 patients)	INR <1.5 In-hospital mortality TEEs Hemostatic effectiveness (ISTH criteria in 4 studies) Additional doses	Fixed vs. standard dose: INR <1.5: OR, 0.3; 95% CI, 0.1–0.8 Order-to-needle time, 39 vs. 72 min Total PCC dose, 22.1 vs. 27.7 IU/kg PCC-to-INR time, 147.4 vs. 192.5 min Higher clinical hemostasis: OR, 1.7; 95% CI, 1.0–2.8 Additional doses: OR, 8.6; 95% CI, 3.0–24.6 INR <1.5: OR, 0.3; 95% CI, 0.1–0.8 Mortality and TEE similar among the RCTs Subgroup analysis: improved effectiveness with fixed dose ≥2000 IU
Brett et al., 2024[71]	Retrospective, single-center study	173 patients with FXaI-related bleeding Fixed dose of 2000 IU or 5000 IU (72 patients) or standard dose of 50 IU/kg (101 patients)	Primary: time between drug order and administration Secondary: total PCC dose, postadministration procedures, hemostasis, 30-day mortality, length of hospitalization	Fixed vs. standard dose: Shorter administration time with fixed dose (4.5 min faster) Hemostasis similar for fixed and standard doses (79.2% and 71.3%) (RR, 1.11; 95% CI, 0.94–1.32) Similar incidence of postsurgery bleeding (fixed dose, 29.2%; standard dose, 36.7%) (RR, 0.80; 95% CI, 0.51–1.24) Similar mortality (fixed dose, 26.4%; standard dose, 35.6%) (RR, 0.73; 95% CI, 0.46–1.17)
Condeni et al., 2024[72]	Meta-analysis of 23 studies (2 RCTs)	2055 patients (63.5% men, median age 77 yr) Fixed dose of ≥1000 IU or standard dose Excluded studies that used <1000 IU and those that involved patients who had obesity	Target INR TEE Time to PCC Survival Cost	Fixed vs. standard dose: Similar percentages of patients had INR <2, TEE, and in-hospital mortality Percentage of patients with INR <1.6 was lower with fixed dose, unless dose was ≥2000 IU or >20 IU/kg Shorter administration time with fixed dose Suggested cutoff of 80 kg for an additional 500-IU fixed dose Cost savings, $581 to $1,657 per patient
Chiasakul et al., 2022[73]	Meta-analysis of 25 observational studies	1760 patients with FXaI-associated major bleeding received PCC Fixed dose of 1500–2000 IU, mean 2025 IU (228 patients), or standard dose of 20–25 IU/kg (1532 patients)	Primary: study-defined clinical hemostatic effectiveness Secondary: mortality, TEE, 4F-PCC use, in-hospital and ICU length of stay, time to 4F-PCC infusion	Fixed vs. standard dose: Similar hemostatic effectiveness (fixed dose, 74%; standard dose, 79%), mortality (fixed dose, 16%; standard dose, 21%), and TEE (fixed dose, 2.9%; standard dose, 4.1%) Longer hospitalization: fixed dose, 7.4 days; standard dose, 5.9 days (P<0.001) Lower mean initial 4F-PCC dose/kg: standard dose 38 IU/kg (95% CI, 32–44), fixed dose 27 IU/kg (95% CI, 26–28) (P<0.001)
Bajdas et al., 2022[74]	Retrospective	265 patients (approx. 60% men) with major, non-ICH bleeding or emergency procedures received 4F-PCC Fixed dose of 1500 IU (90 patients) or standard dose (175 patients)	Primary: hemostatic efficacy at 48 hr (ISTH criteria) Secondary: INR ≤1.5, in-hospital mortality, time to 4F-PCC, cost	Fixed vs. standard dose: Lower hemostatic efficacy (21.7% vs. 37.8%) (P<0.005) Shorter administration time Lower cost (mean reduction, $1,881/patient) Similar in-hospital mortality and INR ≤1.5
Abdoellakhan et al., 2021[75]	Randomized, multicenter, open-label, non-inferiority trial (PROPER3)	199 patients with major non-ICH bleeding received 4F-PCC Fixed dose of 1000 IU or standard dose	Primary: noninferior ISTH hemostatic efficacy between 4 hr and 48 hr Secondary: INR at 1 hr and 24 hr, time to PCC, in-hospital TEE, 30-day all-cause mortality	Underpowered trial owing to early termination for low recruitment Shorter infusion time with fixed dose than standard (difference, 33 min) Similar INR after infusion, in-hospital TEE (1.2% fixed dose vs. 2.3% standard dose), and mortality (4.7% fixed dose vs. 8.1% standard dose)
Elsamadisi et al., 2021[76]	Retrospective	44 patients who had obesity (≥100 kg) received 4F-PCC Fixed dose of 2000 IU vs. standard dose	INR <2 (extracranial bleeding) or <1.5 (ICH) Additional doses Time to PCC 7-Day TEE Mortality Cost	Fixed vs. standard dose: Post-treatment INR: fixed dose, 1.6 (IQR, 1.5–1.9); standard dose, 1.3 (IQR, 1.2–1.5) (P<0.01) Percentage of patients with INR <2, frequency of repeated doses, incidence of TEE, and mortality similar in the two groups Lower costs with fixed dose (savings of $2,419–3,411 per patient)
Mohammadi et al., 2021[77]	Meta-analysis of 10 observational studies and 1 RCT	988 patients with ICH, extracranial hemorrhage, or emergency surgery Fixed dose (mean dose of 1360 IU, approx. 16 IU/kg) or standard dose (approx. 25 IU/kg)	Mortality TEE Target INR Need for a repeat dose Time elapsed for INR reversal Order-to-needle time Length of hospitalization	Fixed vs. standard dose: Lower mortality with fixed dose (RR, 0.65; 95% CI, 0.47–0.90) except for patients with ICH Order-to-needle time 68 min shorter with fixed dose More repeat doses but lower total dose Higher postinfusion INR values Fewer patients with INR <1.5 (RR, 0.87; 95% CI, 0.78–0.96) Similar incidence of TEE and hospitalization
Yohe et al., 2019[78]	Retrospective, single-center	114 patients with major bleeding (42% ICH, 54% men, mean age 75 yr) 4F-PCC at standard dose	Primary: characterize relationship between 4F-PCC and postinfusion INR Secondary: TEE, events ≤10 days after treatment, death from any cause in hospital	Weak linear relationship between 4F-PCC dose and postreversal INR ($R^2 = 0.06$) Each additional 500-IU dose of 4F-PCC dose (in FIX IU) was associated with INR decrease of 0.02 Body weight and baseline INR value not correlated with postreversal INR

War

ABANs

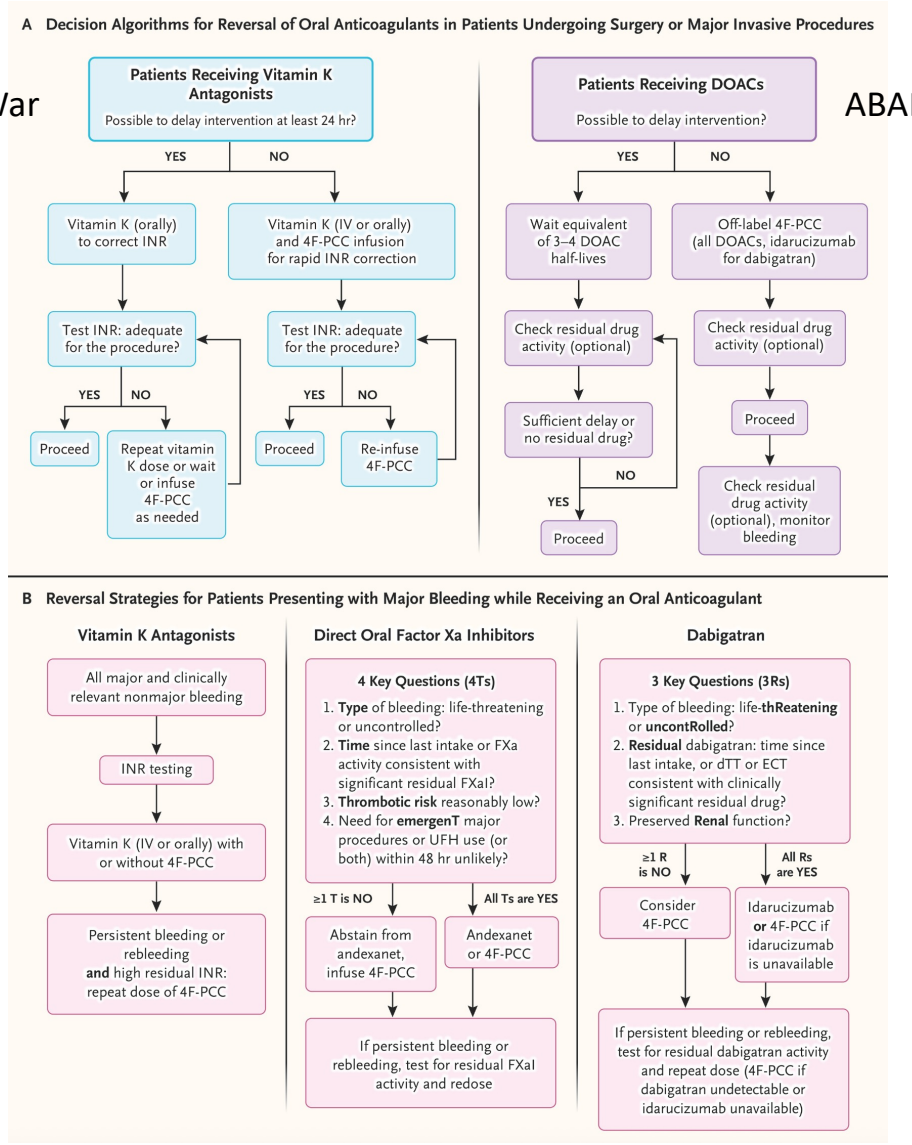

Conclusions

When anticoagulant reversal is needed, the right antidote must be delivered to the right patient in a timely, appropriate, safe, effective way, balancing the need for effective hemostasis and bleeding control against the risk of a life-threatening thrombosis and the burden of cost. Although the ideal antidote, like the ideal anticoagulant, remains largely elusive, the scientific and medical communities have the responsibility to build stronger evidence and refine tools to advance patient-centered, global anticoagulant and prohemostatic care.

Osteosarcoma

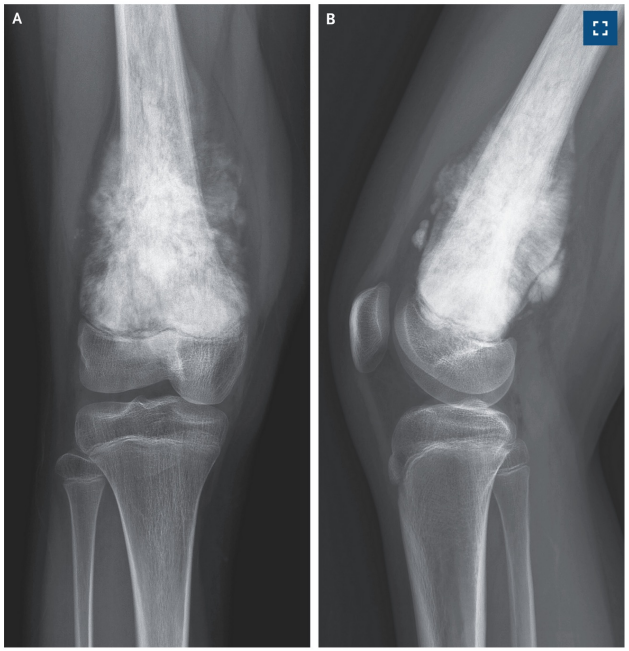

An 11-year-old girl presented to the orthopedic clinic with a 1-month history of right thigh pain that worsened at night. She had no systemic symptoms. Physical examination was notable for soft-tissue swelling over the distal thigh and limited range of motion of the knee on the right side. Radiographs of the knee showed a metaphyseal osteoblastic lesion with ill-defined margins and cortical destruction in the distal femur (Panel A, anteroposterior view; Panel B, lateral view). The mass had a sunburst appearance, a finding that is seen in aggressive bone lesions and that results from the formation of divergent bone spicules as the periosteal reaction to the rapid growth of the tumor. On the basis of subsequent magnetic resonance imaging of the knee and a bone biopsy, a diagnosis of high-grade osteosarcoma was made. Osteosarcoma is the most common primary malignant bone tumor in children. It typically manifests in the second decade of life owing to the rapid bone growth during that stage of development. No distant sites of metastasis were identified on further imaging. Treatment with neoadjuvant chemotherapy, wide excision, reconstruction, and adjuvant chemotherapy was given. After more than 10 years of follow-up, the patient remained cancer-free with independent ambulation.

Neovascularization of the Disk in Proliferative

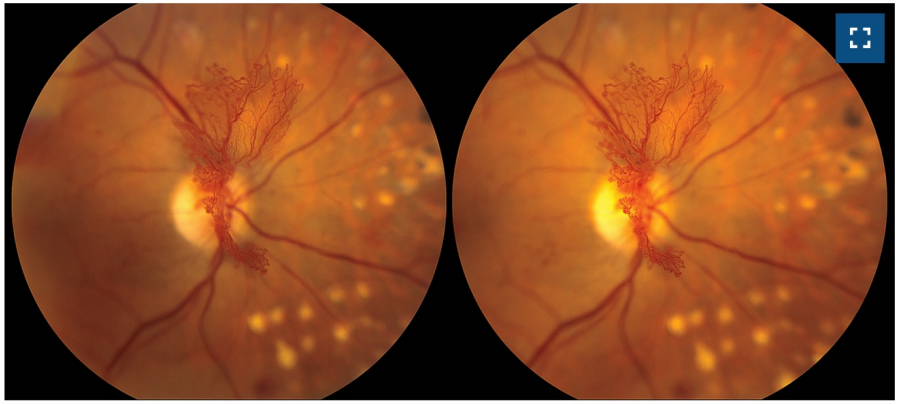

A 58-year-old woman with long-standing type 2 diabetes mellitus complicated by diabetic retinopathy presented to the ophthalmology clinic for an annual eye examination. She had no symptoms affecting her vision. On examination of the right eye, the visual acuity was 20/25. No anterior-segment neovascularization was seen on slit-lamp examination. Dilated funduscopic examination identified prominent neovascularization of the optic disk, which was documented with stereo fundus photography — an imaging technique in which two images of the retina are obtained at slightly different angles and then viewed through a stereoscopic viewer to create a three-dimensional rendering of retinal structures. This patient's stereo fundus photographs showed neovascularization of the disk extending out from the plane of the retina into the vitreous cavity. Scars from previous panretinal photocoagulation were also seen (yellow spots in the image background). In the left eye, the visual acuity was 20/25. Dilated fundus examination showed scars from previous panretinal photocoagulation, but no anterior- or posterior-segment neovascularization was visible. A diagnosis of active proliferative diabetic retinopathy in the right eye was made. Prompt treatment to regress the neovascularization in this condition is indicated because the delicate, newly formed vessels may lead to tractional retinal detachment or hemorrhage. Treatment with panretinal photocoagulation and monthly intravitreal anti–vascular endothelial growth factor injections was given. By 3 months after presentation, the patient had near-complete regression of neovascularization of the disk.

Case 16-2026: A 14-Year-Old Girl with Hypertension

The patient had been in her usual state of health until 10 days before the current admission, when malaise, myalgias, and nausea developed, with five episodes of vomiting. The patient's parents took her to the emergency department of another hospital. On evaluation, the blood pressure was 125/85 mm Hg and the heart rate 120 beats per minute. The patient was actively vomiting and had dry mucous membranes. She appeared to be well developed and nourished. Laboratory test results are shown. Intravenous fluids were administered. The symptoms abated slightly, and the patient was discharged home. During the next 10 days, the vomiting continued, and intermittent fever, epigastric pain, nasal congestion, and cough developed. When the episodes of vomiting increased in frequency, the patient's parents took her back to the emergency department of the other hospital. The blood pressure was 162/112 mm Hg and the heart rate 98 beats per minute. The patient reported nausea; mild tenderness was noted in the left upper quadrant of the abdomen. The blood level of potassium was 2.7 mmol per liter (reference range, 3.5 to 5.1). Tests for severe acute respiratory syndrome coronavirus 2, influenza A and B viruses, and respiratory syncytial virus were negative.

Variable	Reference Range, Other Hospital	10 Days before Current Admission, Other Hospital	Day of Current Admission, Other Hospital	Reference Range, This Hospital†	On Current Admission, This Hospital
Blood					
Hematocrit (%)	33.9–45.0	41.3	38.3	36.0–46.0	35.6
Hemoglobin (g/dl)	11.3–15.0	14.2	13.3	12.0–16.0	12.8
Platelet count (per μl)	189,000–400,000	606,000	559,000	150,000–450,000	458,000
White-cell count (per μl)	4800–10,800	11,000	9500	4500–13,500	7650
Differential count (per μl)					
Neutrophils	1900–8200	9400	5500	1800–8000	3890
Lymphocytes	300–4200	1100	2900	1500–6500	2890
Monocytes	200–800	400	800	200–1500	670
Sodium (mmol/liter)	136–145	134	132	135–145	132
Potassium (mmol/liter)	3.5–5.1	3.1	2.7	3.4–5.0	2.9
Chloride (mmol/liter)	98–107	89	86	98–108	91
Carbon dioxide (mmol/liter)	21–32	30	34	23–32	30
Urea nitrogen (mg/dl)	7–18	9	8	8–25	7
Creatinine (mg/dl)	0.7–1.1	0.7	0.6	0.60–1.50	0.58
Glucose (mg/dl)	74–160	123	117	70–110	98
Calcium (mg/dl)	8.5–10.5	9.7	9.1	8.5–10.5	8.3
Aspartate aminotransferase (U/liter)	12–45	—	21	—	—
Alanine aminotransferase (U/liter)	8–34	—	9	—	—
Alkaline phosphatase (U/liter)	45–504	—	147	—	—
Total bilirubin (mg/dl)	0.2–1.0	—	0.7	—	—
Direct bilirubin (mg/dl)	0.0–0.2	—	<0.2	—	—
Albumin (g/dl)	3.4–5.2	—	3.6	—	—
Total protein (g/dl)	6.4–8.2	—	7.4	—	—
C-reactive protein (mg/liter)	—	—	—	0.0–8.0	57.6
Erythrocyte sedimentation rate (mm/hr)	—	—	—	0–19	98
Urine					
Color	—	—	—	Yellow	Colorless
Clarity	—	—	—	Clear	Clear
Blood	—	—	—	Negative	3+
Glucose	—	—	—	Negative	Negative
Bilirubin	—	—	—	Negative	Negative
Protein	—	—	—	Negative	3+
Ketone	—	—	—	Negative	Negative
Nitrite	—	—	—	Negative	Negative
Leukocyte esterase	—	—	—	Negative	Negative
Specific gravity	—	—	—	1.001–1.035	1.008
Urobilinogen	—	—	—	Negative	Negative
White cells (per high-power field)	—	—	—	0–9	<10
Red cells (per high-power field)	—	—	—	0–2	>100

On examination, the temporal temperature was 36.9°C, the blood pressure 180/116 mm Hg, the heart rate 103 beats per minute, and the respiratory rate 20 breaths per minute. The patient appeared healthy and comfortable, and she was alert, awake, oriented, and cooperative. The neck was supple; a bruit was noted over the left carotid artery. Examination of the heart and lungs showed no abnormalities. The abdomen was nondistended, nontender, and soft, without organomegaly or masses. No acne or excessive hair was present on the face. No rash was noted on exposed skin, and there was no pain or swelling in the joints. The legs were warm, without swelling.

The blood level of potassium was 2.9 mmol per liter (reference range, 3.4 to 5.0), the white-cell count 7650 per microliter (reference range, 4500 to 13,500), and the erythrocyte sedimentation rate 98 mm per hour (reference range, 0 to 19).

On the second hospital day, the headache and vomiting resolved, but the blood pressure remained elevated. Intravenous hydralazine was administered intermittently, amiloride therapy was continued, and amlodipine therapy was started. That evening, the patient reported blurry vision. While she was speaking to a health care worker, she abruptly stopped talking and stared. The blood pressure had increased to 182/111 mm Hg, and the patient was not responsive to voice or sternal rub. The pupils were round and reactive to light. After approximately 15 minutes, she became alert and oriented, but the blurry vision persisted. She was transferred to the pediatric intensive care unit for further treatment.
A diagnostic test was performed.

Differential Diagnosis

This 14-year-old adolescent girl with a history of depression presents with either acute or intermittent hypertension in the context of hypokalemia and elevated inflammatory markers.

Glomerulonephritis

Hypertension is common in patients with glomerulonephritis, and the presence of hematuria and proteinuria in this patient is suggestive of glomerular disease.

Neuroendocrine Disease

Cushing's syndrome (hypercortisolism) can cause hypertension in children, and it is frequently associated with psychiatric disease, which was seen in this patient.

Vascular Disease

Secondary aldosteronism due to abnormalities in the renal vasculature is the most likely cause of this patient's presentation with severe hypertension, mild hypokalemia, and metabolic alkalosis.

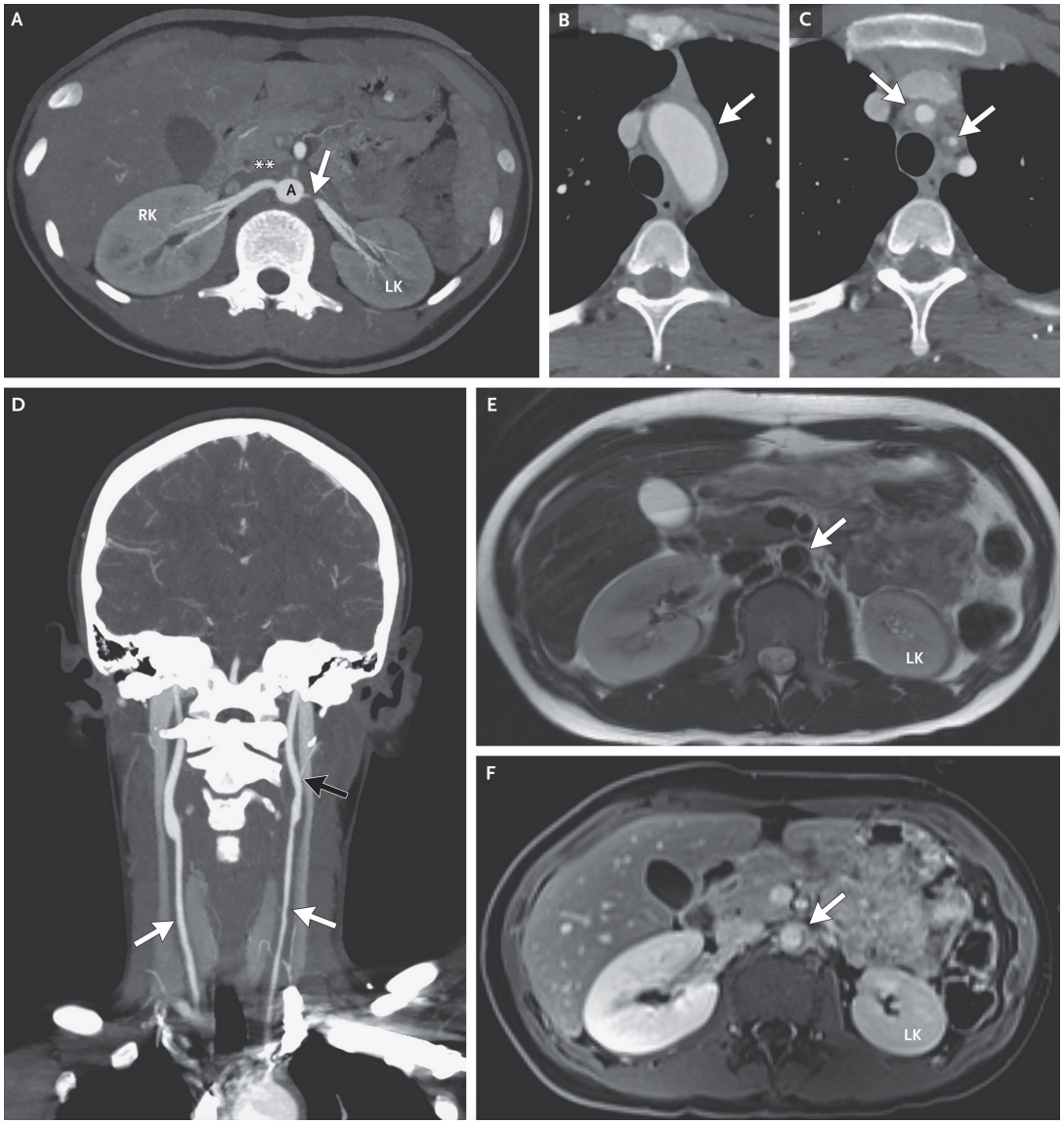

Imaging Studies.

Contrast-enhanced computed tomographic angiography (CTA) of the abdomen was performed. An axial oblique maximum-intensity-projection (MIP)–reformatted image (Panel A) shows severe narrowing of the left renal artery (arrow). Abnormal periaortic soft-tissue thickening is present (asterisks), with a slightly decreased luminal caliber of the abdominal aorta (A). The left kidney (LK) has notable hypoenhancement and atrophy as compared with the right kidney (RK), a finding consistent with chronic, high-grade renovascular obstruction on the left side. Contrast-enhanced CTA of the head, neck, and chest was subsequently performed. Serial axial images (Panels B and C) show abnormal wall thickening (arrows) of the thoracic aortic arch and the origins of the brachiocephalic and left common carotid arteries. In addition, severe luminal narrowing of the left common carotid artery is present. A coronal oblique MIP-reformatted image (Panel D) shows long-segment wall thickening with associated luminal narrowing (white arrows) throughout both common carotid arteries; the finding is more prominent on the left side than on the right side. Severe stenosis is present at the origin of the left external carotid artery (black arrow). Contrast-enhanced magnetic resonance angiography (MRA) of the abdomen was also performed. An axial T2-weighted double inversion recovery image (Panel E) and a nephrographic phase, postcontrast image (Panel F) show abnormal abdominal aortic wall thickening (arrows) with associated contrast enhancement, a finding suggestive of active inflammation. Hypoenhancement and atrophy of the left kidney is visible. Findings on MRA of the head, neck, and chest (not shown) were concordant with previous CTA findings.

Classification Criteria for Takayasu Arteritis in Adults.

Criterion	Status or Points	Status or Points in This Patient
Absolute requirements		
Age ≤60 yr at time of diagnosis	Yes	Yes
Evidence of vasculitis on imaging	Yes	Yes
Additional clinical criteria		
Female sex	+1	+1
Angina or ischemic cardiac pain	+2	—
Arm or leg claudication	+2	—
Vascular bruit	+2	+2
Reduced pulse in arm	+2	—
Carotid-artery abnormality	+2	+2
Difference in systolic blood pressure of ≥20 mm Hg between arms	+1	—
Additional imaging criteria		
No. of affected arterial territories		
One	+1	—
Two	+2	—
Three or more	+3	+3
Symmetric involvement of paired arteries	+1	+1
Involvement of the abdominal aorta with involvement of a renal or mesenteric vessel	+3	+3

FCL Comment

Takayasu was an opthalmologist. No eye findings are given. Takayasu‘s is the pulseless disease. No BPs were measured in other extremities. The metabolic alkalosis and hypokalemia were ignored. No comment about abdominal bruitß

In coordination with the rheumatology team, the patient received glucocorticoid therapy, along with methotrexate and an infusion of infliximab. After 5 months of treatment, repeat renal ultrasonography showed atrophy of the left kidney. Repeat MRA showed poor growth of the left kidney and poor perfusion, with persistent critical stenosis of the left renal artery.

After angioplasty, hypertension resolved, and the patient was discharged while receiving no antihypertensive medications. Repeat Doppler ultrasonography showed continued stenosis of the left renal artery. Treatment with supplemental potassium was indicated for ongoing mild hypokalemia. During this time, the patient had become sexually active. Long-acting reversible contraception was initiated, but the patient discontinued contraception owing to personal preference..

Final Diagnosis

Takayasu arteritis.

Finerenon ist ein selektiver, nicht-steroidaler Mineralokortikoid-Rezeptor-Antagonist (nsMRA). Es blockiert schädliche Wirkungen von Aldosteron auf Herz und Nieren (Entzündung, Fibrose), ohne an Sexualhormonrezeptoren zu binden. Die Indikationen umfassen chronische Nierenerkrankungen bei Typ-2-Diabetes und chronische Herzinsuffizienz.

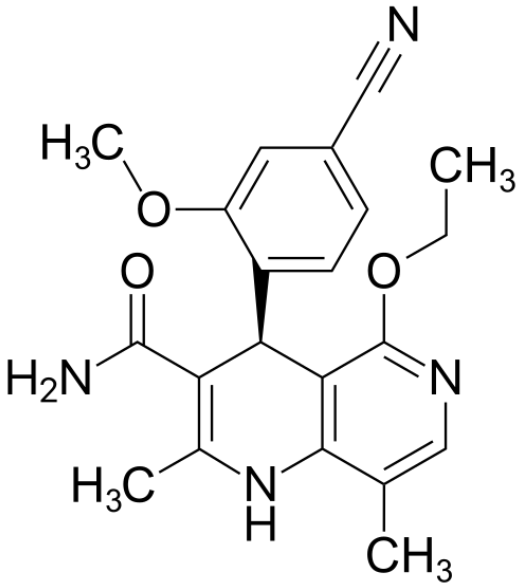

•**Wirkmechanismus:** Finerenon bindet hochaffin an den Mineralokortikoid-Rezeptor (MR) und verhindert dessen Aktivierung. Dadurch wird die Bindung von Rezeptor-Kofaktoren im Zellkern blockiert, was zu einer Reduktion von Entzündungs- und Fibroseprozessen führt.

•**Selektivität:** Im Gegensatz zu älteren Steroid-Antagonisten (wie Spironolacton) ist Finerenon nicht-steroidal. Es weist keine signifikante Bindungsaffinität zu Androgen-, Östrogen- oder Progesteronrezeptoren auf. Typische Nebenwirkungen wie Gynäkomastie (Brustwachstum beim Mann) oder Libidoverlust treten daher so gut wie nicht auf.

•**Metabolisierung:** Die Verstoffwechselung erfolgt in der Leber, überwiegend über das Cytochrom-P450-System (CYP3A4).

•**Halbwertszeit:** Sie liegt bei etwa 2 bis 3 Stunden.

•**Ausscheidung:** Der Wirkstoff wird zu rund 80 % über den Urin und zu 20 % über den Stuhl (in Form inaktiver Metaboliten) eliminiert.

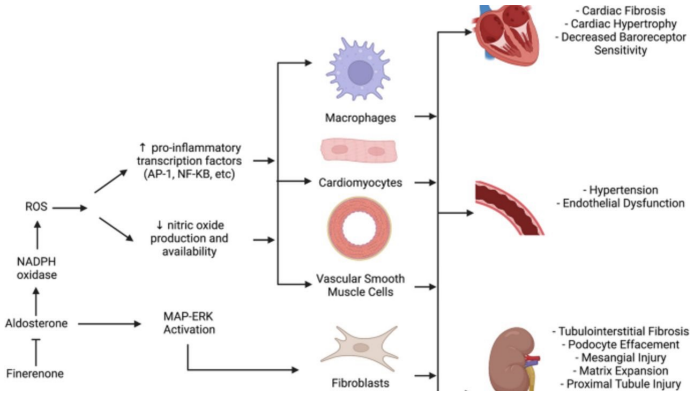

How good is finerenone in CKD?

Efficacy and safety of finerenone in patients with chronic kidney disease: an individual participant data pooled analysis (INFINITY)

Summary

Background Overactivation of the mineralocorticoid receptor is a common pathway for chronic kidney disease (CKD) progression across multiple disease aetiologies. Finerenone, a non-steroidal mineralocorticoid receptor antagonist, has shown kidney and cardiovascular benefits in CKD due to type 2 diabetes, but its efficacy and safety across disease aetiologies, and levels of glycaemia, estimated glomerular filtration rate (eGFR), and albuminuria have not been evaluated. The aim of this study was to evaluate the efficacy and safety of finerenone across the spectrum of CKD.

Methods We conducted an individual participant data meta-analysis of three randomised, double-blind, placebo-controlled trials of finerenone in patients with CKD: FIDELIO-DKD (NCT02540993; Sept 17, 2015, to April 14, 2020), FIGARO-DKD (NCT02545049; Sept 17, 2015, to Feb 2, 2021), and FIND-CKD (NCT05047263; Sept 21, 2021, to Feb 2, 2026). We used Cox regression models to evaluate relative effects on kidney and cardiovascular outcomes. The main kidney outcome was kidney failure or sustained 57% or more decline in eGFR; the main cardiovascular outcome was hospitalisation for heart failure or cardiovascular death. This study was registered with PROSPERO, CRD420251269149.

Findings Across the three trials enrolling 14 574 participants, the mean age was 63·7 years (SD 10·6), 4467 (30·7%) were female, 10 107 (69·3%) were male, mean eGFR was 56·4 mL/min per 1·73 m² (SD 21·4), and median urinary albumin-to-creatinine ratio was 567·4 mg/g (IQR 233·6–1164·7). Finerenone reduced the risk of the composite kidney outcome by 24% versus placebo (22·3 *vs* 28·8 events per 1000 patient-years; hazard ratio 0·76 [95% CI 0·68–0·86]) and kidney failure alone (0·85 [0·74–0·99]). Finerenone reduced the risk of the composite cardiovascular outcome versus placebo (19·1 *vs* 23·9 events per 1000 patient-years; 0·80 [0·70–0·91]), including heart failure hospitalisation (0·78 [0·66–0·92]) and cardiovascular death (0·82 [0·67–0·999]). Finerenone also reduced the risk of all-cause death (0·88 [0·79–0·99]). Treatment effects on the composite kidney outcome were consistent irrespective of glycaemic status, CKD aetiology, baseline eGFR, albuminuria, and use of sodium–glucose co-transporter-2 inhibitors. Hyperkalaemia occurred more frequently with finerenone than with placebo, but the absolute incidence of hyperkalaemia leading to hospitalisation was low.

Interpretation In the studied populations with CKD, finerenone reduced the risk of CKD progression, including kidney failure alone, and reduced heart failure hospitalisation, cardiovascular death, and all-cause death. These findings support finerenone as a foundational therapy for CKD across a broad range of disease aetiologies and levels of glycaemia, eGFR, and albuminuria.

	Finerenone (n=7291)	Placebo (n=7283)	Overall (n=14 574)
Age, years	63·6 (10·5)	63·7 (10·7)	63·7 (10·6)
Sex*			
Female	2310 (31·7%)	2157 (29·6%)	4467 (30·7%)
Male	4981 (68·3%)	5126 (70·4%)	10 107 (69·3%)
Race*			
White	4757 (65·2%)	4760 (65·4%)	9517 (65·3%)
Black	273 (3·7%)	284 (3·9%)	557 (3·8%)
Asian	1860 (25·5%)	1868 (25·6%)	3728 (25·6%)
Other†	401 (5·5%)	371 (5·1%)	772 (5·3%)
Region			
Europe, Australia, and Israel	3527 (48·4%)	3550 (48·7%)	7077 (48·6%)
Asia	1750 (24·0%)	1734 (23·8%)	3484 (23·9%)
North America	1096 (15·0%)	1085 (14·9%)	2181 (15·0%)
Latin America	753 (10·3%)	754 (10·4%)	1507 (10·3%)
Others	165 (2·3%)	160 (2·2%)	325 (2·2%)
eGFR, mL/min per 1·73 m²	56·3 (21·3)	56·4 (21·5)	56·4 (21·4)
eGFR category, mL/min per 1·73 m²			
<45	2617 (35·9%)	2613 (35·9%)	5230 (35·9%)
45 to <60	1918 (26·3%)	1931 (26·5%)	3849 (26·4%)
≥60	2755 (37·8%)	2737 (37·6%)	5492 (37·7%)
UACR, mg/g	566·6 (231·8–1155·5)	568·3 (235·2–1173·2)	567·4 (233·6–1164·7)
UACR category, mg/g			
<300	2218 (30·4%)	2155 (29·6%)	4373 (30·0%)
300 to ≤1000	2884 (39·6%)	2917 (40·1%)	5801 (39·8%)
>1000	2187 (30·0%)	2208 (30·3%)	4395 (30·2%)
BMI, kg/m²	30·9 (6·1)	30·9 (6·0)	30·9 (6·1)
Mean systolic blood pressure, mm Hg	136·0 (14·3)	135·9 (14·4)	136·0 (14·4)
Mean HbA_{1c}, %	7·5 (1·5)	7·5 (1·5)	7·5 (1·5)
Potassium, mmol/L	4·4 (0·4)	4·4 (0·4)	4·4 (0·4)
History of cardiovascular disease			
Atherosclerotic cardiovascular disease	3063 (42·0%)	3060 (42·0%)	6123 (42·0%)
Atrial fibrillation or atrial flutter	594 (8·1%)	571 (7·8%)	1165 (8·0%)
Heart failure	501 (6·9%)	541 (7·4%)	1042 (7·1%)
Concomitant medications			
Angiotensin-converting enzyme inhibitors	2753 (37·8%)	2758 (37·9%)	5511 (37·8%)
Angiotensin receptor blockers	4529 (62·1%)	4520 (62·1%)	9049 (62·1%)
SGLT2 inhibitors	570 (7·8%)	572 (7·9%)	1142 (7·8%)
Statins	5068 (69·5%)	5193 (71·3%)	10 261 (70·4%)

Data are reported as n (%), mean (SD), or median (IQR). eGFR=estimated glomerular filtration rate. FSGS=focal segmental glomerulosclerosis. HbA_{1c}=glycated haemoglobin. SGLT2=sodium–glucose co-transporter-2. UACR=urine albumin-to-creatinine ratio. *Sex and race were self-reported by the participants. Participants reporting more than one race were categorised as multiple race. †American Indian or Alaska native, Hawaiian or other Pacific Islander, or not reported, or multiple.

Table 1: **Characteristics of participants at baseline**

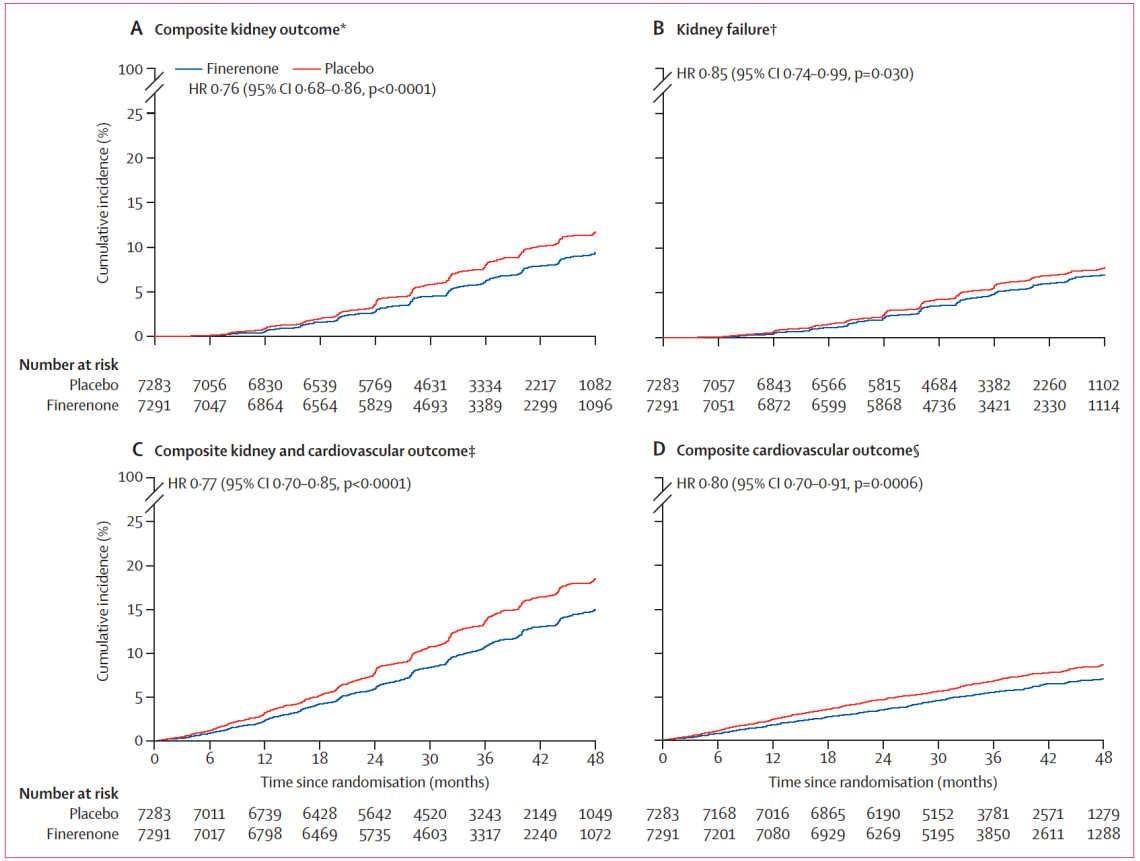

Figure 1: **Cumulative incidence functions for key efficacy outcomes**
Cumulative incidence curves of efficacy outcomes estimated using Aalen–Johansen methods accounting for mortality as a competing risk. Outcomes were assessed in time-to-event analyses. eGFR=estimated glomerular filtration rate. HR=hazard ratio. *The composite kidney outcome was a 57% or more decline in eGFR or kidney failure. †Kidney failure was defined as sustained eGFR less than 15 mL/min per 1·73 m² or initiation of chronic dialysis or kidney transplantation. ‡Comprises the composite kidney outcome, or heart failure hospitalisation or cardiovascular death. §Heart failure hospitalisation or cardiovascular death.

	Events or participants		Event rate per 1000 patient-years		HR (95% CI)	p value
	Finerenone (n=7291)	Placebo (n=7283)	Finerenone	Placebo		
Kidney failure or ≥57% decline in eGFR	460	589	22·3	28·8	0·76 (0·68–0·86)	<0·0001
Kidney failure, ≥57% decline in eGFR, or cardiovascular death	612	763	29·7	37·3	0·79 (0·71–0·88)	<0·0001
Kidney failure, ≥57% decline in eGFR, heart failure hospitalisation, or cardiovascular death	786	997	38·6	49·6	0·77 (0·70–0·85)	<0·0001
Kidney failure	346	399	16·7	19·4	0·85 (0·74–0·99)	0·030
Dialysis or kidney transplantation	189	240	8·5	10·9	0·77 (0·64–0·94)	0·0089
Heart failure hospitalisation	263	334	12·0	15·3	0·78 (0·66–0·92)	0·0024
Heart failure hospitalisation or cardiovascular death	420	520	19·1	23·9	0·80 (0·70–0·91)	0·0006
Cardiovascular death	182	220	8·1	9·9	0·82 (0·67–0·999)	0·049
All-cause death	569	642	25·4	28·8	0·88 (0·79–0·99)	0·026

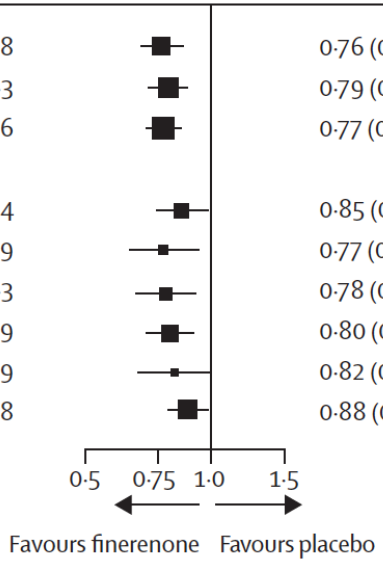

Figure 2: **Kidney, cardiovascular, and mortality outcomes in the overall INFINITY population**

Shown are prespecified kidney and cardiovascular efficacy outcomes, assessed in time-to-event analyses. Kidney failure was defined as sustained eGFR <15 mL/min per 1·73 m^2, initiation of chronic dialysis, or kidney transplantation. Cardiovascular death in this analysis excluded deaths classified as undetermined. eGFR=estimated glomerular filtration rate. HR=hazard ratio.

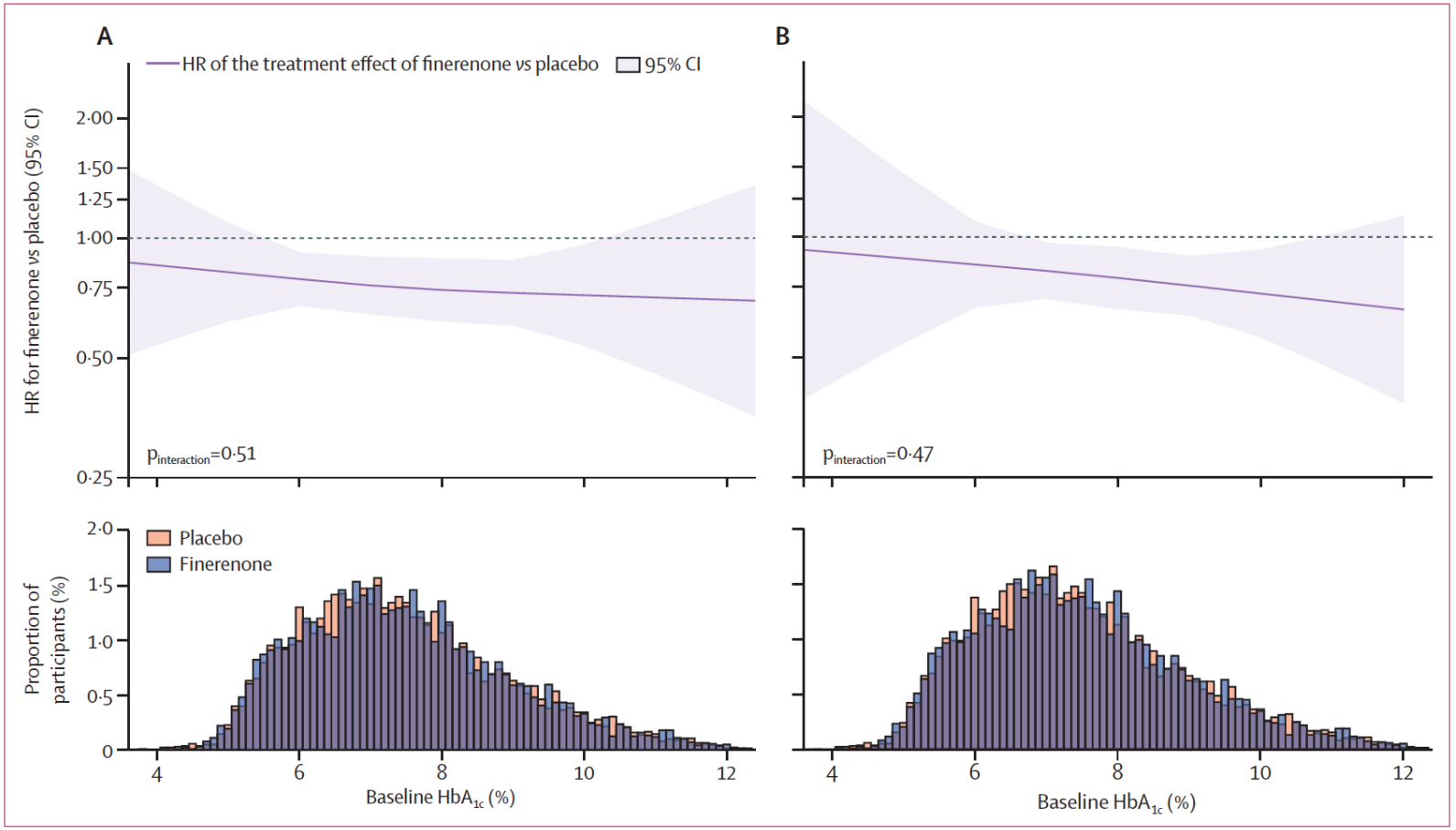

***Figure 3*: Effects of finerenone on the composite kidney outcome and the composite cardiovascular outcome across the spectrum of glycated haemoglobin**

The solid line shows the HR for the treatment effect of finerenone relative to placebo on the main composite kidney outcome (A) and the main composite cardiovascular outcome (B), with the shading indicating the 95% CI. The kidney composite outcome included a sustained 57% or more decline in eGFR or kidney failure. The cardiovascular composite outcome included hospitalisation for heart failure or cardiovascular death. The distribution of baseline HbA_{1c} is shown in the histograms at the bottom of each panel. HbA_{1c}=glycated haemoglobin. HR=hazard ratio.

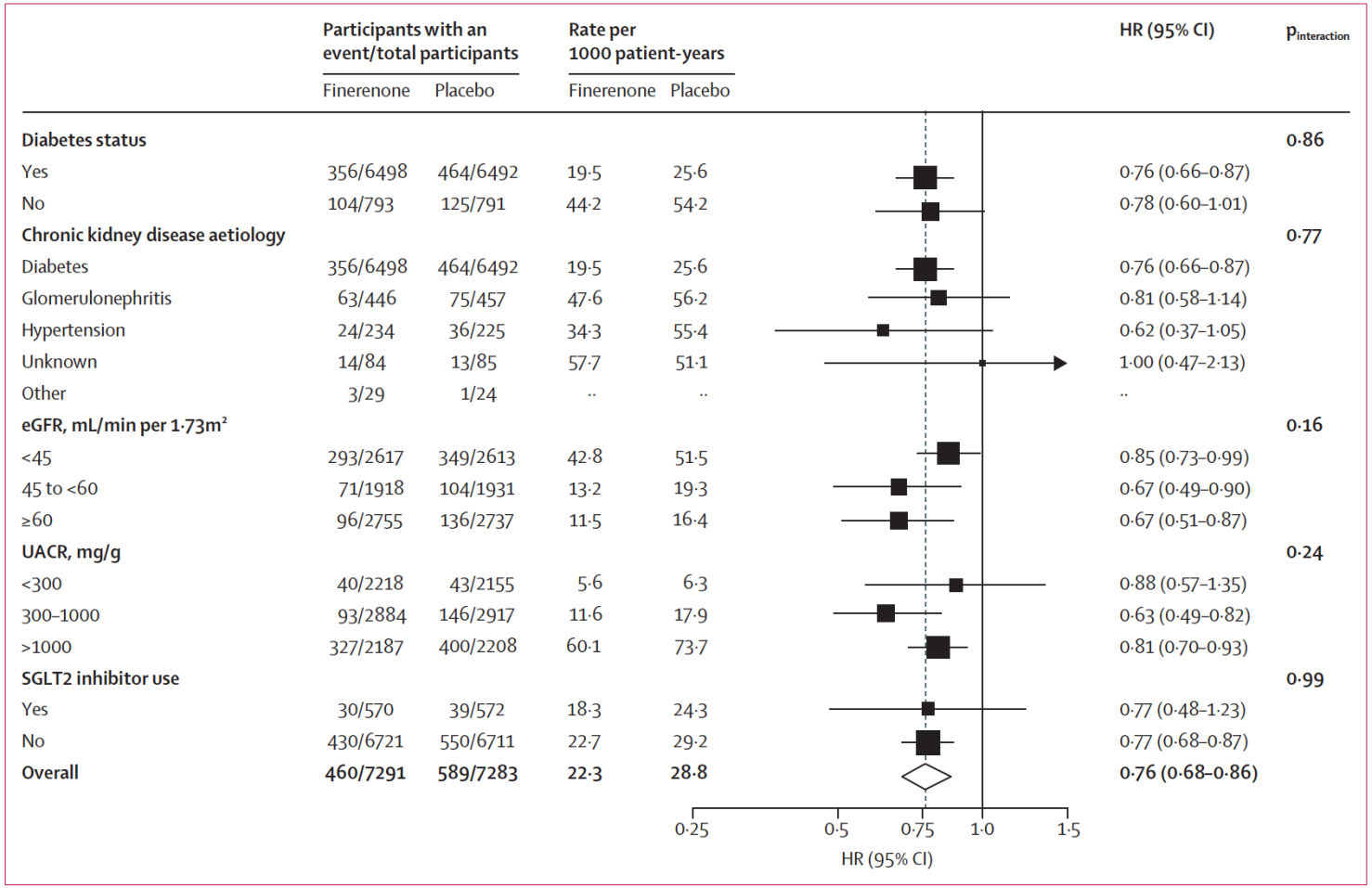

Figure 4: **Effect of finerenone on the composite kidney outcome across prespecified subgroups**

Analyses conducted based on stratified Cox models fitted across subgroup categories, including covariates treatment, subgroup, and the respective interaction. Heterogeneity between subgroups was assessed via the interaction p-value. eGFR=estimated glomerular filtration rate. HR=hazard ratio. SGLT2=sodium–glucose co-transporter-2. UACR=urinary albumin-to-creatinine ratio.

	Finerenone (n=7282)	Placebo (n=7265)
Any treatment-emergent adverse event	6124 (84·1%)	6109 (84·1%)
Any treatment-emergent adverse event leading to permanent discontinuation of study drug	431 (5·9%)	373 (5·1%)
Any treatment-emergent serious adverse event	2220 (30·5%)	2349 (32·3%)
Treatment-emergent serious adverse event leading to permanent discontinuation of study drug	146 (2·0%)	162 (2·2%)
Hypotension	350 (4·8%)	224 (3·1%)
Acute kidney injury*	243 (3·3%)	259 (3·6%)
Serious acute kidney injury requiring hospitalisation*	94 (1·3%)	94 (1·3%)
Any treatment-emergent hyperkalaemia	1043 (14·3%)	553 (7·6%)
Leading to permanent discontinuation of study drug	122 (1·7%)	39 (0·5%)
Any serious hyperkalaemia	77 (1·1%)	21 (0·3%)
Requiring hospitalisation	68 (0·9%)	15 (0·2%)
Life threatening	5 (0·1%)	5 (0·1%)
With fatal outcome	0	0
Any treatment-emergent hypokalaemia	74 (1·0%)	165 (2·3%)
Any serious hypokalaemia	3 (<0·1%)	11 (0·2%)
Requiring hospitalisation	2 (<0·1%)	11 (0·2%)
Potassium level		
<3·5 mmol/L	256/7058 (3·6%)	564/7035 (8·0%)
>5·5 mmol/L	1218/7154 (17·0%)	565/7128 (7·9%)
>6·0 mmol/L	245/7201 (3·4%)	98/7179 (1·4%)

Data are n (%) or n/N (%). Adverse events that started or worsened after the first dose of study drug up to 3 days after any temporary or permanent interruption of study drug were considered as treatment-emergent adverse events.
*Preferred term.

Table 2: **Treatment-emergent adverse events**

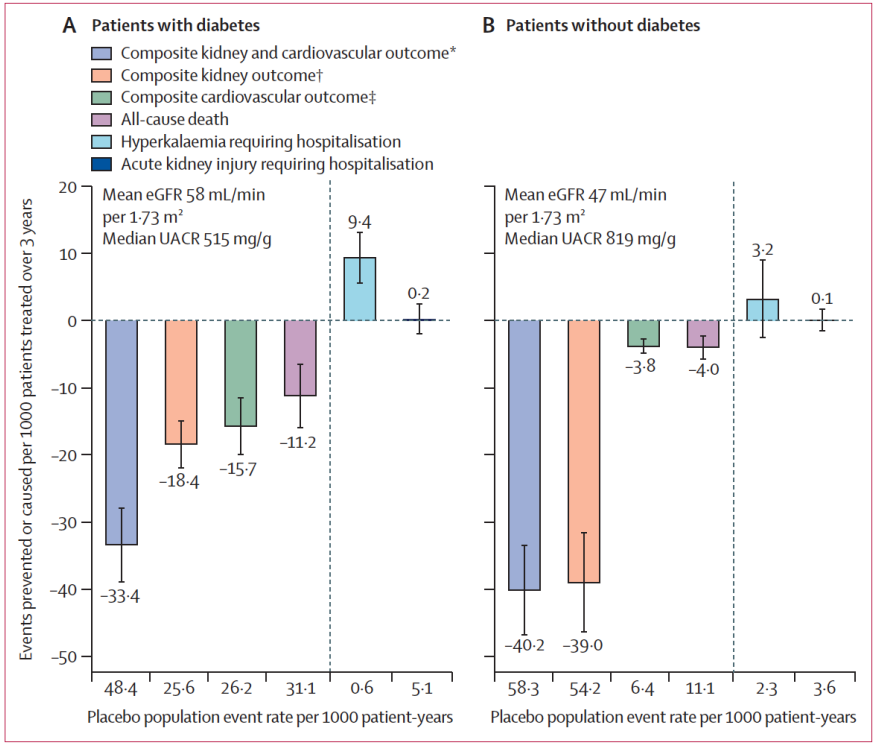

Figure 5: **Estimated absolute effects of finerenone per 1000 patients treated over 3 years by diabetes status**
Estimated absolute numbers of events prevented (negative numbers) or caused (positive values) per 1000 patients treated for 3 years are shown. Error bars represent SE estimated from uncertainty in the hazard ratios. Placebo population event rates are the numbers of events per 1000 patient-years in the placebo groups of all trials in the relevant subpopulation. eGFR=estimated glomerular filtration rate. UACR=urinary albumin-to-creatinine ratio. *The composite kidney outcome, or heart failure hospitalisation or cardiovascular death. †Sustained 57% or more decline in eGFR relative to baseline or kidney failure. Kidney failure was defined as sustained eGFR <15 mL/min per 1·73 m² or initiation of chronic dialysis or kidney transplantation. ‡Heart failure hospitalisation or cardiovascular death. Cardiovascular death in this analysis excluded deaths classified as undetermined.

Research in context

Evidence before this study

In a systematic review conducted in 2024, we searched PubMed and MEDLINE from database inception to July 24, 2024, for phase 3, randomised, double-blind, placebo-controlled trials evaluating the efficacy and safety of finerenone, a nonsteroidal mineralocorticoid receptor antagonist, using the terms "finerenone" and "randomized controlled trial". We applied no language restrictions to this search. The review identified two phase 3 trials in patients with chronic kidney disease (CKD) and type 2 diabetes: FIDELIO-DKD and FIGARO-DKD. Together, these trials enrolled 12 990 participants with a median follow-up of 3 years. The trials showed that finerenone reduced the risk of CKD progression and cardiovascular events, findings that supported regulatory approval and subsequent recommendations in clinical practice guidelines for this population. However, most cases of CKD worldwide are not attributable to diabetes, and at the time of the systematic review there was no robust evidence regarding the efficacy or safety of finerenone in patients with CKD without diabetes. Since then, the FINEARTS-HF trial showed that finerenone reduced heart failure events in 6001 individuals with heart failure with mildly reduced or preserved ejection fraction. Although this trial included individuals without diabetes, it was not designed to assess kidney outcomes. Consequently, guideline recommendations for finerenone in CKD have remained restricted to patients with diabetes.

Added value of this study

More recently, the FIND-CKD trial showed that finerenone reduced the rate of kidney function loss in patients with CKD who did not have diabetes, extending the evidence for finerenone beyond CKD and type 2 diabetes, but without providing a comprehensive evaluation of effects on kidney and cardiovascular outcomes across the full spectrum of CKD, or reliable estimates on outcomes such as kidney failure and mortality. To address this limitation, we updated the previous systematic review and conducted an individual participant data meta-analysis of the FIDELIO-DKD, FIGARO-DKD, and FIND-CKD trials. In 14 574 individuals followed up for a median of 3·1 years, finerenone reduced the risk of a composite kidney outcome comprising kidney failure or sustained 57% or more decline in estimated glomerular filtration rate (eGFR; hazard ratio 0·76 [95% CI 0·68–0·86]), with clear reduction in kidney failure alone (0·85 [0·74–0·99]). Finerenone reduced the risk of heart failure hospitalisation or cardiovascular death (0·80 [0·70–0·91]), driven by both heart failure hospitalisation (0·78 [0·66–0·92]) and cardiovascular death (0·82 [0·67–0·999]). In addition, finerenone also reduced the risk of all-cause death (0·88 [0·79–0·99]). Effects on the composite kidney and cardiovascular outcomes were broadly consistent across a range of prespecified subgroups, including glycaemic status, cause of kidney disease, eGFR, albuminuria, and use of sodium–glucose co-transporter-2 inhibitors. Although finerenone increased the incidence of hyperkalaemia compared with placebo (14·3% *vs* 7·6%), events leading to hospitalisation were uncommon (0·9% *vs* 0·2%) with no deaths attributable to hyperkalaemia. Although the absolute risk of cardiovascular events and mortality differed by diabetes status, absolute estimates showed that the net kidney, cardiovascular, and mortality benefits of finerenone outweighed adverse effects, irrespective of diabetes status.

Implications of all the available evidence

The totality of the randomised evidence supports the role of finerenone as a foundational therapy to improve kidney and cardiovascular outcomes in patients with CKD across a broad range of disease aetiologies, spectrum of glycaemia, eGFR, and albuminuria.

Der **Endothelin-A-Rezeptor** ist ein G-Protein-gekoppelter Rezeptor im menschlichen Körper, der eine **entscheidende Rolle bei der Regulierung des Blutdrucks** und des Gefäßtonus spielt.

Physiologische Funktionen

•**Vasokonstriktion**: Befindet sich auf glatten Gefäßmuskelzellen und vermittelt eine starke Gefäßverengung.

•**Zellproliferation**: Reguliert das Wachstum von Gefäßmuskelzellen und trägt zum Gefäßumbau (Remodeling) bei.

•**Flüssigkeitsbalance**: Beeinflusst die Natrium- und Wasserretention in den Nieren.

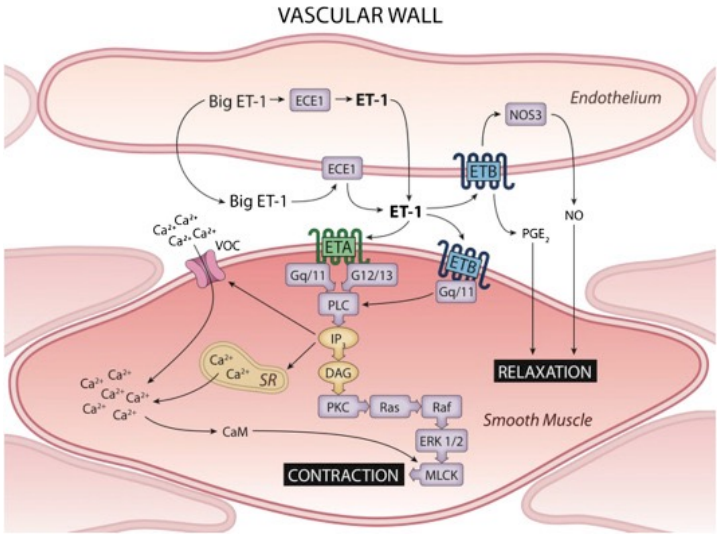

ETB-R is said to release NO; therefore „good“

Unterschied zum ETB Rezeptor

Während der ETA-Rezeptor auf den Muskelzellen primär gefäßverengend wirkt, befindet sich der ETB-Rezeptor hauptsächlich auf den Endothelzellen. Seine Aktivierung führt über die Freisetzung von Stickstoffoxid (NO) zu einer Gefäßerweiterung (Vasodilation) und dient dem Abbau von überschüssigem Endothelin.

Atrasentan ist ein selektiver Endothelin-A-Rezeptorantagonist (ERA). Das verschreibungspflichtige Medikament wird zur Senkung der Proteinurie (Eiweißausscheidung im Urin) bei Patienten mit primärer Immunglobulin-A-Nephropathie (IgAN) eingesetzt, bei denen ein hohes Risiko für eine rasche Verschlechterung der Nierenfunktion besteht.

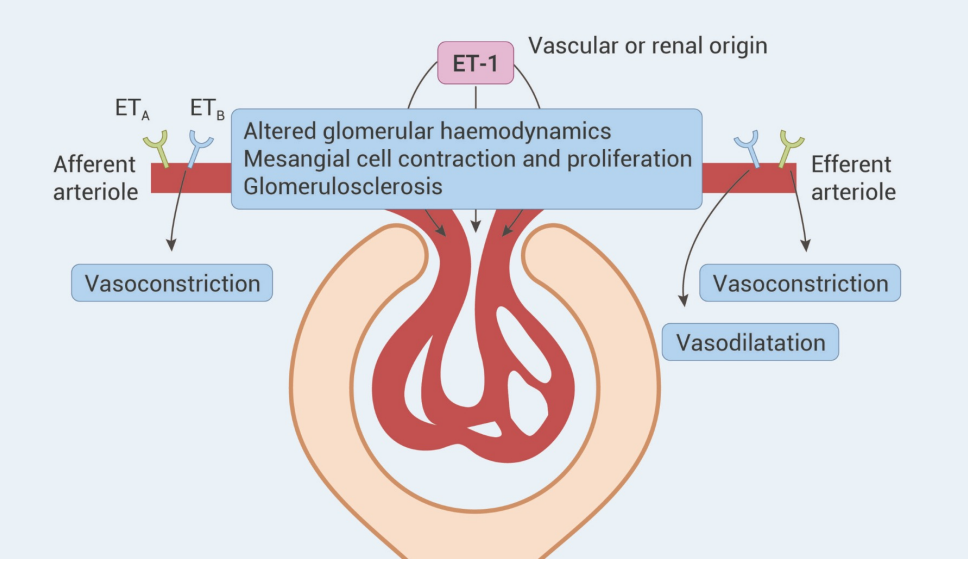

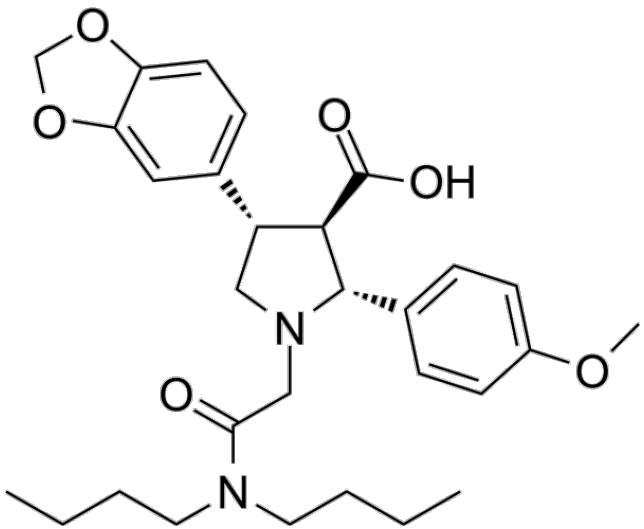

Does atrasentan help?

Atrasentan in patients with IgA nephropathy (ALIGN): final 2·5-year results from a randomised, double-blind, placebo-controlled, phase 3 trial

Summary

Background Atrasentan, a selective endothelin A receptor antagonist, reduced proteinuria in the prespecified interim analysis (week 36) of the ALIGN trial in adults with IgA nephropathy. We assessed whether atrasentan slowed estimated glomerular filtration rate (eGFR) decline after 2·5 years' treatment.

Methods We performed a randomised, double-blind, placebo-controlled, phase 3 trial (133 sites, 20 countries). Adults with biopsy-proven IgA nephropathy, eGFR of at least 30 mL/min per 1·73 m², and urinary protein excretion of at least 1·0 g/day while receiving renin–angiotensin system inhibition were enrolled (main stratum). An exploratory stratum enrolled participants also receiving an SGLT2 inhibitor. Participants were randomly assigned (1:1) to oral atrasentan 0·75 mg once daily or placebo for 132 weeks, followed by a 4-week off-treatment follow-up. The key secondary endpoint was change from baseline to week 136 in eGFR in the main stratum, assessed in all randomised patients (excluding data after intercurrent events, defined as initiation of restricted or alternative IgA nephropathy medications or kidney replacement therapy). Safety was assessed in all randomised patients who received at least one dose of study treatment. ALIGN is registered with ClinicalTrials.gov, NCT04573478; the double-blind section is complete, and the open-label extension is ongoing.

Findings Between March 15, 2021, and April 28, 2023, 404 participants were randomly assigned (main stratum: 340; SGLT2 inhibitor stratum: 64). In the main stratum, change from baseline in eGFR at week 136 was −7·5 mL/min per 1·73 m² (95% CI −9·2 to −5·8) with atrasentan and −9·9 mL/min per 1·73 m² (−11·7 to −8·1) with placebo (between-group difference 2·4 mL/min per 1·73 m²; 95% CI −0·1 to 4·8; p=0·057). The between-group difference in eGFR change from baseline at end of treatment (week 132) was 2·6 mL/min per 1·73 m² (95% CI 0·1–5·0), and the difference in total eGFR slope (baseline to week 136) was 1·4 mL/min per 1·73 m² per year (95% CI 0·5–2·3). In the SGLT2 inhibitor stratum, the difference in eGFR change from baseline at week 136 between atrasentan and placebo was 9·1 mL/min per 1·73 m² (95% CI 3·0–15·2). Treatment-emergent adverse events were well balanced between atrasentan and placebo, with no new safety signals. In the main stratum, fluid retention adverse events occurred in 24 (14%) of 169 patients receiving atrasentan and 20 (12%) of 170 receiving placebo.

Interpretation Atrasentan reduced proteinuria and preserved kidney function after 2·5 years. This effect was present with or without concomitant SGLT2 inhibitor use. Atrasentan was well tolerated.

	Main stratum (non-SGLT2 inhibitor)		SGLT2 inhibitor stratum		Pooled strata (main + SGLT2 inhibitor strata)	
	Atrasentan (n=170)	Placebo (n=170)	Atrasentan (n=32)	Placebo (n=32)	Atrasentan (n=202)	Placebo (n=202)
Age, years						
Mean (SD)	45·8 (12·7)	43·7 (11·2)	47·3 (12·7)	47·1 (11·5)	46·0 (12·7)	44·2 (11·3)
Median (IQR)	46·0 (38·0–54·0)	43·0 (35·0–50·0)	47·5 (38·0–56·0)	44·5 (37·0–55·5)	46·0 (38·0–54·0)	43·5 (35·0–51·0)
Sex						
Male	103 (61%)	93 (55%)	21 (66%)	17 (53%)	124 (61%)	110 (54%)
Female	67 (39%)	77 (45%)	11 (34%)	15 (47%)	78 (39%)	92 (46%)
Race						
Asian	89 (52%)	97 (57%)	12 (38%)	14 (44%)	101 (50%)	111 (55%)
Black	4 (2%)	1 (1%)	1 (3%)	0	5 (2%)	1 (0%)
Other	15 (9%)*	14 (8%)†	3 (9%)‡	0	18 (9%)	14 (7%)
White	62 (36%)	58 (34%)	16 (50%)	18 (56%)	78 (39%)	76 (38%)
Bodyweight, kg						
Mean (SD)	77·2 (20·3)	76·7 (21·1)	81·5 (22·6)	82·0 (27·1)	77·9 (20·6)	77·6 (22·1)
Median (IQR)	73·8 (63·4–89·4)	72·8 (63·6–83·7)	77·5 (66·1–93·0)	76·0 (63·2–99·5)	74·5 (63·4–89·4)	73·1 (63·6–84·3)
Mean (SD) blood pressure, mm Hg§						
Diastolic	79·4 (9·6)	78·9 (8·9)	83·2 (11·0)	79·2 (7·9)	80·0 (9·9)	78·9 (8·8)
Systolic	125·1 (13·0)	123·1 (12·3)	126·3 (13·9)	125·3 (12·0)	125·3 (13·1)	123·4 (12·3)
Mean (SD) duration of disease, years¶	5·3 (5·6)	5·7 (6·2)	6·2 (6·1)	5·2 (4·9)	5·4 (5·7)	5·6 (6·0)
Median (IQR) total urinary protein excretion, g/day‖	1·8 (1·3–2·6)	1·8 (1·3–2·6)	2·1 (1·5–2·6)	1·9 (1·4–2·8)	1·9 (1·4–2·6)	1·9 (1·3–2·7)
Median (IQR) 24-h UPCR, g/g‖	1·4 (1·0–2·0)	1·4 (1·1–1·9)	1·3 (1·1–1·9)	1·4 (1·0–2·0)	1·4 (1·0–2·0)	1·4 (1·1–1·9)
UPCR distribution‖						
<1·5 g/g	91 (54%)	93 (55%)	18 (56%)	19 (59%)	109 (54%)	112 (55%)
≥1·5 g/g	79 (46%)	77 (45%)	14 (44%)	13 (41%)	93 (46%)	90 (45%)
Median (IQR) 24-h UACR, g/g‖	1·1 (0·8–1·5)	1·1 (0·8–1·5)	0·9 (0·7–1·3)	1·0 (0·8–1·3)	1·0 (0·8–1·5)	1·1 (0·8–1·5)
Mean (SD) eGFR, mL/min per 1·73 m²**	58·1 (23·6)	59·7 (24·3)	57·4 (23·5)	48·6 (20·2)	58·0 (23·5)	57·9 (24·0)
eGFR distribution**						
≤60 mL/min per 1·73 m²	103 (61%)	100 (59%)	19 (59%)	23 (72%)	122 (60%)	123 (61%)
>60 mL/min per 1·73 m²	67 (39%)	70 (41%)	13 (41%)	9 (28%)	80 (40%)	79 (39%)
Mean (SD) BNP, pg/mL††	22·2 (21·3)	20·4 (20·8)	20·5 (22·6)	23·4 (25·8)	22·0 (21·5)	20·8 (21·6)
Medication‡‡						
Use of RAS inhibitor						
ACE inhibitor only	48 (28%)	51 (30%)	10 (31%)	9 (28%)	58 (29%)	60 (30%)
ARB only	121 (71%)	115 (68%)	22 (69%)	22 (69%)	143 (71%)	137 (68%)
Both	0	1 (1%)	0	0	0	2 (1%)
None	1 (1%)	3 (2%)	0	1 (3%)	1 (0%)	3 (1%)
Use of diuretics§§	26 (15%)	17 (10%)	7 (22%)	7 (22%)	33 (16%)	24 (12%)

Data are n (%) unless otherwise stated. ACE=angiotensin-converting enzyme. ARB=angiotensin receptor blocker. ATC=Anatomical Therapeutic Chemical. BNP=B-type natriuretic peptide. eGFR=estimated glomerular filtration rate. RAS=renin–angiotensin system. UACR=urine albumin-to-creatinine ratio. UPCR=urine protein-to-creatinine ratio. *Other includes American Indian or Alaska Native (n=4), not reported (n=3), multiple races reported (n=8). †Other includes American Indian or Alaska Native (n=1), not reported (n=1), multiple races reported (n=12). ‡Other includes not reported (n=3). §Baseline blood pressure value is based on the arithmetic mean of the triplicate results collected at the last assessment on or before study day 1. ¶Duration of IgA nephropathy (time from most recent biopsy to baseline) is calculated as number of years between the most recent date of biopsy and first dose date. ‖Baseline 24-h UPCR, UACR, and total urine protein values are based on the geometric mean of the two latest samples on or before study day 1. **Baseline eGFR value is based on the arithmetic mean of the two latest samples on or before study day 1. ††Baseline BNP values below the lower limit of quantification (2·0 pg/mL) are imputed as 1·9 pg/mL. ‡‡Medications coded using the WHO dictionary B3 202509. §§Includes drugs with a WHO dictionary ATC class of "diuretics".

Table 1: **Patient baseline characteristics**

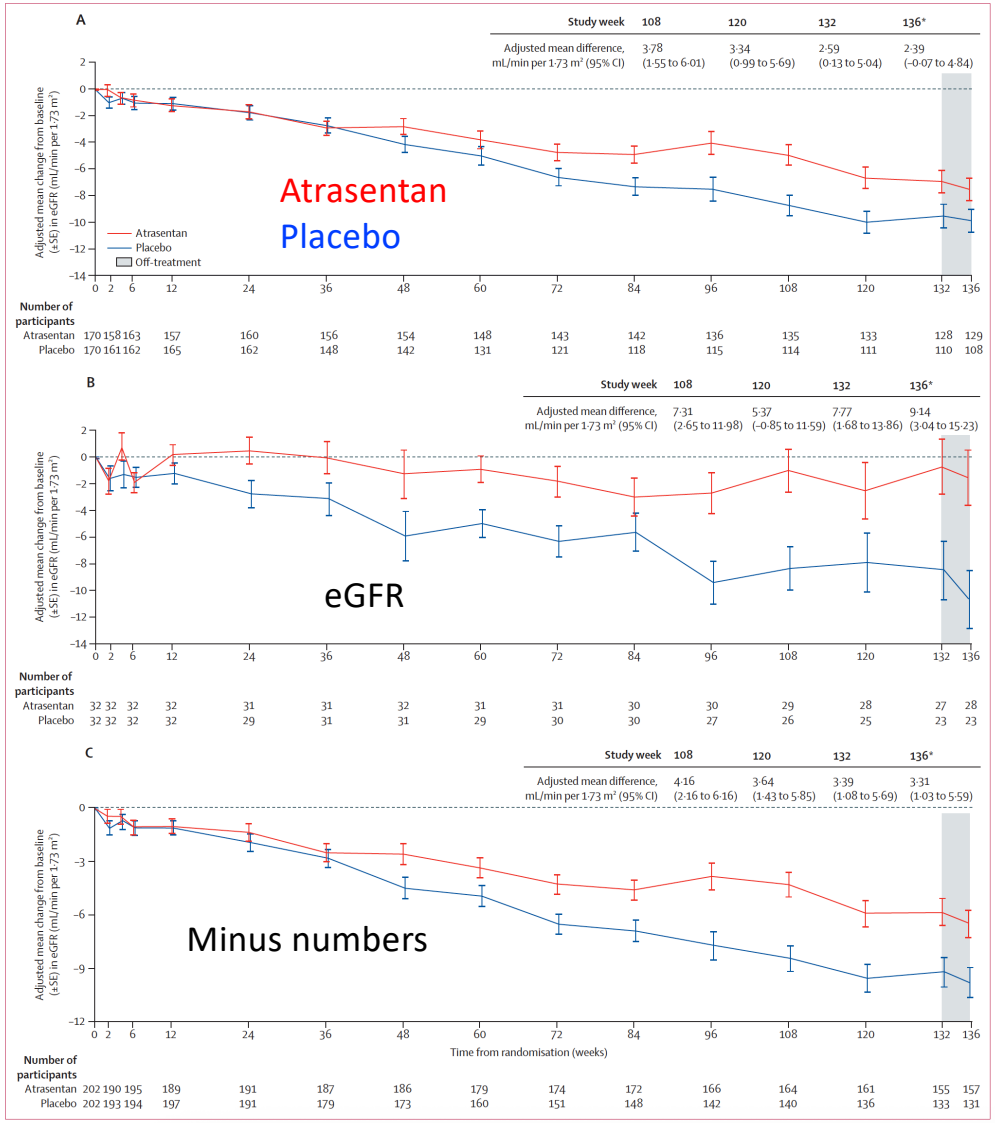

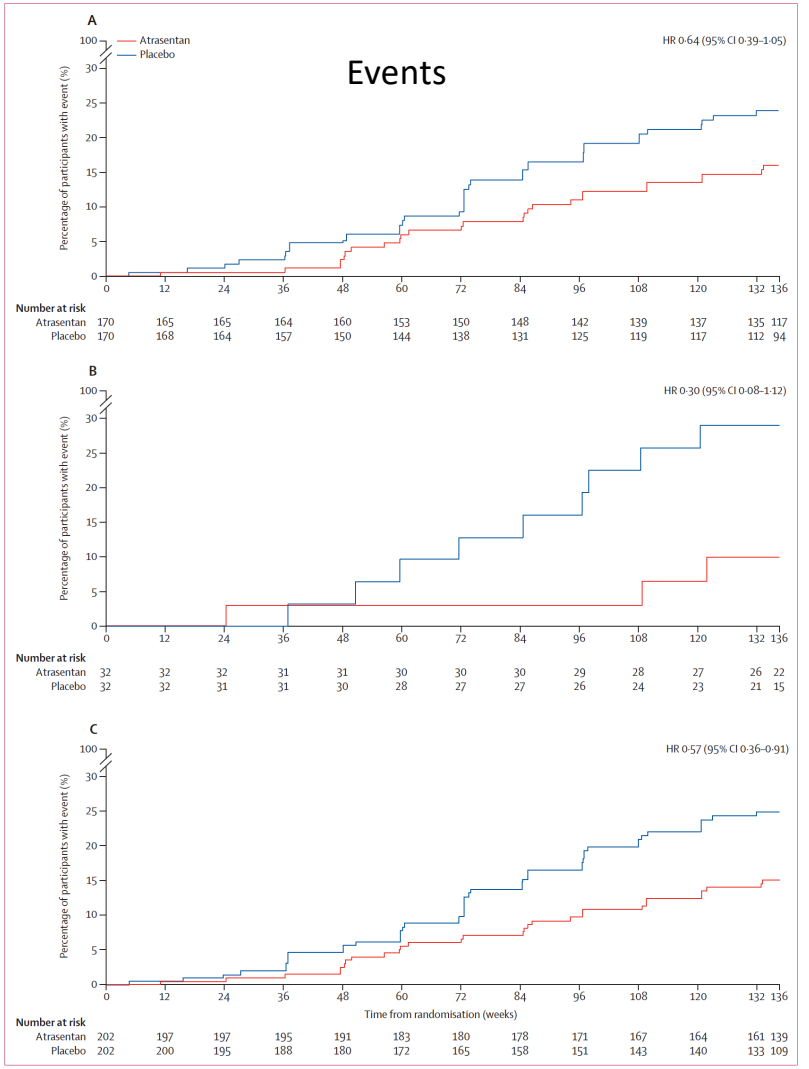

***Figure 3*: Kaplan–Meier curves for composite kidney outcome with ≥30% reduction in eGFR in the main stratum (A), SGLT2 inhibitor stratum (B), and pooled strata (C)**

Time from randomisation reflects actual time to event and not the specified study visit window. eGFR=estimated glomerular filtration rate. HR=hazard ratio.

	Main stratum		SGLT2 inhibitor stratum	
	Atrasentan (n=169)	Placebo (n=170)	Atrasentan (n=32)	Placebo (n=32)
Any TEAE	157 (93%)	159 (94%)	30 (94%)	27 (84%)
TEAEs occurring in >10% of patients in either group*				
COVID-19	39 (23%)	44 (26%)	3 (9%)	4 (13%)
Nasopharyngitis	27 (16%)	18 (11%)	8 (25%)	5 (16%)
Peripheral oedema	22 (13%)	15 (9%)	3 (9%)	2 (6%)
Hyperkalaemia	19 (11%)	14 (8%)	1 (3%)	2 (6%)
Influenza	19 (11%)	14 (8%)	2 (6%)	3 (9%)
Upper respiratory tract infection	16 (9%)	23 (14%)	2 (6%)	3 (9%)
Pyrexia	16 (9%)	14 (8%)	4 (13%)	1 (3%)
Back pain	13 (8%)	20 (12%)	2 (6%)	5 (16%)
Headache	12 (7%)	14 (8%)	5 (16%)	5 (16%)
Nausea	12 (7%)	10 (6%)	4 (13%)	4 (13%)
Vomiting	6 (4%)	2 (1%)	3 (9%)	4 (13%)
Arthralgia	9 (5%)	9 (5%)	0	4 (13%)
Any serious TEAE	24 (14%)	26 (15%)	3 (9%)	4 (13%)
Any severe TEAE	22 (13%)	17 (10%)	2 (6%)	1 (3%)
Any treatment-related TEAE	36 (21%)	24 (14%)	6 (19%)	3 (9%)
Any treatment-related serious TEAE	1 (1%)	1 (1%)	0	0
Any TEAE leading to death†	1 (1%)	1 (1%)	0	0
Any TEAE leading to study drug discontinuation	6 (4%)	10 (6%)	1 (3%)	2 (6%)
Any TEAE leading to study discontinuation	0	0	0	0
Any TEAE of special interest‡	48 (28%)	34 (20%)	3 (9%)	7 (22%)
Anaemia	19 (11%)	7 (4%)	0	3 (9%)
Cardiac failure	0	0	0	0
Fluid retention	24 (14%)	20 (12%)	3 (9%)	2 (6%)
Vasodilation or hypotension	14 (8%)	11 (6%)	1 (3%)	2 (6%)
Any serious TEAE of special interest	1 (1%)	1 (1%)	0	1 (3%)
Any moderate or severe TEAE of special interest	13 (8%)	15 (9%)	0	1 (3%)
Any TEAE of special interest leading to discontinuation of study drug	0	0	1 (3%)	0

Data are n (%). Adverse events were coded using MedDRA, version 28.1. Shown are TEAEs that emerged or worsened in severity on or after the date of first study drug administration and within 30 days after the last dose of study drug. FMQ=Food and Drug Administration Medical Query. MedDRA=Medical Dictionary for Regulatory Activities. TEAE=treatment-emergent adverse event. *Adverse events are ordered by descending frequency in the main stratum (atrasentan group). †Deaths due to amyotrophic lateral sclerosis in the atrasentan group and pneumonia in the placebo group (these events were assessed as not related to the study drug). ‡Adverse events of special interest are shown according to FMQ category, using FMQ peripheral oedema—narrow and peripheral oedema—broad for fluid retention, FMQ anaemia—narrow for anaemia, FMQ hypotension—narrow for vasodilation or hypotension, and FMQ heart failure—narrow for cardiac failure.

Table 2: **TEAEs in the main and SGLT2 inhibitor strata**

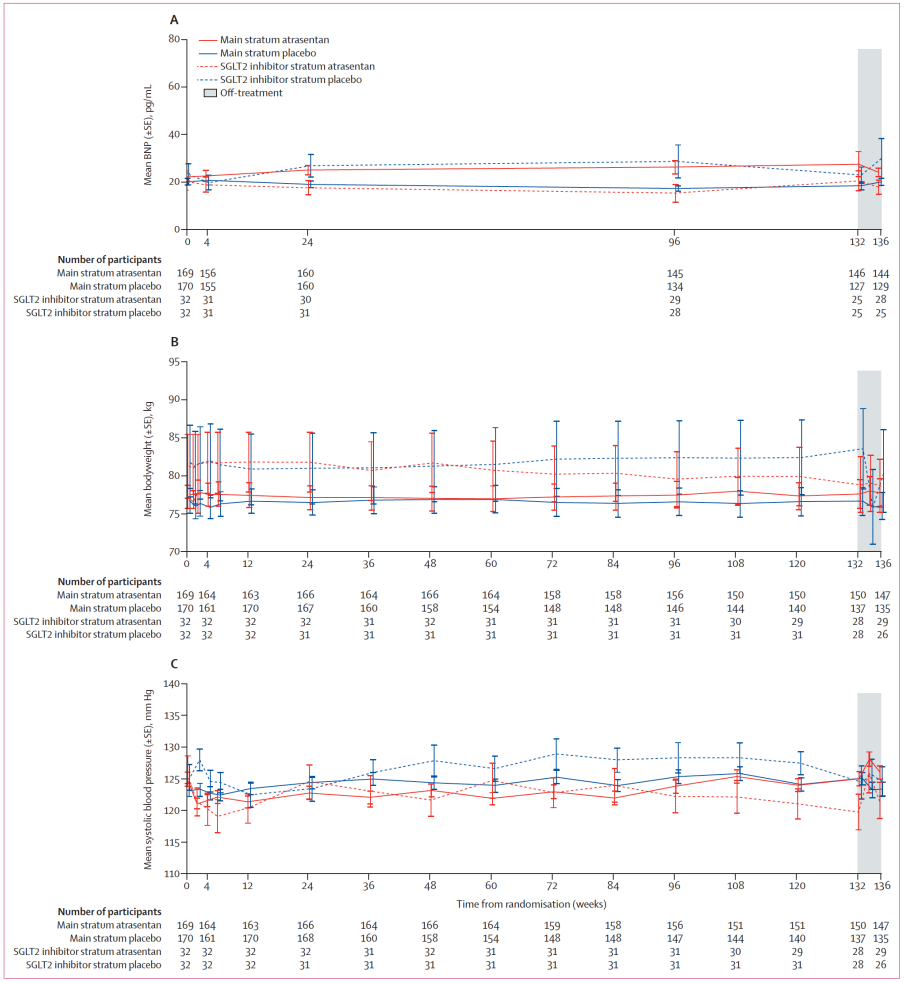

(Figure 4 continues on next page)

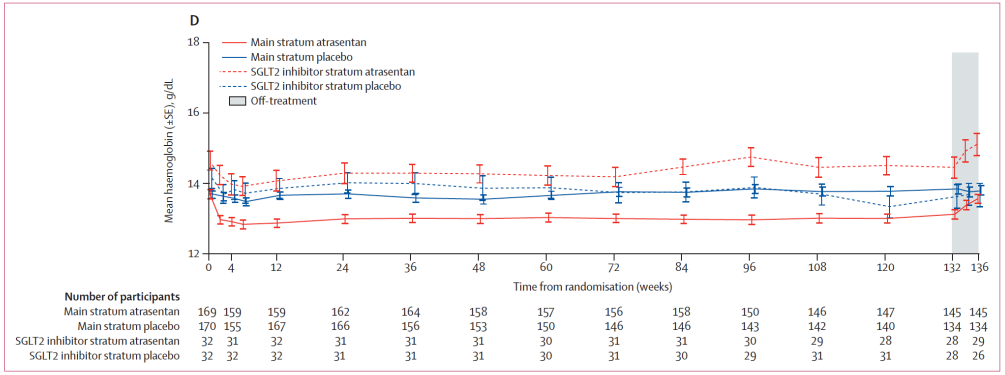

Figure 4: **Values by study visit from baseline to week 136 in the main and SGLT2 inhibitor strata for BNP (A), bodyweight (B), systolic blood pressure (C), and haemoglobin (D)**
In the main stratum, BNP concentrations remained stable over the treatment duration with the mean within the reference ranges by age for a healthy person and returned to nearly pre-treatment values during the off-treatment follow-up. Reference ranges of BNP (pg/mL): age 0–44 years: 2·7–33·3; age 45–54 years: 2·7–46·7; age 55–64 years: 2·7–53·2; age 65–74 years: 2·7–72·3; age ≥75 years: 2·7–176·0. In the main stratum, haemoglobin concentrations remained stable and within the reference ranges for a healthy person over the treatment duration and returned to nearly pre-treatment values during the off-treatment follow-up. Reference ranges of haemoglobin (g/dL): female age 12–65 years: 11·6–16·2; female age ≥66 years: 11·0–16·1; male age 18–65 years: 13·0–17·5; male age ≥66 years: 13·0–17·7. BNP=B-type natriuretic peptide.

Implications of all the available evidence

The ALIGN results, together with prior studies, suggest that selective endothelin A receptor antagonism with atrasentan provides early and sustained proteinuria reduction and preserves kidney function in patients with IgA nephropathy, while being well tolerated. Given the directionally concordant effects in the main and exploratory SGLT2 inhibitor strata, these findings support atrasentan as a non-immunosuppressive option that can be added on top of supportive care. Collectively, these data support consideration of atrasentan as a component of long-term disease management that could improve kidney survival in patients with IgA nephropathy.

Der Hauptgrund für die zusätzliche Stimulation des Glukagonrezeptors (neben GLP-1 und GIP) bei Retatrutid ist die **Steigerung des Energieverbrauchs (Kalorienverbrennung)**. Während GLP-1 und GIP vor allem das Hungergefühl reduzieren und die Insulinausschüttung fördern, kurbelt Glukagon den Stoffwechsel an.

Die wichtigsten Mechanismen und der therapeutische Nutzen in der Übersicht:

•**Gesteigerte Energieverbrennung:** Die Aktivierung des Glukagonrezeptors regt die Thermogenese an, wodurch der Körper im Ruhezustand mehr Kalorien verbrennt.

•**Fettverbrennung (Lipolyse):** Sie fördert den Abbau von Fettreserven zur Energiegewinnung und beschleunigt die Oxidation von Leberfetten.

•**Synergieeffekt:** Die potenzielle blutzuckersteigernde Wirkung von Glukagon wird durch die starken blutzuckersenkenden Effekte der gleichzeitig stimulierten GLP-1- und GIP-Rezeptoren mehr als ausgeglichen.

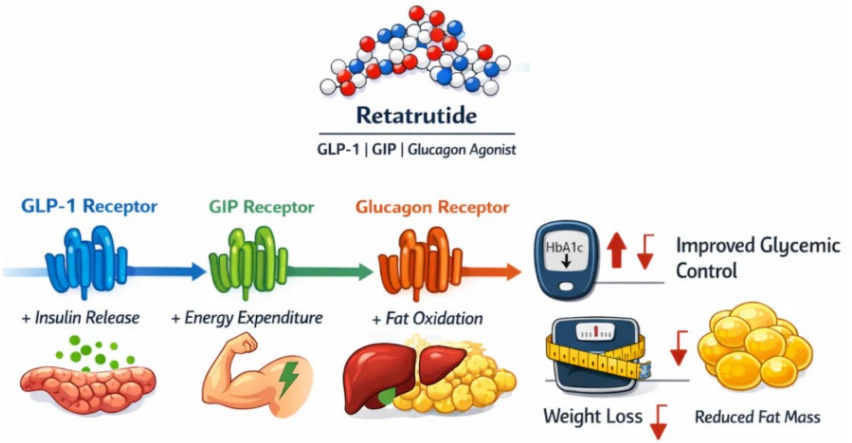

Retatrutide & Glucagon Signaling in Type 2 Diabetes

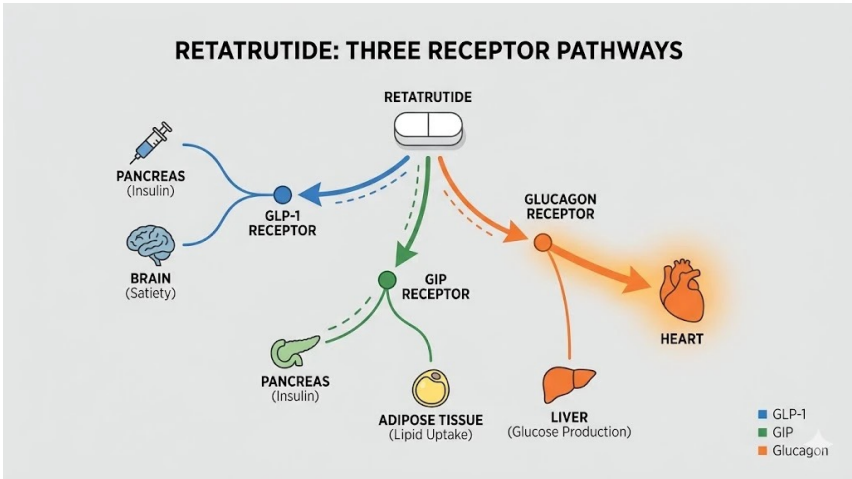

A triple threat for obesity diabetes

Efficacy and safety of retatrutide, a GIP, GLP-1, and glucagon receptor agonist, in people with type 2 diabetes and inadequate glycaemic control with diet and exercise (TRANSCEND-T2D-1): a double-blind, randomised, phase 3 trial

Summary

Background Retatrutide is a GIP, GLP-1, and glucagon triple hormone receptor agonist, under clinical development for type 2 diabetes, obesity, and related complications. We aimed to assess the efficacy and safety of retatrutide as a monotherapy in people with type 2 diabetes that is inadequately controlled by diet and exercise alone.

Methods In this 40-week, phase 3, randomised, double-blind, placebo-controlled trial at 48 sites in the USA, Mexico, and India, we recruited adults (aged ≥18 years) with type 2 diabetes that is inadequately controlled by diet and exercise alone, glycated haemoglobin (HbA_{1c}) between 7·0% and 9·5% (53–80 mmol/mol), and BMI of at least 23 kg/m². Participants were randomly assigned (1:1:1:1) to receive retatrutide (4 mg, 9 mg, or 12 mg) or placebo by once-weekly subcutaneous injection. The primary endpoint was the change in HbA_{1c} concentration from baseline to week 40. A key secondary endpoint was the percentage change in bodyweight from baseline to week 40. This trial is registered with ClinicalTrials.gov, NCT06354660, and is completed.

Findings Between April 10, 2024, and April 21, 2025, 930 participants were screened and 537 (296 [55%] female and 241 [45%] male) were randomly assigned: 134 to retatrutide 4 mg, 133 to retatrutide 9 mg, 136 to retatrutide 12 mg, and 134 to placebo. Baseline mean age was 48·8 years (SD 12·1), mean HbA_{1c} concentration was 7·9% (SD 1·1), mean duration of diabetes was 2·5 years (SD 4·4), and mean BMI was 35·8 kg/m² (SD 7·0). 490 (91%) participants completed the treatment period on study drug and 504 (94%) completed the study. For the treatment regimen estimand, the mean change from baseline in HbA_{1c} concentration was –1·69% (SE 0·11) with retatrutide 4 mg, –1·86% (0·10) with 9 mg, and –1·94% (0·08) with 12 mg, versus –0·81% (0·12) with placebo, resulting in estimated treatment differences versus placebo of –0·88% (95% CI –1·18 to –0·59) with retatrutide 4 mg, –1·04% (–1·32 to –0·76) with 9 mg, and –1·12% (–1·39 to –0·85) with 12 mg (all p<0·0001). The mean percentage change from baseline in bodyweight was –11·5% (SE 0·7) with retatrutide 4 mg, –13·9% (0·8) with 9 mg, and –15·3% (0·8) with 12 mg, versus –2·6% (0·5) with placebo. The most frequent adverse events with retatrutide were generally mild to moderate gastrointestinal events, which subsided over time. Study intervention discontinuations due to adverse events were 2–5% with retatrutide and 0% with placebo. No severe hypoglycaemia was reported. Two deaths occurred during the study, both in the retatrutide 4 mg group and unrelated to the study drug.

Interpretation Retatrutide showed significant improvements in glycaemic control and bodyweight reduction as a monotherapy in adults with type 2 diabetes that is inadequately controlled with diet and exercise alone, with an adverse event profile consistent with molecules with GLP-1 agonist activity, supporting its potential as an effective treatment for type 2 diabetes.

	Retatrutide 4 mg (n=134)	Retatrutide 9 mg (n=133)	Retatrutide 12 mg (n=136)	Placebo (n=134)
Age, years	47·9 (12·2)	50·2 (12·1)	49·2 (12·1)	48·0 (12·2)
Sex				
Female	71 (53%)	79 (59%)	80 (59%)	66 (49%)
Male	63 (47%)	54 (41%)	56 (41%)	68 (51%)
Race				
American Indian or Alaska Native	50 (37%)	50 (38%)	49 (36%)	45 (34%)
Asian	41 (31%)	41 (31%)	43 (32%)	45 (34%)
Black or African American	5 (4%)	5 (4%)	8 (6%)	9 (7%)
White	36 (27%)	33 (25%)	35 (26%)	35 (26%)
Ethnicity				
Hispanic or Latino	72 (54%)	71 (53%)	71 (52%)	69 (51%)
Not Hispanic or Latino	62 (46%)	62 (47%)	65 (48%)	65 (49%)
Country				
India	41 (31%)	40 (30%)	41 (30%)	42 (31%)
Mexico	54 (40%)	54 (41%)	55 (40%)	53 (40%)
USA	39 (29%)	39 (29%)	40 (29%)	39 (29%)
HbA_{1c} concentration				
%	7·9 (1·1)	8·0 (1·0)	7·9 (1·0)	7·9 (1·1)
mmol/mol	63·1 (11·9)	64·4 (11·3)	62·7 (10·8)	62·5 (12·1)
HbA_{1c} category				
≤8·0%	79 (59%)	70 (53%)	90 (66%)	85 (63%)
>8·0%	55 (41%)	63 (47%)	46 (34%)	49 (37%)
Fasting serum glucose concentration				
mg/dL	137·8 (52·6)	144·7 (59·6)	129·9 (53·3)	131·8 (51·8)
mmol/L	7·7 (2·9)	8·0 (3·3)	7·2 (3·0)	7·3 (2·9)
Duration of type 2 diabetes, years	2·3 (4·3)	2·9 (5·3)	2·5 (4·0)	2·4 (4·1)
Previous use of antihyperglycaemic medications	23 (17%)	20 (15%)	20 (15%)	19 (14%)
Bodyweight, kg	99·6 (23·3)	95·1 (21·9)	99·6 (25·1)	93·3 (18·6)
BMI, kg/m²	36·6 (7·4)	35·6 (6·7)	36·4 (7·1)	34·7 (6·5)
Waist circumference, cm	113·7 (15·9)	110·4 (13·9)	113·3 (16·6)	109·2 (13·9)
Triglycerides, mg/dL	176·9 (138·3)	174·2 (124·8)	172·7 (102·9)	174·7 (105·6)
Non-HDL cholesterol, mg/dL	135·3 (39·0)	138·4 (39·0)	139·4 (38·8)	142·9 (40·4)
Blood pressure, mm Hg				
Systolic	124·4 (10·0)	125·7 (11·0)	125·4 (10·9)	124·2 (9·9)
Diastolic	79·6 (7·0)	79·2 (7·8)	79·3 (6·2)	79·0 (6·8)
eGFR, mL/min per 1·73 m²	85·0 (22·5)	88·3 (22·4)	86·7 (22·1)	87·0 (23·2)

Data are mean (SD) or n (%). Randomly allocated population. HbA_{1c}=glycated haemoglobin. eGFR=estimated glomerular filtration rate.

Table 1: **Baseline demographics and clinical characteristics**

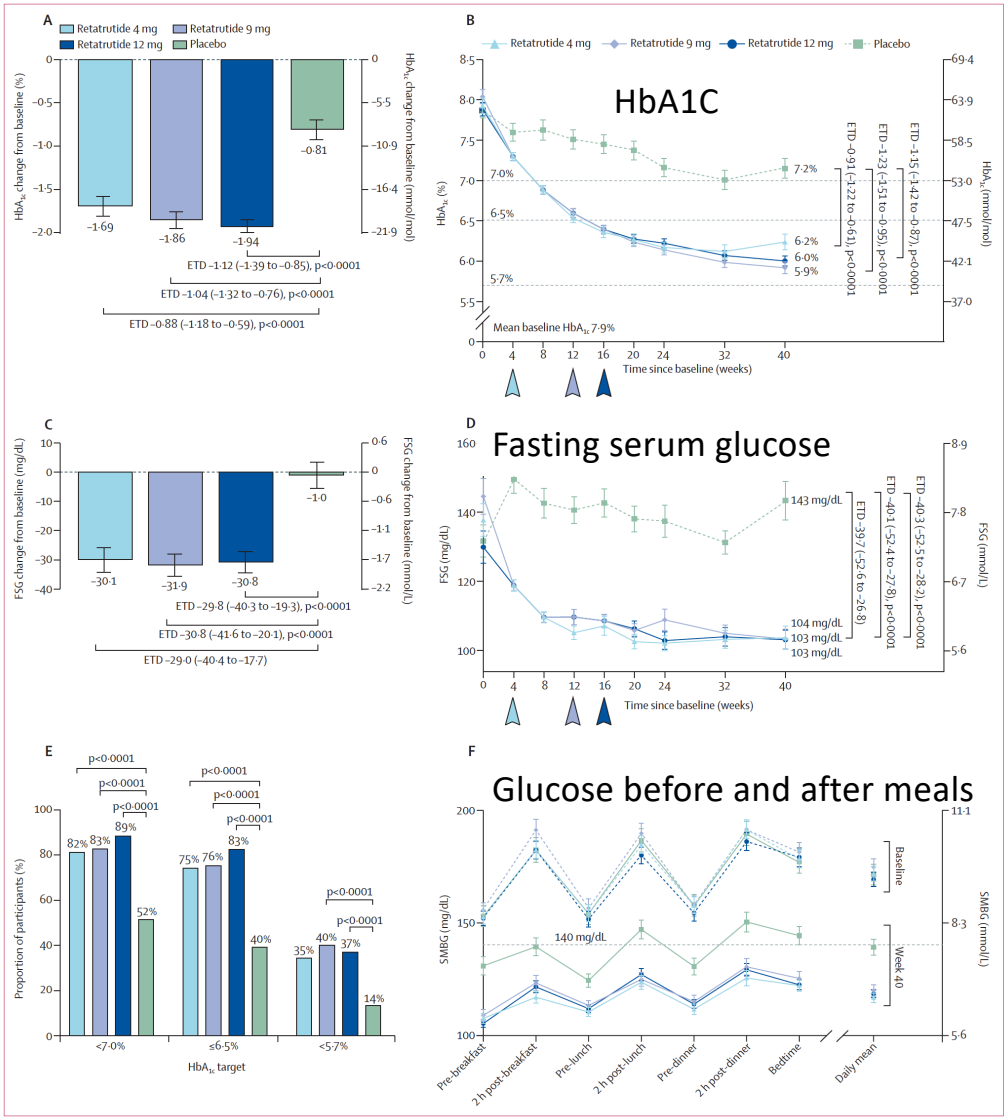

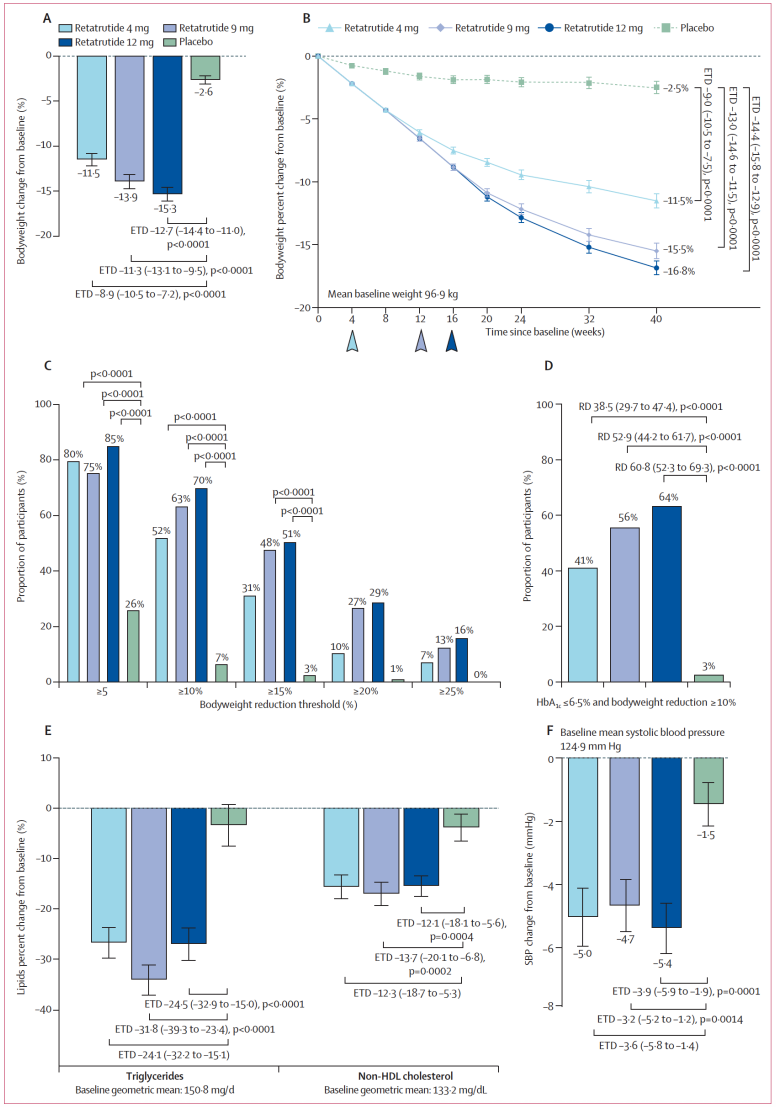

Figure 3: **Effects of retatrutide on bodyweight, lipids, and systolic blood pressure**

Data are model-based estimate unless otherwise noted. Error bars represent SE. Arrows indicate when the randomly assigned doses of retatrutide (4 mg, 9 mg, and 12 mg) were reached. Only p values controlled for multiplicity (family-wise type I error) are shown. CIs were not adjusted for multiplicity and should not be used for hypothesis testing. (A) Percentage change from baseline in bodyweight at 40 weeks from ANCOVA with multiple imputation (treatment regimen estimand). (B) Percentage change from baseline in bodyweight over 40 weeks from mixed-model repeated measures (efficacy estimand). (C) Proportion of participants reaching the indicated bodyweight reduction thresholds at 40 weeks from logistic regression with multiple imputation (treatment regimen estimand) with p values for risk difference. (D) Proportion of participants reaching the composite target of HbA_{1c} less than or equal to 6·5% (48 mmol/mol) and 10% or more bodyweight reduction from baseline at 40 weeks from logistic regression with multiple imputation (treatment regimen estimand) with risk difference. (E) Percentage change from baseline in serum triglycerides and non-HDL cholesterol at 40 weeks from ANCOVA with multiple imputation (treatment regimen estimand). (F) Change from baseline in systolic blood pressure at 40 weeks from ANCOVA with multiple imputation (treatment regimen estimand). ETD=estimated treatment difference. HbA_{1c}=glycated haemoglobin. RD=risk difference.

	Retatrutide 4 mg (n=134)	Retatrutide 9 mg (n=133)	Retatrutide 12 mg (n=136)	Placebo (n=134)
Participants with one or more treatment-emergent adverse events	84 (63%)	85 (64%)	85 (63%)	77 (57%)
Serious adverse events	6 (4%)	1 (1%)	5 (4%)	2 (1%)
Deaths*	2 (1%)	0	0	0
Adverse events leading to study intervention discontinuation	3 (2%)	6 (5%)	7 (5%)	0
Gastrointestinal adverse events leading to study intervention discontinuation	0	1 (1%)	4 (3%)	0
Upper abdominal pain	0	0	1 (1%)	0
Constipation	0	0	1 (1%)	0
Dyspepsia	0	0	1 (1%)	0
Nausea	0	1 (1%)	1 (1%)	0
Treatment-emergent adverse events occurring in 5% or more of participants in any treatment group				
Diarrhoea	25 (19%)	35 (26%)	31 (23%)	6 (4%)
Nausea	22 (16%)	26 (20%)	36 (26%)	5 (4%)
Vomiting	21 (16%)	20 (15%)	24 (18%)	3 (2%)
Hyperglycaemia	5 (4%)	10 (8%)	5 (4%)	35 (26%)
Decreased appetite	10 (7%)	15 (11%)	11 (8%)	2 (1%)
Headache	5 (4%)	8 (6%)	7 (5%)	13 (10%)
Abdominal distension	7 (5%)	8 (6%)	13 (10%)	3 (2%)
Constipation	6 (4%)	11 (8%)	10 (7%)	1 (1%)
Asthenia	5 (4%)	5 (4%)	5 (4%)	9 (7%)
Fatigue	1 (1%)	8 (6%)	10 (7%)	4 (3%)
Pain	3 (2%)	5 (4%)	4 (3%)	11 (8%)
Abdominal discomfort	6 (4%)	10 (8%)	4 (3%)	1 (1%)
Nasopharyngitis	6 (4%)	2 (2%)	4 (3%)	9 (7%)
Upper abdominal pain	7 (5%)	1 (1%)	5 (4%)	7 (5%)
Back pain	4 (3%)	3 (2%)	2 (1%)	10 (7%)
Eructation	1 (1%)	2 (2%)	7 (5%)	0
Other treatment-emergent adverse events of interest				
Hypoglycaemia (blood glucose <54 mg/dL)	0	2 (2%)	1 (1%)	0
Severe hypoglycaemia	0	0	0	0
Initiation of rescue therapy for severe hyperglycaemia	3 (2%)	9 (7%)	2 (1%)	26 (19%)
Arrhythmias and cardiac conduction disorders	4 (3%)	2 (2%)	1 (1%)	0
Malignancies	3 (2%)	0	0	1 (1%)
Adjudication-confirmed major adverse cardiovascular events	3 (2%)	0	0	0
Cholelithiasis	0	1 (1%)	3 (2%)	0
Dysesthesia	6 (4%)	3 (2%)	6 (4%)	0
Injection site reactions	2 (1%)	2 (2%)	2 (1%)	1 (1%)

Data are n (%). Safety analysis set. Participants might be counted in more than one category. Number of episodes was reported if available. MedDRA version 28.1. *Deaths are also included as serious adverse events and discontinuations due to adverse events.

Table 2: **Adverse events**

Research in context

Evidence before this study

The American Diabetes Association standards of care recommend a target glycated haemoglobin (HbA_{1c}) of less than 6·5% for individuals with type 2 diabetes who are in good health and have low treatment risks. Furthermore, the standards of care suggest that a sustained bodyweight loss of greater than 10% could have disease-modifying effects and possibly lead to remission of diabetes. We searched PubMed on March 13, 2026, using the terms "glucagon-like peptide 1 receptor agonist", "glucose-dependent insulinotropic polypeptide", "glucagon", "retatrutide", "triple agonist", "type 2 diabetes", "obesity", and "chronic weight management", with no date or study duration restrictions. The results of the search showed that GLP-1 monoreceptor agonists and a dual GIP and GLP-1 receptor agonist have shown robust weight reduction efficacy in individuals with type 2 diabetes. The GIP and GLP-1 receptor agonist tirzepatide has shown superior effects on glycaemic control and bodyweight compared with selective GLP-1 receptor agonism (dulaglutide and semaglutide). However, the weight reduction efficacy of these agents is generally attenuated in trial participants with type 2 diabetes compared with participants without type 2 diabetes, highlighting an unmet need for therapies delivering robust weight reduction alongside glycaemic control. Additionally, treatment of hyperglycaemia without suitable weight reduction can leave people with type 2 diabetes at a high risk of cardiometabolic complications associated with obesity and overweight, such as hypertension, dyslipidaemia, metabolic dysfunction-associated steatotic liver disease, and cardiovascular disease. Retatrutide, a GIP, GLP-1, and glucagon triple hormone agonist, might further enhance weight reduction, as targeting the glucagon receptor has been shown to increase energy expenditure, suppress appetite, and enhance fat metabolism while providing meaningful improvement in glycaemic control. In a phase 2 clinical trial in 281 people with type 2 diabetes (NCT04867785), treatment with retatrutide resulted in greater bodyweight reduction compared with a selective GLP-1 receptor agonist (dulaglutide).

Added value of this study

TRANSCEND-T2D-1 is the first phase 3 clinical trial of retatrutide for the treatment of type 2 diabetes. We investigated the efficacy and safety of retatrutide (4 mg, 9 mg, or 12 mg) compared with placebo as a monotherapy for 40 weeks. Treatment with retatrutide resulted in significant reductions in HbA_{1c} and fasting serum glucose compared with placebo. The proportion of participants reaching glycaemic targets of less than 7·0%, less than or equal to 6·5%, and less than 5·7% were also significant for all tested retatrutide doses at week 40. Treatment with retatrutide also resulted in significant bodyweight reduction, beyond that observed in similar studies of molecules with GLP-1 agonist activity. The composite endpoints of reaching the target of HbA_{1c} concentration of 6·5% or less and the potentially disease-modifying threshold of weight reduction of 10% or more was reached by more than half of participants receiving retatrutide, showing the efficacy of retatrutide in improving glycaemic control while simultaneously driving clinically meaningful weight reduction. Retatrutide also improved other cardiometabolic outcomes, including lipid profile and blood pressure. The safety profile was overall consistent with molecules with GLP-1 agonist activity, with the most commonly reported adverse events being gastrointestinal in nature. Together, TRANSCEND-T2D-1 showed that triple hormone receptor agonist retatrutide could deliver robust weight reduction alongside glycaemic control in early type 2 diabetes, potentially addressing an unmet need for effective therapies that act on both endpoints simultaneously for people with type 2 diabetes.

Implications of all the available evidence

The results of the TRANSCEND-T2D-1 study show potent glucose-lowering effects of retatrutide in people with early type 2 diabetes, accompanied by significant bodyweight reduction. The safety results were similar to those reported for molecules with GLP-1 agonist activity. This first phase 3 trial of retatrutide in type 2 diabetes supports the use of retatrutide as a monotherapy for early type 2 diabetes. Retatrutide is being investigated in the additional TRANSCEND-T2D clinical trials for use in different populations with type 2 diabetes, including in direct comparison with other available therapies.

Chronic Kidney Disease 1

Advances in the diagnosis and detection of chronic kidney disease

Chronic kidney disease affects 788–844 million adults worldwide and is projected to become the fifth leading cause of death by 2040. Global burden estimates remain limited by ascertainment bias and inadequate access to testing, particularly in low-income and middle-income countries. Advances in detection include improved estimation of glomerular filtration rate (GFR) using cystatin C and the recognition of albuminuria as a key marker for screening and risk stratification. Kidney biopsy is improving diagnostic accuracy and prognostic prediction, and multiomics approaches are advancing our understanding of disease mechanisms and hold promise for precision medicine. Advanced imaging and artificial intelligence are enabling non-invasive diagnostics and case detection. Population screening strategies using estimated GFR and albuminuria are increasingly cost-effective, particularly with the availability of novel therapies. Disease-specific prediction models support individualised risk stratification and clinical decision-making. However, inequitable access, limited validation across diverse populations, gaps in biomarker standardisation, and insufficient health-care system capacity constrain implementation globally. Addressing these challenges requires coordinated investment in diagnostics, workforce training, laboratory infrastructure, and health-care system strengthening alongside continued technological advancement.

Didn‘t we know these things in 1968?

Panel: Advances and priorities in CKD diagnosis and detection

What has changed in the past decade?

- Improved glomerular filtration rate (GFR) estimation with cystatin C for diagnosis and accurate risk prediction
- Recognition of albuminuria as a key marker for screening and risk stratification
- Prediction models incorporating multiple aspects of diseases including biopsy data and imaging
- Improved imaging techniques for non-invasive assessment of kidney structure and function
- Improved understanding of biopsy value for diagnosis, prognosis, and molecular profiling
- Systems biology approach to discovery through multiomics integration
- International consortia for precision medicine, genetics, and understanding chronic kidney disease (CKD) in underserved populations
- Artificial intelligence (AI) and digital health technologies to support accessible CKD detection and monitoring, and to facilitate patient-centred care

What should clinicians and health systems do differently now?

For clinical practice

- Use cystatin C under recommended conditions
- Screen for albuminuria according to guidelines
- Apply recommended risk prediction models during nephrology referral, patient counselling, and kidney replacement therapy preparation
- Biopsy when diagnosis uncertain: enables disease-specific therapies and molecular profiling
- Point-of-care creatinine in setting where resources are scarce
- Raise awareness and promote education early in people with CKD or at high risk of CKD

For health system and policy

- Embed CKD detection within non-communicable disease prevention and management frameworks and clinical workflows
- Adopt standardised albuminuria screening protocols
- Ensure equitable access to diagnostic tools
- Invest in point-of-care testing infrastructure in low-resource settings
- Implement AI-enabled diagnostics in primary care settings with low nephrology access

What is not ready?

- Unclear clinical utility and standardisation of emerging biomarkers
- Validation of dynamic and static imaging for diagnosis and follow-up
- Multiomics approaches for routine clinical application
- Cost-effectiveness uncertainty for advanced diagnostics
- Generalisability, transparency, and implementation barriers of AI models
- Unified and consistent recognition within national policy frameworks of the importance of CKD

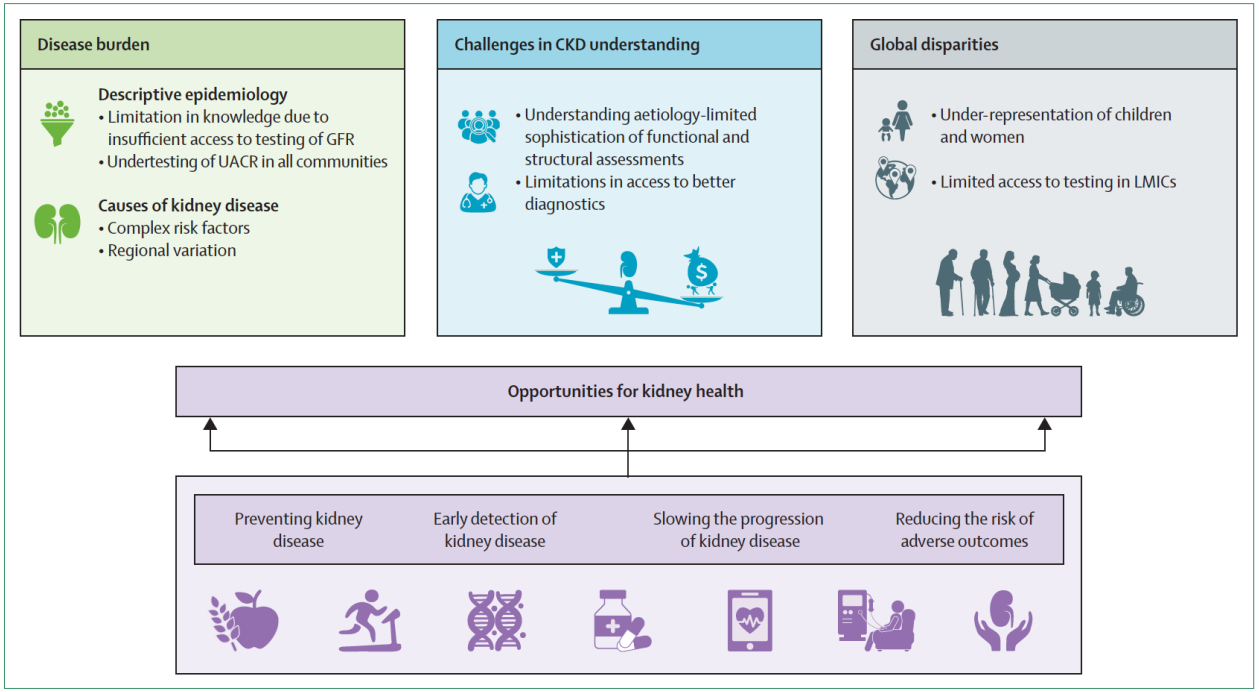

Figure 1: **Key barriers to and opportunities for kidney health**
CKD=chronic kidney disease. GFR=glomerular filtration rate. UACR=urinary albumin-to-creatinine ratio.

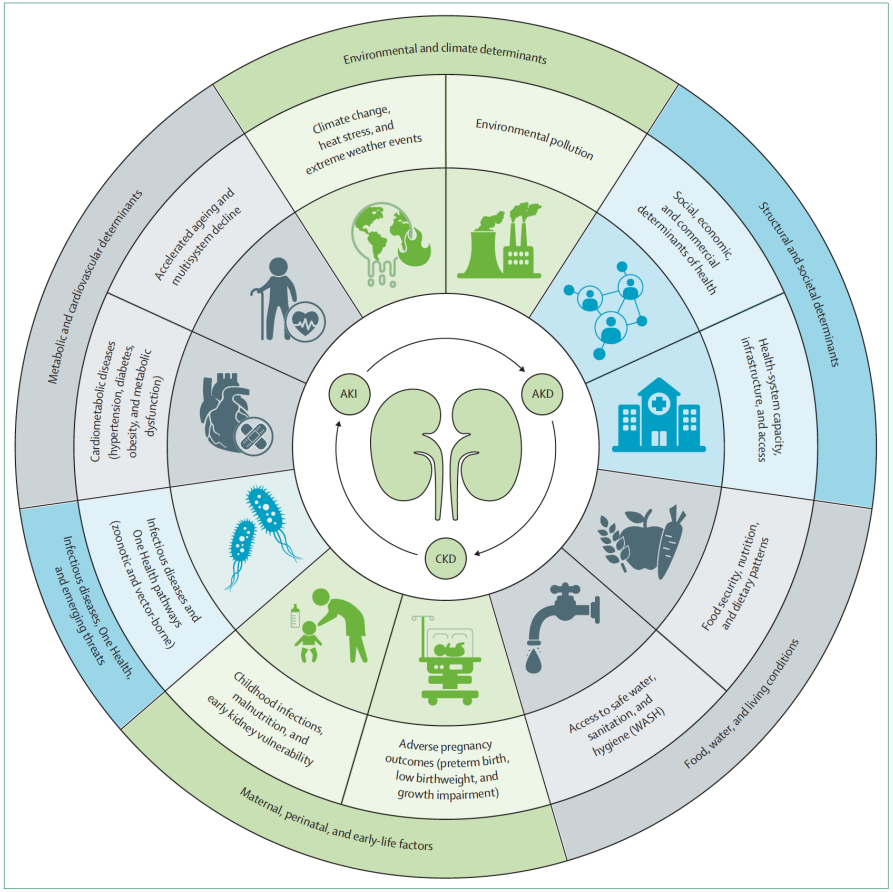

Figure 2: **Complex and inter-related social determinants contribute to the rising burden of kidney disease**
CKD=chronic kidney disease. AKI=acute kidney injury. AKD=acute kidney disease. WASH=water, sanitation, and hygiene.

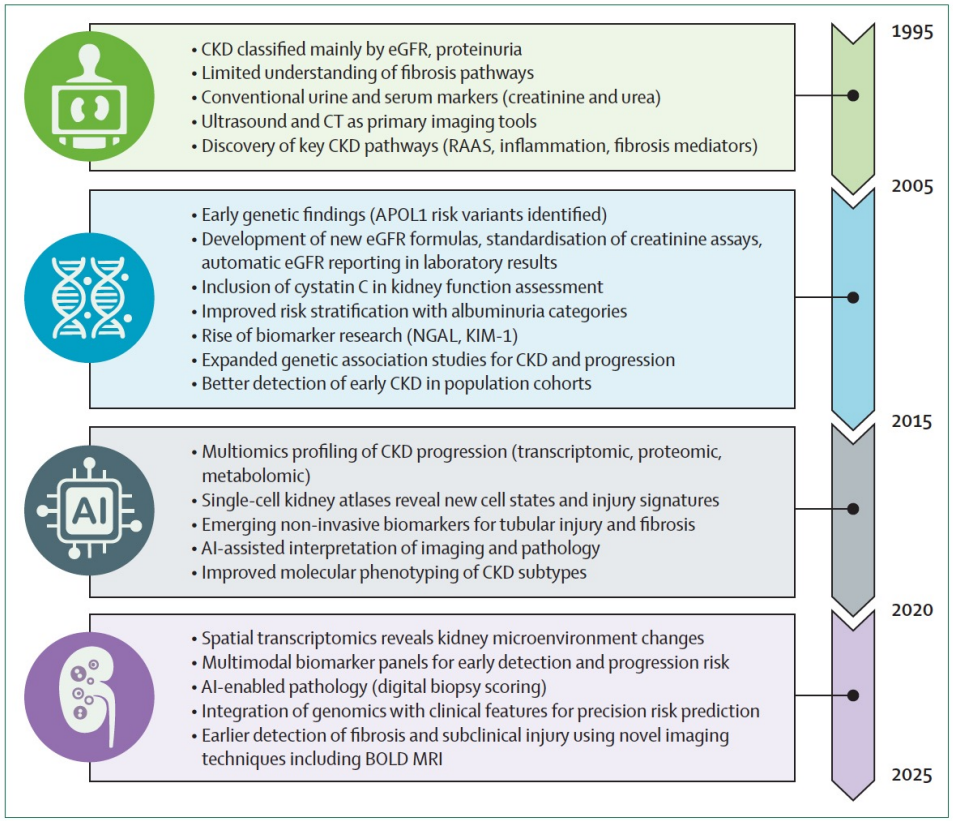

Figure 3: **Advances in CKD mechanistic understanding and diagnostics**
CKD=chronic kidney disease. eGFR=estimated glomerular filtration rate. RAAS=renin–angiotensin–aldosterone system. KIM-1=kidney injury molecule-1. AI=artificial intelligence. BOLD MRI=blood oxygen level-dependent MRI.

Lots of biomarkers; which do we need?

	Mechanism and function	Clinical relevance
Traditional biomarkers for routine clinical use		
Serum creatinine and eGFR	Creatinine is produced by muscles as a by-product of the breakdown of creatine; it is freely filtered in the glomerulus and in part reabsorbed by tubular structures	As GFR measurement is complex, multiple equations use creatinine levels as an indirect measure of GFR; accuracy is reduced in older patients and individuals with less or more muscle mass, obesity, exercise, diet, and AKI
Urine albumin-to-creatinine ratio	Most common proteins in the urine in kidney diseases; measured accurately even in normal levels	Values integrated in the CKD staging system; prognostic predictor of CKD risk; less prone to inaccuracies in measurement than urine protein assays
Cystatin C	Synthesised by all cells, freely filtered by the glomerulus with complete tubular reabsorption and catabolisation; no tubular secretion	Levels increase earlier and faster in AKI; equations combining serum creatinine and cystatin C give a more accurate estimate of GFR than creatinine-based equations alone; less influenced by muscle mass and gender than serum creatinine
Parathyroid hormone	Established marker of secondary hyperparathyroidism, secreted by the parathyroid gland	A predictor of CKD progression and cardiovascular morbidity and mortality
Emerging biomarkers for selective or near-term use		
β2M	Produced by all nucleated cells (MHC class 1 molecule); progressively accumulates as GFR declines	Strong predictor of kidney failure and all-cause mortality; GFR equations combining BTP and β2M predict kidney failure more accurately than traditional markers; levels are less influenced by muscle mass and gender than serum creatinine
BTP	Mainly produced by epithelial cells in the choroid plexus; catalyst in the prostaglandin pathway	Increased urinary and plasma levels correlate with serum creatinine and cystatin C levels; GFR equations combining BTP and β2M predict kidney failure more accurately than traditional markers; levels are less influenced by muscle mass and gender than serum creatinine
N-acetyl-α-D-glucosaminidase	Enzyme indicating tubular injury	Urinary levels as a marker of systemic inflammation and proteinuria
Uromodulin (Tamm–Horsfall protein)	Exclusively produced in the tubular cells; protective function in UTI; reflects tubular damage and nephron mass	Urinary and serum levels predict CKD progression; strong predictive value between serum uromodulin levels and eGFR
FGF23	Mainly produced by osteocytes and osteoblasts; major role in bone metabolism (phosphate metabolism)	Elevated early in CKD and is a major predictor of CKD progression and cardiovascular mortality
NGAL	Released during tubular injury and inflammation, produced by inflammatory cells in the liver and kidneys	Early marker of AKI and has prognostic value in CKD progression
Kidney injury molecule 1	Marker of proximal tubular injury	Mucin domain elevated in urine and plasma in AKI and CKD; correlates with urine albumin-to-creatinine ratio, inflammation, and fibrosis in the kidney; potential therapeutic target
Liver-type fatty acid-binding protein	Produced by liver and proximal tubular cells	Increased urinary levels are linked with tubulo-interstitial damage in AKI and is also associated with CKD progression
IGFBP7 and TIMP-2	IGFBP7 is secreted by proximal tubule cells, and TIMP-2 by distal tubule cells; tubular stress protein expressed with ongoing injury	Often checked together (Nephrocheck); good predictive value in the first 12 h of AKI
GDF-15	Produced in cardiac myocytes and in kidneys	Associated with progression of CKD and adverse cardiovascular outcomes; key biomarker in haemodialysis patients
Galectin-3	Produced in epithelial cells, macrophages and fibroblasts	Raised levels in CKD; predicts rapid decline in kidney function and cardiovascular mortality
Urinary soluble CD163	Shed from activated macrophages infiltrating the kidney; reflects local intrarenal macrophage activation and inflammation	Urinary levels indicate active glomerular inflammation; useful non-invasive marker of disease activity in immune-mediated kidney diseases (eg, lupus nephritis, ANCA-associated vasculitis)

(Table continues on next page)

	Mechanism and function	Clinical relevance
(Continued from previous page)		
Research-grade biomarkers		
Klotho	Reno-protective and anti-ageing molecule; predominantly expressed in the kidneys	Deficiency leads to CKD progression; positive correlation between serum and urinary levels and eGFR; potential therapeutic target
DKK3	Tubular stress protein expressed with ongoing injury	Urinary levels linked to CKD progression and proteinuria; marker indicating poor prognosis
Sclerostin	Secreted by osteocytes; inhibits bone formation and indirectly activates osteoclast activity	High levels are correlated with low GFR and a marker of CKD progression
NLRP3 inflammasome	Activates caspase-1, which cleaves pro-inflammatory cytokines (ie, IL-1β and IL-18); promotes inflammation and fibrosis	Predicts CKD progression
TNF receptors (1 and 2)	Circulating receptors of TNF, activated by binding of circulating TNF	Early biomarkers in different kidney diseases and predictive of progression in CKD and all-cause mortality
Calprotectin	Released from myeloid cells; acute phase reactant	Predictor of new-onset CKD and is a marker of vascular calcification and increased cardiovascular mortality in patients with CKD; also increased in immune-mediated kidney diseases
Ficolins	Part of the lectin pathway of the complement system	Elevated levels associated with CKD progression, poor allograft function, and increased risk of infectious complications
Soluble UPAR	Expressed at low levels in endothelial cells, podocytes, and immunologically active cells (monocytes and lymphocytes)	High levels are predictive of AKI and is also predictive of progressive kidney function decline and development of CKD
TGF-β	Cytokine involved in tissue inflammation and fibrosis	Blood levels associated with progressive kidney fibrosis and decline in function therapeutic target
Podocyte markers (podocalyxin, podocin, and nephrin)	Markers of podocyte injury in proteinuric kidney diseases	Podocalyxin urinary levels are raised in immune-mediated kidney diseases and have a prognostic value; urinary podocyte-derived markers—including podocin, podocalyxin, and nephrin—have been investigated as biomarkers for pre-eclampsia, with mixed evidence on their comparative diagnostic accuracy; nephrinuria is a biomarker in early diagnosis of proteinuric kidney disease
Testican-2	Released from podocytes	Higher levels indicate higher GFR; positive correlation with kidney health
Urinary exosomes	Vesicles excreted by the kidney that contain proteins and nucleic acids; these excreted molecules reflect the pathophysiological state of the kidney	Multiple miRNAs and other molecules (complement factor 5 and 9, ceruloplasmin, CD36, C-megalin, etc) are upregulated in various kidney disease; needs further characterisation for future clinical application

ANCA=antineutrophil cytoplasmic antibody. AKI=acute kidney injury. BTP=β trace protein. CKD=chronic kidney disease. eGFR=estimated glomerular filtration rate. miRNA=microRNA (ribonucleic acid). UTI=urinary tract infection.

***Table*: Biomarkers in CKD: from routine clinical use to research frontiers**

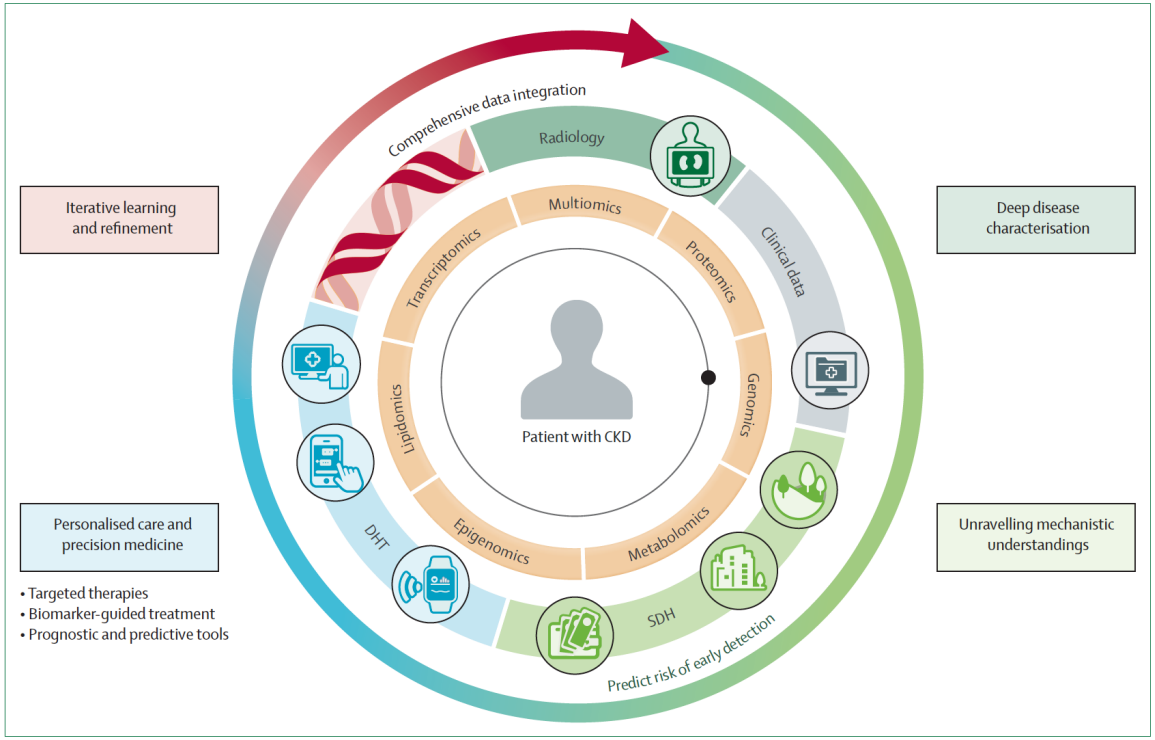

Figure 4: **Integrative, patient-centred framework for advancing CKD care**
CKD=chronic kidney disease. DHT=digital health technology. SDH=social determinants of health.

Several gaps in current knowledge and practice remain, including standardisation and access to sophisticated testing, and a lack of understanding of the differential ranges, thresholds, sensitivities, and specificities of these tools by age, sex and geography. These gaps are further delineated in the second paper of this Series, where we offer an in-depth discussion on sex differences in biological processes that affect development and progression of CKD and responsiveness to treatment; and in the third paper, we discuss successful treatments, informed by advances in understanding biological processes, and the need for ongoing evidence generation to better understand best therapies and responsiveness for different subgroups of people living with CKD.

Chronic Kidney Disease 2

Advances in understanding the impact of sex on kidney health and disease

Biological differences exist between males and females in kidney structure and function, leading to sex heterogeneity in the presentation and outcomes of chronic kidney disease (CKD) and response to novel therapeutics. However, treatment guidelines ignore sex-specific differences. This Series paper provides an integrated discussion of the complexity of sex differences in the context of kidney health and disease, from biology through clinical characteristics, treatment, evidence generation, and reporting. Throughout, we consider the effect of genetics, epigenetic regulation, and the role of sex hormones. We highlight substantial opportunities that exist for policy makers, scientific organisations, journal editors, funders, and individuals to change the current paradigm. Strategic and systematic acknowledgment, exploration, and reporting of these differences is needed in future research to continue to advance our understanding of pathophysiology, diagnostics, and novel therapeutics for CKD.

Chronic Kidney Disease (CKD) is slightly more common in women than in men, affecting approximately 14% of women compared to 12% to 13% of men globally.

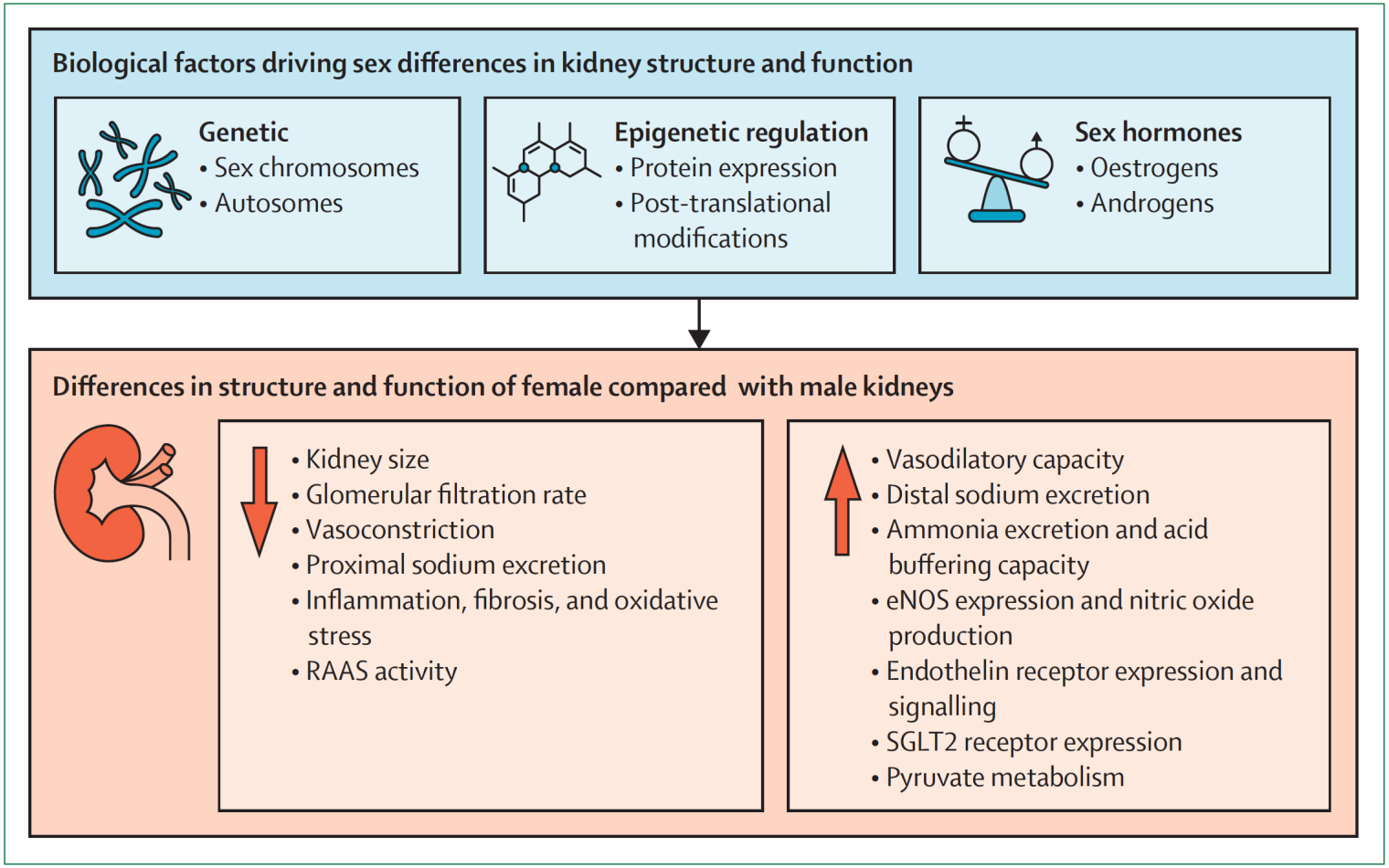

Figure 1: **Biological sex differences in kidney structure and function**

eNOS=endothelial nitric oxide synthase. RAAS=renal–angiotensin–aldosterone system.

Panel: Effects of sex and gender on the most common drugs

Pharmacokinetics[29,97,98]

Absorption (assuming oral administration)

- Higher gastric pH, which decreases weak acid absorption and increases weak base absorption, with evidence for an increased effect during pregnancy
- Increased gastrointestinal transit time, prolonging the absorption window and increasing overall absorption, with evidence for an increased effect during pregnancy

Distribution

- Lower body weight, smaller organ size, lower lean tissue mass, and higher fat mass
- Lower plasma volume and lower blood flow rate, with evidence for an increased effect during pregnancy
- Higher unbound drug fraction, with evidence for an increased effect during pregnancy
- Hydrophilic drugs have a lower volume of distribution, higher peak plasma levels, and a shorter duration of action
- Lipophilic drugs have a higher volume of distribution, lower peak plasma levels, and a longer duration of action

Metabolism (cytochrome P450 system)

- Higher CYP3A4 activity, with evidence for an increased effect during pregnancy
- Lower CYP2D6 activity, with evidence for an increased effect during pregnancy
- Lower CYP1A2 activity, with evidence for a decreased effect during pregnancy
- Females might have higher or lower exposure to drugs and their metabolites than males

Excretion

- Lower glomerular filtration rate, with evidence for an increased effect during pregnancy
- Altered active secretion in proximal tubule
- Reduced drug elimination and longer half-lives

Evidence for sex differences in pharmacokinetics for therapeutics used in chronic kidney disease (CKD)

- Loop diuretics (torasemide): higher peak serum concentration, area under curve (AUC), clearance time, and half-life
- Endothelin receptor antagonists (atrasentan): higher AUC and peak serum concentration
- Angiotensin receptor blockers (losartan): higher AUC and peak serum concentration
- Direct renin inhibitors (aliskiren): higher AUC and peak serum concentration

Pharmacodynamics[22,29,30,98–100]

Effects of sex hormones on receptor expression, binding, and signal transduction, leading to a different outcome from same delivered treatment

Evidence for sex differences in pharmacodynamics for therapeutics used in CKD

- Angiotensin converting enzyme inhibitors (class level): similar effects at half dose used in males
- Angiotensin receptor blockers (losartan and irbesartan): differential effect on kidney failure and cardiovascular outcomes
- SGLT2 inhibitors (class level): higher adverse event rate in females but similar effects on glycated haemoglobin (HbA1c) and cardiovascular events
- GLP1-receptor agonists (class level): greater weight loss and higher adverse event rate in females but similar effects on HbA1c and cardiovascular events
- Diuretics (torasemide): more frequent electrolyte disturbance including hospitalisations
- Endothelin receptor antagonists (atrasentan): more effective kidney failure reduction but higher heart failure events
- Direct renin inhibitors (aliskerin): higher rate of diarrhoea

Drug–drug interactions[101]

Females take more unique medications than males, including non-prescription drugs, herbal remedies and hormonal therapies for contraception and menopause, which can lead to changes to pharmacokinetics or pharmacodynamics

Evidence for sex differences in drug–drug interactions for therapeutics used in CKD

GLP1-receptor agonists (tirzepatide): causes reduced peak serum concentration and AUC for oral contraceptives

	Policy ororganisational level (eg, government, research funders, or journals or editorial boards)	Collaboration level (eg, research consortia and clinical trial organisations)	Individual physician level
Improve awareness of the biological relevance of sex differences in kidney health and disease	Highlight sex (in policy documents and national campaigns) as an important and characterisable factor that influences health and disease; inclusion of sex differences in educational curricula for biological, clinical, and pharmaceutical sciences	Provide education on sex differences in kidney health and disease; promote interdisciplinary research (eg, basic science, social science, statisticians, epidemiologists, and clinicians); mandate engagement with educational resources for relevant personnel	Engage with educational materials to understand the relevance of sex differences in research and practice; engage with local students, colleagues, and mentors to share education on sex differences
Improve representation of female cells, animals, and human participants in research	Subscribe to and enforce guidance for consideration of sex and gender in study design, analysis plans, results reporting, and interpretation (ie, Sex and Gender Equity in Research guidelines 2016)[150]	Consider experimental design to facilitate inclusion of both sexes in animal research (see guidance from National Centre for the Replacement, Refinement and Reduction of Animals in Research)[152] unless single sex study is strongly justified; consider stage of life cycle in research design (prepuberty or postpuberty, pregnancy, and premenopause or postmenopause); design pragmatic clinical trial protocols that promote female participation; consider support for caregivers in clinical trial design; targeted increases in proportion of female participants invited to trial screening	Be mindful of sex disparities when approaching potential participants for clinical studies
Improve reporting of sex differences in research	Formal integration of sex and gender considerations in funding policy and application processes; mandatory reporting of the sex of cells, tissues, and animals and human participants; mandatory reporting of sex-disaggregated efficacy and safety data in research outputs to facilitate later meta-analysis	Two-step data collection for sex at birth and current gender identity; normalise the measurement and reporting of reproductive health and sex hormone levels in clinical studies; integrate sex (and gender) into statistical analysis plans—eg, include sex as an explicit biological variable and assess interaction with other variables; reanalysis of existing efficacy and safety data through a sex lens (requires sharing of raw data and publication of sex-disaggregated data)	Be mindful of sex considerations when designing, analysing, reporting, reviewing, and interpreting research
Reduce sex disparities in treatment of CKD	Generate guidance documents to reduce sex and gender disparities in provision of CKD care (eg, Association for Diagnostics & Laboratory Medicine/ National Kidney Foundation guidance to improve equity in CKD care 2023)[153]	Engage with actionable advice to reduce sex-disparities and gender-disparities in CKD care; use advances in digital health-care technologies and artificial intelligence to identify diagnosis and treatment gaps	Audit of local practice to identify sex discrepancies in the identification or treatment of CKD; identify local barriers to providing sex-equitable CKD care; develop local strategies to overcome barriers to providing equitable CKD care

CKD=chronic kidney disease.

Table: **Opportunities and recommendations to improve understanding of sex differences in kidney health and disease**

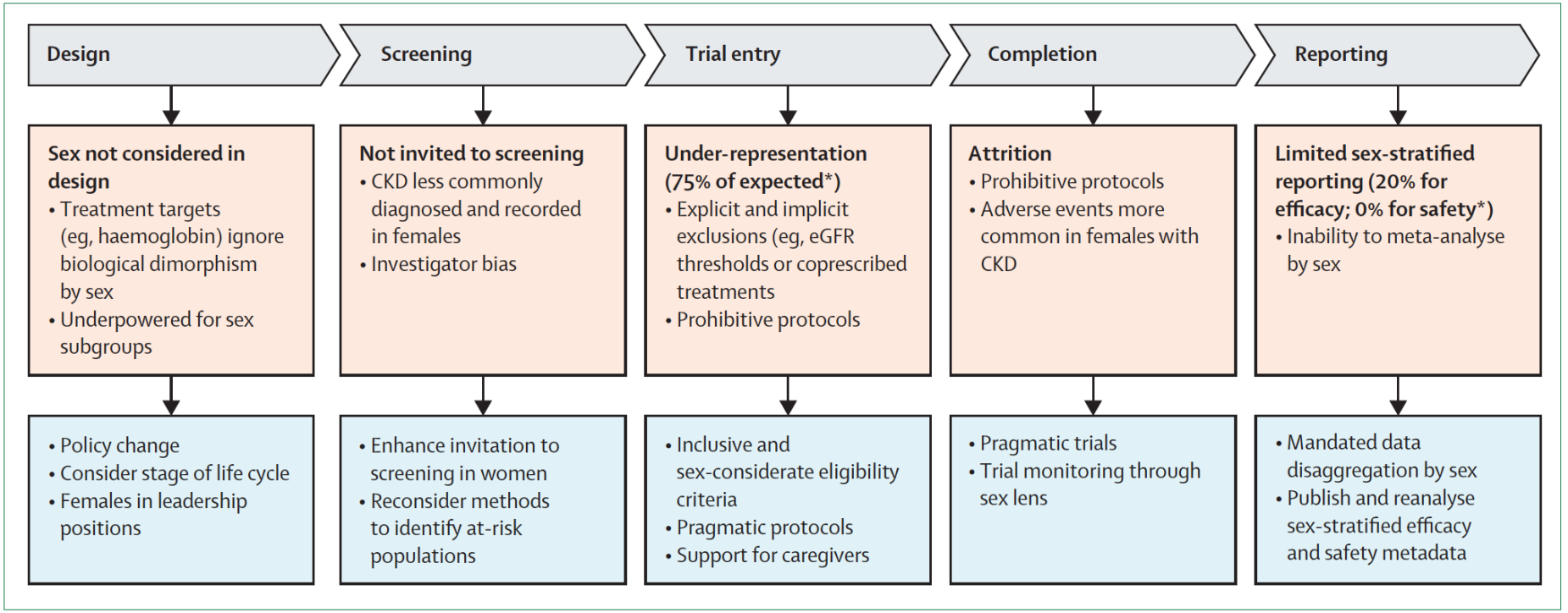

***Figure* 3: Issues affecting clinical evidence base for CKD in females**

CKD=chronic kidney disease. eGFR=estimated glomerular filtration rate. *In a systematic review and meta-analysis of 192 CKD trials.[144]

Conclusion

Sex differences in kidney structure, function, and propensity to disease are necessary and expected results of physiology that have evolved to optimise reproduction. Substantial gains have been made in our appreciation of the sex differences in kidney health and disease. Strategic and systematic acknowledgment, exploration, and reporting of these differences is required in future research, or we risk derailing substantial efforts to advance our understanding of pathophysiology and novel therapeutics for CKD, which are discussed in detail in the first and third Series papers.[2,3]

Chronic Kidney Disease 3

Chronic kidney disease, complex conditions, and advancing therapeutics: new hope and challenges

Chronic kidney disease (CKD) is increasingly recognised as a complex, multisystem condition that rarely occurs in isolation. This Series paper outlines major advances in therapeutics that target shared inflammatory, metabolic, and fibrotic pathways across CKD, cardiovascular disease, diabetes, obesity, and infection. Novel therapeutics, including SGLT2 inhibitors, non-steroidal mineralocorticoid receptor antagonists, and GLP receptor agonists, show substantial benefits for slowing CKD progression and improving cardiovascular outcomes, with combination strategies showing additive potential. This Series paper discusses complexities for therapeutic decision-making in CKD, highlighting multimorbidity, frailty, and polypharmacy care as major challenges for implementation in general or primary care settings. We identify under-recognised, groups of patients at high risk with infection and cancer-related CKD, in whom early detection and integrated care could markedly improve outcomes. Finally, we call for more inclusive and representative evidence generation, improved CKD screening within other disease pathways, and coordinated implementation of emerging therapies to reduce the global burden of CKD.

Key messages

- Novel chronic kidney disease (CKD) therapeutics (including SGLT2 inhibitors, non-steroidal mineralocorticoid receptor antagonists, and GLP-1 receptor agonists) and emerging agents can now preserve kidney function, reduce albuminuria, slow progression, and improve cardiovascular outcomes across diverse CKD populations. Multiple new drug classes are in late-phase development.
- Evidence suggests additive benefits when combining novel CKD therapeutics, although randomised evidence is awaited. Fixed-dose polypills might simplify prescribing but remain untested in CKD and underused in cardiovascular disease due to regulatory and dosing challenges.
- Multimorbidity, polypharmacy, frailty, and sarcopenia complicate prescribing, increase adverse events, and reduce confidence in applying trial evidence. Guidance for managing CKD in these complex populations is inconsistent, and safety data for high-risk groups remain scarce, making individualised treatment challenging, particularly in primary care.
- CKD risk and progression are amplified by cancer and its therapies, infections, autoimmune disease, and cardiometabolic conditions. Integrating CKD screening and treatment into disease-specific management may improve CKD outcomes but is rarely implemented.
- CKD trials under-represent advanced CKD and kidney failure, older adults (>75 years), females, individuals with multimorbidity, patients with frailty, children, and populations in low-income and middle-income countries. The absence of these populations from CKD trials limits generalisability and delays access to effective treatments. More inclusive trial design and individual-level data sharing are urgently needed.

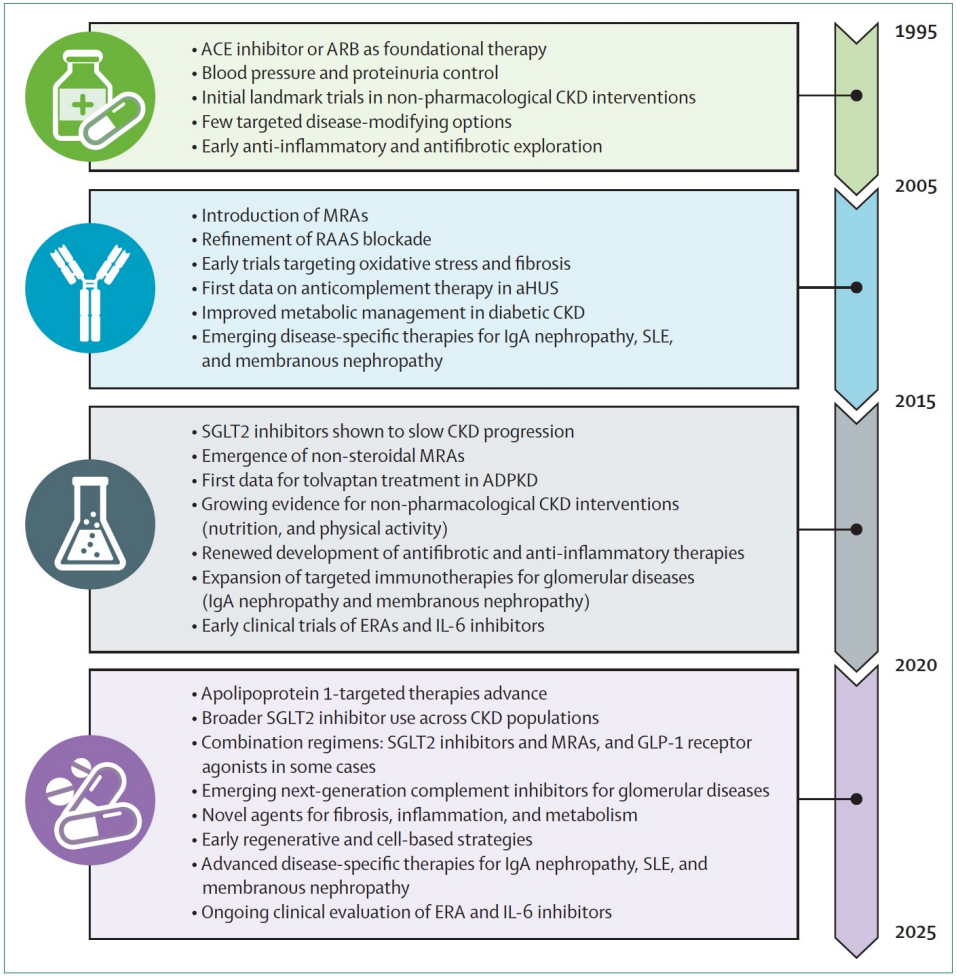

Figure 1: **Advances in CKD therapeutic discovery**
ACE=angiotensin-converting enzyme. ADPKD=autosomal dominant polycystic kidney disease. ARB=angiotensin II receptor blocker. CKD=chronic kidney disease. ERA=endothelin receptor antagonist. MRA=mineralocorticoid receptor antagonist. RAAS=renin–angiotensin–aldosterone system. HUS=haemolytic uraemic syndrome. SLE=systemic lupus erythematosus.

	Selected mechanisms	Populations	Outcomes	Considerations
Existing evidence and implemented in clinical practice				
RAS inhibitors (ACE inhibitors and ARBs)	Reduce glomerular hydraulic pressure and the ultrafiltration of plasma proteins; reduce cell growth, inflammation, and fibrosis; and reduce cardiac remodelling	There is evidence for use of RAS inhibitors in people with CKD and albuminuria, CKD and hypertension, and heart failure with reduced and preserved ejection fraction (with or without CKD)	Reduce blood pressure and proteinuria; slow decline in kidney function; and reduce risks of kidney failure and cardiovascular disease in CKD populations[9]	STOP-ACEi trial: no benefit to stopping RAS inhibitors in advanced CKD to increase or preserve eGFR;[10] target trial emulation suggests that RAS inhibitor discontinuation in CKD is associated with higher rate of major cardiovascular events and death;[11,12] continuing RAS inhibitors in advancing CKD might be preferable to discontinuation in the absence of a strong indication to stop (such as severe hyperkalaemia)
SGLT2 inhibitors	Promote natriuresis, change in tissue sodium handling and glycosuria, with a range of downstream effects beyond plasma glucose control, including enhanced tubuloglomerular feedback, reduced intraglomerular pressure, reduction in plasma volume and systemic blood pressure, improved vascular function, and reduced uric acid, inflammation, and oxidative stress[13]	There is evidence for use of SGLT2 inhibitors in people with CKD with and without diabetes, including a range of glomerular diseases; people with type 2 diabetes; and people with heart failure with reduced and preserved ejection fraction; more evidence is required to support SGLT2 inhibitor use in children with CKD (NCT07107945), people with advanced CKD[14] and kidney failure (dialysis and kidney transplantation)[14]	Reduce AKI, CKD progression (by over 1 mL/min per 1·73m^2 per year on average, corresponding to approximately 57% improvement in eGFR decline compared with untreated individuals,[15] albuminuria, heart failure diagnoses, hospitalisation for heart failure, cardiovascular death, and all-cause mortality[16–24]	Early (within 2–4 weeks) drop in eGFR is commonly observed but is considered a protective mechanism due to reduced intraglomerular pressure[19,20]
Non-steroidal MRAs	Reduces oxidative activity, fibroblast proliferation, pro-fibrotic mediators, and immune and inflammatory mediators, leading to reduced tubular and podocyte injury, reduced fibrosis and glomerulosclerosis, reduced inflammation and vascular injury, and net vasodilation[25]	There is evidence for use of non-steroidal MRAs in people with CKD with type 2 diabetes and albuminuria and people with heart failure with reduced and preserved ejection fraction; evidence is required to support use in children with CKD (trial in progress),[26] people with CKD without type 2 diabetes (trials in progress),[27,28] and people with kidney failure (dialysis and kidney transplantation; no trials in progress)	Reduce proteinuria, prevention of the AKI to CKD transition, slows CKD progression, reduces cardiovascular events, particularly heart failure[27,29,30]	Not currently recommended in patients who have uncontrolled serum potassium, advanced CKD, or kidney failure because of safety concerns, primarily relating to risk of hyperkalaemia
Incretin analogues (GLP-1 receptor agonists; dual GLP-1 receptor agonists and GIPs; dual GLP-1 receptor agonists and glucagon agonists; and triple GLP-1 receptor agonists, GIPs, and glucagon agonists)	Reduces glycaemia, improves insulin sensitivity, decreases glucagon and free fatty acid concentrations, suppresses appetite (through increased satiety and slowed gastric emptying), decreases bodyweight, and downregulates proteomic profiles associated with cardiovascular disease risk[31,32]	There is evidence for use of incretin analogues in people with type 2 diabetes and people with CKD with type 2 diabetes; evidence is required for use in children with CKD (no trials in progress); CKD without overweight or obesity or type 2 diabetes (no trials in progress); and CKD with overweight or obesity, with or without type 2 diabetes (trials in progress)[33,34]	Reduces major adverse kidney and cardiovascular events; slows rate of eGFR decline by over 1 mL/min/1·73m^2 per year[35]	Significant (12·7%) GLP-1 receptor agonist treatment discontinuation due to adverse (mainly gastrointestinal) events in the trials;[36] treatment discontinuation might be higher in clinical practice (over 50% at 1 year) than in trials, and more common in patients who do not have type 2 diabetes or who lack access to an appropriate source of funding for treatment[37]

(Table continues on next page)

	Selected mechanisms	Populations	Outcomes	Considerations
(Continued from previous page)				
In development (awaiting further evidence or not implemented in clinical practice)				
Endothelin receptor antagonists	Endothelin receptor A antagonists promote vasoconstriction, cell proliferation, and matrix accumulation; endothelin receptor B antagonists lead to vasodilation and antiproliferative and antifibrotic effects[38]	People with CKD and type 2 diabetes;[39,40] people with CKD with albuminuria;[41] two endothelin receptor antagonists (atrasentan and sparsentan)[42,43] are already licensed for use in IgA nephropathy	Atrasentan reduced albuminuria and kidney function decline, but at the expense of increased risks of fluid retention and heart failure, particularly in women;[39,40] zibotentan with dapagliflozin enhanced albuminuria reduction and mitigated fluid retention in patients with CKD[41]	Zibotentan in combination with dapagliflozin being tested in CKD with albuminuria for CKD outcomes in phase 3 trial (NCT06087835)
Aldosterone synthase inhibitors	Blocks the adverse effects of aldosterone for kidney and cardiovascular health (see non-steroidal MRAs), but additionally target direct effects of aldosterone that are not mediated by altered gene expression (such as deleterious cardiac remodelling)	People with CKD and albuminuria[44] and people with CKD and uncontrolled hypertension[45]	Vicadrostat in combination with empagliflozin dose-dependently reduced albuminuria in patients with albuminuric CKD;[44] baxdrostat reduced systolic blood pressure[45]	Vicadrostat in combination with empagliflozin being testing for kidney and cardiovascular protection in patients with CKD and albuminuria (NCT06531824);[46] baxdrostat in combination with dapagliflozin is being tested to slow CKD progression, and reduce albuminuria, kidney, and cardiovascular events among participants with CKD and hypertension (NCT06268873)
Anti-IL-6 ligand monoclonal antibodies	Inhibits IL-6: a key component in the inflammatory cascade leading to development of thrombosis and atherosclerosis	People with moderate to severe CKD[47]	Ziltivekimab reduced biomarkers of inflammation and thrombosis that are implicated in the development of atherosclerosis[47]	Therapeutic efficacy of ziltivekimab for reducing cardiovascular outcomes in patients with CKD and systemic inflammation is being tested in ongoing phase 3 trial (NCT05021835)
Small soluble guanylate cyclase molecule activator	Enhances nitric oxide production and nitric oxide signalling, improving endothelial function	People with CKD with diabetes and without diabetes	Avenciguat lowered albuminuria[48]	NA
Complement inhibitors	Inhibit the main soluble component of the innate immune system; complement activation and over-activity plays a role in the pathogenesis of a range of glomerular diseases, including IgA nephropathy, membranous nephropathy, lupus nephritis, C3 glomerulopathy, dense deposit disease, diabetic nephropathy, and hypertensive nephrosclerosis	Under investigation in phase 1, 2, and 3 trials across a range of diseases[49]	NA	NA
Apolipoprotein-1 blockers (small molecule inhibitors and gene therapy)	Apolipoprotein-1 is an innate immunity gene; gene variants protect against African trypanosomiasis but can cause rapidly progressive proteinuric CKD for those carrying one or two apolipoprotein-1 risk variants; blocking expression or activity of gene might reduce CKD progression	People with apolipoprotein-1 associated CKD	Small molecule inhibitors of the apolipoprotein-1 channel reduce proteinuria[50]	Beyond proof of efficacy in phase 3 trials, successful implementation will require broader genetic testing to identify individuals at risk

APOL1

ACE=angiotensin-converting enzyme. AKI=acute kidney injury. ARB=angiotensin receptor blockers. CKD=chronic kidney disease. eGFR=estimated glomerular filtration rate. GIP=glucose-dependent insulinotropic polypeptide. MRA=mineralocorticoid receptor antagonists. NA=not applicable. RAS=renin-angiotensin system.

Table: **Novel and emerging drug therapeutics in the prevention and treatment of CKD**

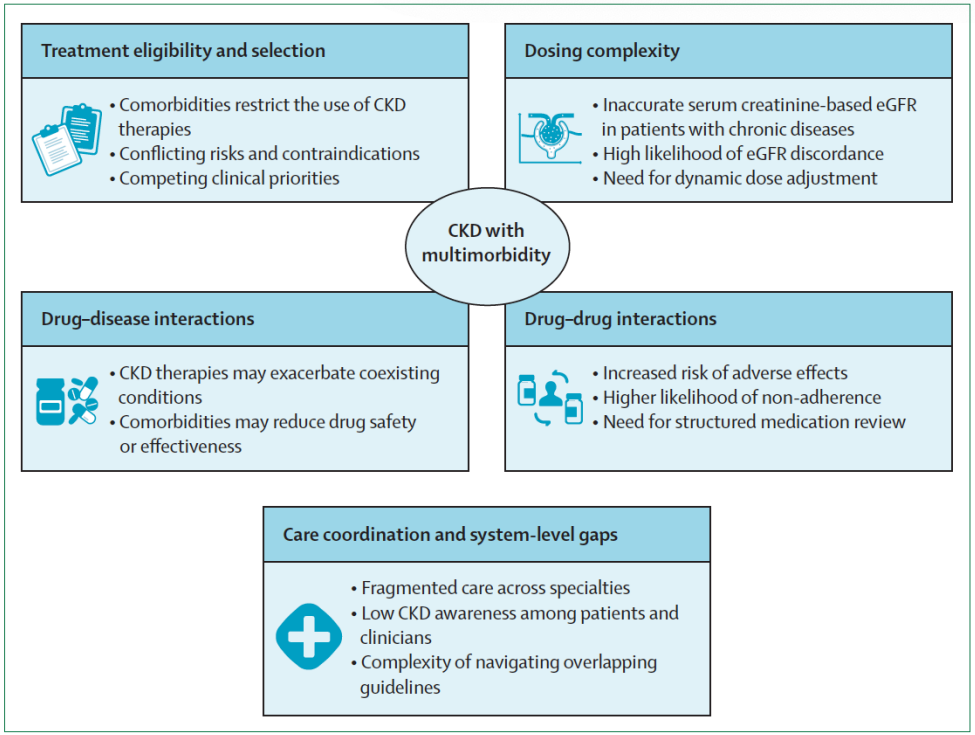

Figure 2: **How multimorbidity complicates CKD management**
CKD=chronic kidney disease. eGFR=estimated glomerular filtration rate.

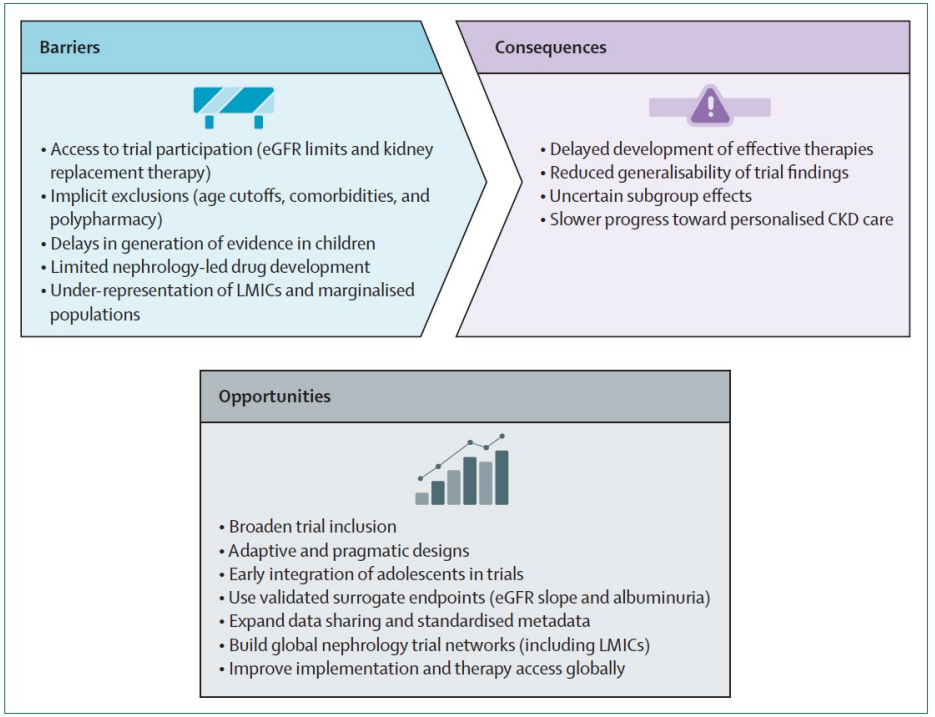

Figure 3: **Effect of CKD on evidence generation and opportunities for improvement**
CKD=chronic kidney disease. eGFR=estimated glomerular filtration rate. LMICs=low-income and-middle income countries.

Panel 1: **Outstanding questions and key research priorities**

Representativeness of chronic kidney disease (CKD) populations in CKD trials

- Key trials of CKD therapeutics do not adequately represent the populations they seek to treat
- Trials commonly recruit from specialist settings in high-income countries (HICs), rather than primary or general care and low-income and middle-income countries (LMICs), where most patients with CKD exist
- Trial participants are typically younger, less often female, and have lower levels of multimorbidity than in community settings
- Exclusions might be explicit, implicit, or subjective
- Serious adverse event rates are typically lower in trials than in community settings

Representation of patients with CKD in trials of other conditions

- Low representation of patients with advanced CKD, and those with kidney failure with or without replacement therapy are almost absent, across trials for other chronic medical conditions, including heart failure, cancer, and infections

Opportunities for improvement

- Ongoing efforts to improve trial efficiency, pragmatic, decentralised delivery, and representativeness
- Improved confidence in surrogate markers of CKD progression and kidney failure (eGFR slope,[178] change in albuminuria,[179] or a composite of both measures[180]) offer opportunities to identify off-target therapeutic benefits and harms for CKD progression
- Collaborative consortia[181] and data-sharing platforms[182] have improved access to individual-participant level data and offer flexibility and power to assess subgroup-specific effects across broad populations

Key research priorities

- Key therapeutic gaps and target populations are highlighted in the table
- Improve representation in LMICs and in under-studied, marginalised, and vulnerable populations in HICs
- Evidence for novel CKD therapeutics in children
- Evidence to improve cardiovascular disease outcomes in patients with advanced CKD and kidney failure
- Integrate surrogate markers of CKD progression in non-CKD trials
- Approaches to CKD prevention in populations at high risk such as those with cancer and infections
- Design standard set of mandatory trial metadata (eg, age, sex, comorbidity count, and baseline eGFR subgroups and their interactions) to facilitate secondary meta-analysis for subgroup effects

Panel 2: Series recommendations

Clinical

- Integrate CKD detection, screening, monitoring, and treatment for populations at high-risk (eg, pregnancy, cancer, infections, autoimmune, multisystem, and cardiometabolic disease) in local or regional care pathways
- Recognise albuminuria as a strong, independent, and modifiable risk factor for adverse CKD and cardiovascular outcomes even when eGFR appears normal
- Prioritise early, combination treatment of CKD where appropriate to prevent adverse CKD and cardiovascular outcomes: individualised decisions and application of clinical judgement remain necessary for complex patients

Research

- Acknowledge heterogeneity of CKD populations in research, considering demographic and clinical characteristics, pathophysiology of CKD, and geographical distribution
- Integrate consideration of sex differences to the design, reporting, and review of research as default
- Report subgroup metadata to facilitate meta-analysis and maximise use of existing research

Formalising a shared and more inclusive research agenda that acknowledges the heterogeneity of patients with CKD across pathophysiology, demographic, and clinical characteristics (including sex, gender, age, and medical history), and geographical region would be expected to improve the understanding of CKD epidemiology, targeted therapeutic development, specificity of clinical guidance, and the personalisation of CKD care.

Nicotinamidadenindinukleotid (*Nicotinamid*-*Adenin*-*Dinukleotid*, abgekürzt **NAD**) ist ein Coenzym, das formal ein Hydridion überträgt (zwei Elektronen, kurz: 2 e^-, und ein Proton, H^+). Es ist an zahlreichen Redoxreaktionen des Stoffwechsels der Zelle beteiligt.

NAD+ und **NADH** bilden das wichtigste Redoxpaar unseres Stoffwechsels und sind für die zelluläre Energieproduktion, DNA-Reparatur und Langlebigkeit (Longevity) unerlässlich.

Detaillierte Unterschiede lassen sich wie folgt zusammenfassen:

•**NAD+ (Oxidierte Form):** Nimmt Elektronen und Protonen auf. Es ist der zentrale Elektronenakzeptor im Körper (ein "Taxi"), der Nährstoffe oxidiert und als Coenzym essenzielle Reparaturenzyme aktiviert.

•**NADH (Reduzierte Form):** Entsteht, wenn NAD+ zwei Elektronen und ein Wasserstoffion aufnimmt. NADH transportiert diese Energie in die Mitochondrien, um dort das lebenswichtige **ATP** (Zellenergie) zu erzeugen.

Die Elektronenaufnahme wird als Reduktion bezeichnet, weil sich die **Oxidationszahl** (Ladung) des Atoms **verringert**. Der Begriff stammt ursprünglich aus der Metallurgie, bei der die Reduktion von Erz auf die **Gewinnung (Verringerung) des reinen Metalls** durch den Sauerstoffverlust zurückgeführt wurde.

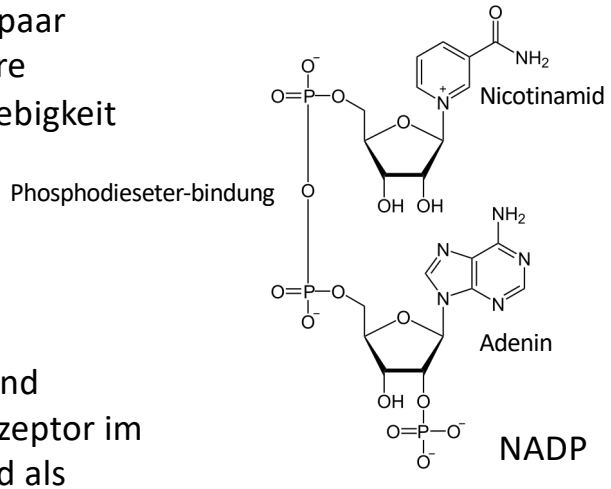

NADP

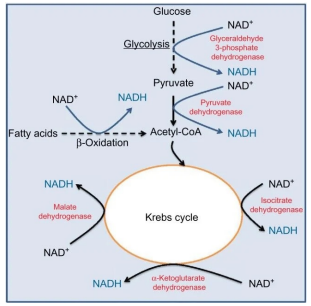

Energie-Produktion

NADH für Katabole Reaktionen;
NADPH für anabole Reaktonen
O_2 bringt NADH zurück zu NAD+

15-Hydroxyprostaglandin Dehydrogenase (15-PGDH) is the primary rate-limiting enzyme responsible for the metabolic inactivation of prostaglandins, most notably **prostaglandin E2 (PGE2)**.

$$PGE_2 + NAD^+ \xrightarrow{15\text{-PGDH}} 15\text{-keto-}PGE_2 + NADH + H^+$$

The placental metabolic clock

NAD+ depletion triggers a countdown to birth in mice

A decline in the availability of oxidized nicotinamide adenine dinucleotide (NAD^+) is an important trigger of aging across diverse species, including yeast, nematodes, and mammals. Decreased concentrations of this metabolic molecule drive progressive losses of physiological function across various tissues. Ciampa *et al* report that NAD^+ depletion in the placenta is not merely a marker of tissue fatigue. Rather, NAD^+ decline is a regulatory component of a precisely orchestrated metabolic countdown that determines when a new life is brought into existence. More generally, this discovery reframes the role of NAD^+ in metabolism, development, and aging.

The physiological clock uncovered by Ciampa *et al*. couples the placenta's metabolic state directly to a specific enzymatic process. The authors show that 15-hydroxy prostaglandin dehydrogenase (15-PGDH)— an enzyme that prevents premature labor by degrading the labor-promoting factor prostaglandin E_2 (PGE_2)—requires NAD^+ as an essential coenzyme. As pregnancy reaches its term, placental NAD^+ levels drop sharply, rendering 15-PGDH inactive. The accumulation of PGE_2 then triggers parturition. What drives the steep NAD^+ decline that occurs just before labor? Ciampa *et al*. found that it does not result from increased degradation by NAD^+-consuming enzymes, but rather from a marked reduction in NAD^+ synthesis. Metabolomic analyses showed substantially decreased amounts of NAD^+ precursors, such as maternal-derived nicotinamide (NAM), nicotinamide mononucleotide, and kynurenine, just before birth. Furthermore, the concentration of phosphoribosyl pyrophosphate (PRPP) was also decreased. PRPP is an essential cosubstrate for nicotinamide phosphoribosyltransferase (NAMPT), the rate-limiting enzyme in the NAD^+ salvage pathway, in which NAM is recycled into NAD^+. This dual constraint—a reduced supply of maternal-derived NAD^+ precursors coupled to a bottleneck in the placental synthesis machinery—forces the placenta into irreversible NAD^+ starvation. Therefore, through a process of maternal-fetal communication, NAD^+ availability acts as a signal that guides the birth of a new life.

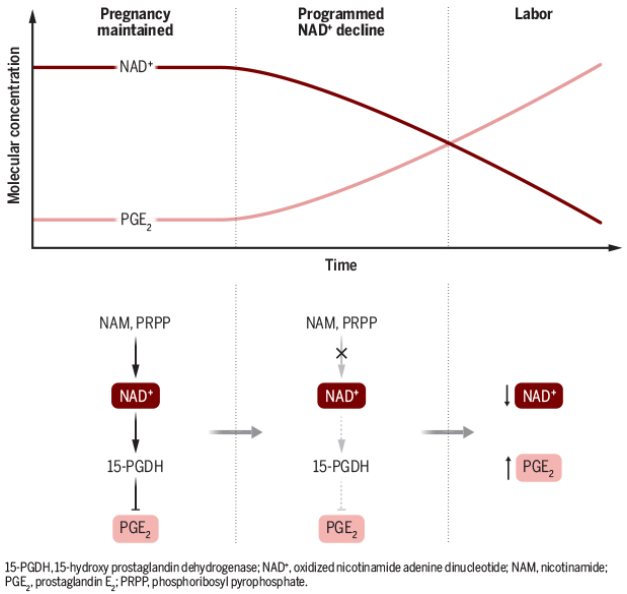

15-PGDH,15-hydroxy prostaglandin dehydrogenase; NAD+, oxidized nicotinamide adenine dinucleotide; NAM, nicotinamide; PGE_2, prostaglandin E_2; PRPP, phosphoribosyl pyrophosphate.

A metabolic trigger for labor in mice

Throughout gestation, placental NAD^+ levels are maintained to support the activity of 15-PGDH, an enzyme that degrades PGE_2 to prevent premature labor. As pregnancy reaches its terminus, a precipitous drop in placental NAD^+ concentrations caused by decreased amounts of NAD^+ precursors (NAM and PRPP) and decreased NAD^+ synthesis renders 15-PGDH inactive. The resulting surge in PGE_2 is a signal for parturition.

The findings by Ciampa *et al*. are clinically relevant because they uncover a potential strategy to prevent unexplained preterm births or to precisely control the induction of labor. The authors' concept of programmed NAD^+ decline has even broader implications. This localized metabolic exhaustion and its consequences mirror the process of programmed cell death (apoptosis) that is essential for development and maturation in many species—for example, to shed a tadpole's tail or to sculpt human digits. Both apoptosis and the placenta's metabolically programmed NAD^+ decline are mechanisms of decay that nature might have repurposed to shape life's most important transitions. As the changing role of the placenta from pregnancy to labor illustrates, the end of one tissue's life is the catalyst for the beginning of another. In this regard, aging could also be viewed not merely as a process of decline, but as an active, vital system that ensures the succession of generations by coordinating transitions across life stages. Ultimately, by decoding and controlling the switch of the NAD^+-driven program, humans may be able to achieve the vision of "productive aging" —a concept that emphasizes a healthy lifespan and the continued contribution of individuals to society from the beginning to the end of their lives.

$$PGE_2 + NAD^+ \xrightarrow{\text{15-PGDH}} \text{15-keto-}PGE_2 + NADH + H^+$$

Big Tobacco didn't just sell cigarettes. It shaped what Americans eat.

A new series of articles in the American Journal of Public Health explored the history and health impacts of ultra-processed foods and drew a direct line between their rise and Big Tobacco. During the 1980s, two of the biggest tobacco companies, Philip Morris (now known as Altria) and R.J. Reynolds (now Reynolds American), diversified their business holdings at a time of declining cigarette sales by aggressively expanding into the food industry. (Both companies did not respond to requests for comment.)

The two companies managed to acquire a long list of major brands, such as General Foods, Kraft, Del Monte, Nabisco and 7Up. Food became such a central part of their businesses that, at one point, it accounted for about 30 percent of R.J. Reynolds's portfolio and about half of Philip Morris's. The companies have since shed these holdings.

One of the articles examined more than 100 internal industry documents that became public through litigation against tobacco companies. As lead author Tera Fazzino, an addiction researcher and associate professor at the University of Kansas, explained to me, the companies not only integrated their food and tobacco distribution and sales operations but also directly applied lessons from tobacco manufacturing to food products.

For instance, king-size sodas, cookies and other food products were modeled on king-size cigarettes, which had successfully increased consumption. “Light” and “low-fat” foods similarly mirrored earlier efforts to sell “light” and “low-tar” cigarettes. Companies even used the same technology that extracted nicotine from tobacco to reduce fat in food — and targeted the same consumers.

“They developed these [nicotine] products to specifically retain customers who might otherwise have quit due to health concerns,” Fazzino said. “Then they did the exact same thing with their food products.”

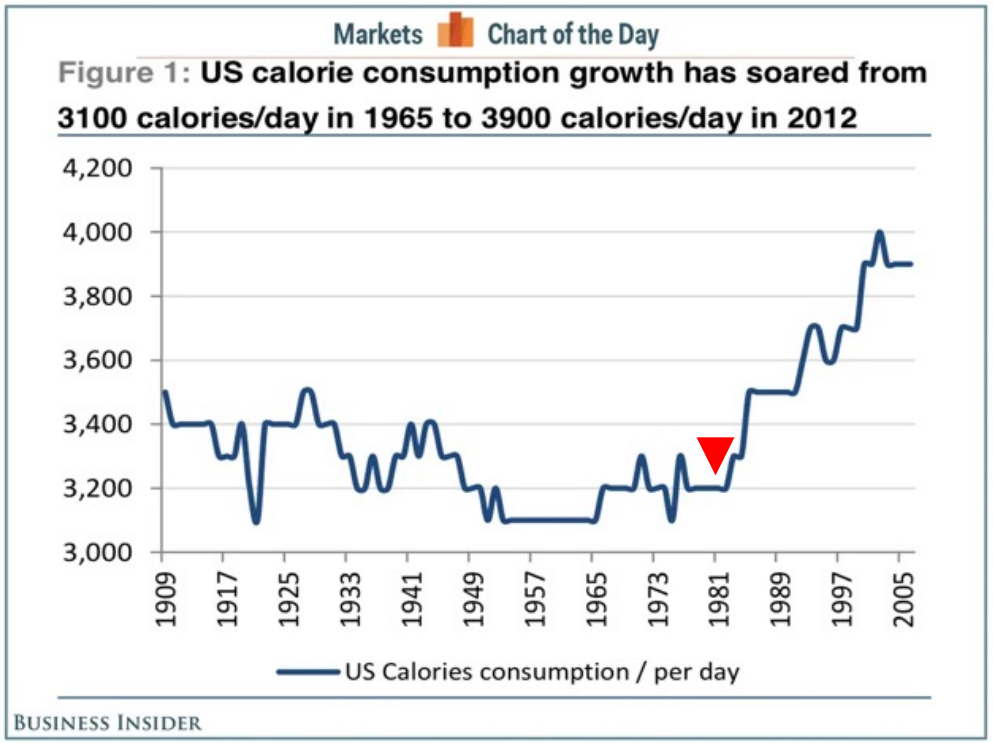

1980‘s Big tobacco buys into big food